

Winter 2002

# Genetic basis of adaptive radiation in East African cichlids

Richard Craig Albertson  
*University of New Hampshire, Durham*

Follow this and additional works at: <https://scholars.unh.edu/dissertation>

---

## Recommended Citation

Albertson, Richard Craig, "Genetic basis of adaptive radiation in East African cichlids" (2002). *Doctoral Dissertations*. 98.  
<https://scholars.unh.edu/dissertation/98>

This Dissertation is brought to you for free and open access by the Student Scholarship at University of New Hampshire Scholars' Repository. It has been accepted for inclusion in Doctoral Dissertations by an authorized administrator of University of New Hampshire Scholars' Repository. For more information, please contact [nicole.hentz@unh.edu](mailto:nicole.hentz@unh.edu).

## INFORMATION TO USERS

This manuscript has been reproduced from the microfilm master. UMI films the text directly from the original or copy submitted. Thus, some thesis and dissertation copies are in typewriter face, while others may be from any type of computer printer.

**The quality of this reproduction is dependent upon the quality of the copy submitted.** Broken or indistinct print, colored or poor quality illustrations and photographs, print bleedthrough, substandard margins, and improper alignment can adversely affect reproduction.

In the unlikely event that the author did not send UMI a complete manuscript and there are missing pages, these will be noted. Also, if unauthorized copyright material had to be removed, a note will indicate the deletion.

Oversize materials (e.g., maps, drawings, charts) are reproduced by sectioning the original, beginning at the upper left-hand corner and continuing from left to right in equal sections with small overlaps.

ProQuest Information and Learning  
300 North Zeeb Road, Ann Arbor, MI 48106-1346 USA  
800-521-0600

UMI<sup>®</sup>



**GENETIC BASIS OF ADAPTIVE RADIATION  
IN EAST AFRICAN CICHLIDS**

**BY**

**R. CRAIG ALBERTSON  
BS, University of New Hampshire, 1996  
MS, University of New Hampshire, 1999**

**DISSERTATION**

**Submitted to the University of New Hampshire  
in Partial Fulfillment of  
the Requirements for the Degree of**

**Doctor of Philosophy  
in  
Zoology**

**December, 2002**

UMI Number: 3070969

Copyright 2002 by  
Albertson, Richard Craig

All rights reserved.

UMI<sup>®</sup>

---

UMI Microform 3070969

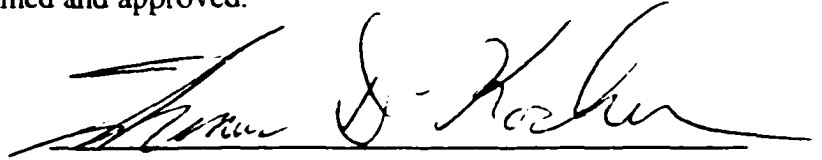
Copyright 2003 by ProQuest Information and Learning Company.  
All rights reserved. This microform edition is protected against  
unauthorized copying under Title 17, United States Code.

---

ProQuest Information and Learning Company  
300 North Zeeb Road  
P.O. Box 1346  
Ann Arbor, MI 48106-1346

**ALL RIGHTS RESERVED**  
© 2002  
R. Craig Albertson

This dissertation has been examined and approved.



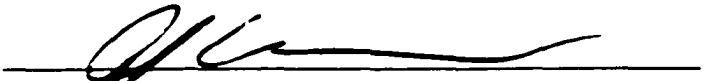
Dissertation Director, Dr. Thomas D. Kocher  
Professor of Zoology and Genetics



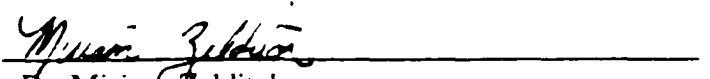
Dr. Jessica A. Bolker  
Professor of Zoology



Dr. J. Todd Streelman  
Postdoctoral Research Fellow in Genetics



Dr. John Collins  
Associate Professor of Biochemistry



Dr. Miriam Zelditch  
Associate Research Scientist, Museum of  
Paleontology, University of Michigan



Dr. James Hanken  
Professor of Zoology, Harvard University

Aug 30, 2002  
Date

## TABLE OF CONTENTS

LIST OF TABLES .....	vi
LIST OF FIGURES .....	vii
ABSTRACT .....	ix

CHAPTER	PAGE
INTRODUCTION .....	1
I. REVISITING THE 'PEACEFUL CONDOMINIUM': HABITAT PARTITIONING IN FORAGING SPACE.....	17
Abstract .....	17
Introduction .....	18
Materials and Methods .....	21
Results .....	25
Discussion .....	28
II. ASSESSING MORPHOLOGICAL DIFFERENCES IN AN ADAPTIVE TRAIT: A LANDMARK-BASED MORPHOMETRIC APPROACH.....	47
Abstract .....	47
Introduction .....	49
Materials and Methods .....	52
Results .....	57
Discussion .....	63
III. GENETIC BASIS OF ADAPTIVE SHAPE DIFFERENCES IN THE CICHLID HEAD.....	88
Abstract .....	88
Introduction .....	89



Materials and Methods .....	91
Results .....	97
Discussion .....	102
<b>IV. A GENETIC LINKAGE MAP FOR LAKE MALAWI'S ROCK-DWELLING</b>	
<b>CICHLIDS, THE MBUNA.....</b>	<b>115</b>
Abstract .....	115
Introduction .....	116
Materials and Methods .....	117
Results .....	123
Discussion .....	126
<b>V. GENETIC DETERMINANTS AND GENOMIC "HOT-SPOTS" IN THE</b>	
<b>ADAPTIVE RADIATION OF EAST AFRICAN CICHLIDS.....</b>	<b>138</b>
Abstract .....	138
Introduction .....	140
Materials and Methods .....	142
Results .....	146
Discussion .....	150
<b>APPENDICES.....</b>	<b>162</b>
Appendix A.....	163
Appendix B.....	164
Appendix C.....	168
<b>LITERATURE CITED.....</b>	<b>186</b>

## LIST OF TABLES

Table 1. Developmental Units .....	14
Table 2.1. Description of Anatomical Landmarks .....	71
Table 2.2. Results of DFA .....	72
Table 2.3. Functional Differences Between Species .....	73
Table 4.1. Comparative Map .....	132
Table 4.2. Segregation of Color and Sex .....	133
Table 5.1. Results of QTL Analysis .....	155

## LIST OF FIGURES

Figure 1. Proposed Phylogenetic History of Lake Malawi Cichlids .....	15
Figure 2. Anatomical ‘Hot-Spots’ .....	16
Figure 1.1. Map of Thumbi West Island .....	36
Figure 1.2. Results for Jaw Width .....	37
Figure 1.3. Morphotypic Classes .....	38
Figure 1.4. Results for Depth Distribution .....	39
Figure 1.5. Results for Foraging Area .....	40
Figure 1.6. Results for Slope.. .....	41
Figure 1.7. Results for Shelter .....	42
Figure 1.8. Results for Sediments .....	43
Figure 1.9. Results for Feeding Mode .....	44
Figure 1.10. Summary of Microhabitat Partitioning .....	45
Figure 1.11. Mechanism of Habitat Partitioning .....	46
Figure 2.1. Study Species .....	74
Figure 2.2. Lower Jaw Lateral .....	75
Figure 2.3. Lower Jaw Ventral .....	76
Figure 2.4. Maxilla .....	77
Figure 2.5. Premaxilla .....	78
Figure 2.6. Neurocranium .....	79
Figure 2.7. Vomer .....	80
Figure 2.8. Results of TPS – Lower Jaw Lateral .....	81
Figure 2.9. Results of TPS – Lower Jaw Ventral .....	82
Figure 2.10. Results of TPS – Maxilla .....	83
Figure 2.11. Results of TPS – Premaxilla .....	84
Figure 2.12. Results of TPS – Neurocranium .....	85

Figure 2.13. Results of TPS – Vomer .....	86
Figure 2.14. Histograms of CV1 .....	87
Figure 3.1. Craniofacial Morphology .....	108
Figure 3.2. Description of Multivariate Analysis .....	109
Figure 3.3. Results of Castle-Wright Estimator – Head Morphology .....	110
Figure 3.4. Results of Castle-Wright Estimator – Dentition .....	112
Figure 3.5. Histograms of PC1 .....	113
Figure 3.6. Correlation Analysis .....	114
Figure 4.1. Pedigree of Experimental Population .....	134
Figure 4.2. Genetic Linkage Map .....	135
Figure 4.3. Segregation of Sex and Color .....	137
Figure 5.1. Phenotypic Effects of QTL Genotypes .....	158
Figure 5.2. Linkage Map Showing QTL Positions .....	160

## ABSTRACT

### GENETIC BASIS OF ADAPTIVE MORPHOLOGICAL RADIATION IN CICHLID FISHES

by

R. CRAIG ALBERTSON

UNIVERSITY OF NEW HAMPSHIRE, DECEMBER, 2002

East African cichlids are a paramount example of adaptive morphological radiation. The most dramatic difference among species occurs in oral jaw design and correlates with ecological niche partitioning. Convergent evolution of trophic forms between lakes suggests a common mechanism. What combination of intrinsic and extrinsic factors constitute this mechanism still remains to be seen. The goal of this dissertation was to examine the genetic basis of shape differences between two closely related cichlid species that employ alternate modes of feeding. This was achieved through a number of independent experiments. First, I used field data to characterize the way in which foraging habitat was partitioned between sympatric rock-dwelling species from Lake Malawi. Second, morphological differences between two species that employ alternate modes of feeding, *Labeotropheus fuelleborni* and *Metriaclima zebra*, were quantified via geometric morphometrics. I found that specific aspects of shape predicted differences in feeding performance. In this experiment I also developed the phenotypic characters that were used in subsequent experiments. Next, the genetic bases of these morphological characters were biometrically estimated using the Castle-Wright estimator. I estimated between 1 and 11 factors to control shape differences in various

traits. Specific traits were also shown to segregate together in hybrid progeny, suggesting a degree of pleiotropy among genes that underlie differences in the cichlid feeding apparatus. Finally, I constructed a genetic linkage map for Lake Malawi's rock-dwelling cichlids, and identified quantitative trait loci (QTL) that affected shape differences in the cichlid head. Segregation at 136 molecular markers was studied in 173 F<sub>2</sub> hybrids. The final linkage map consisted of 126 markers distributed over 24 linkage groups and 838 cM. QTL were detected for sex, color, and 15 morphological traits that distinguish the shape of the feeding apparatus in *L. fuelleborni* and *M. zebra*. At every stage of this dissertation results are related to the developmental and functional biology of the cichlid head.

## INTRODUCTION

East African cichlids have undergone an extraordinary evolutionary radiation. Lakes Victoria, Tanganyika and Malawi each contain several hundred endemic species. Molecular and geological studies suggest that these radiations are extremely recent (Meyer, 1993; Kocher et al., 1995). Lake Malawi and its endemic cichlid fauna are less than a million years old (Meyer et al., 1990), but it contains well over 500 cichlid species, and much of this radiation probably occurred within the last 25,000 years (Owen et al. 1990; Scholtz and Rosendahl 1988). Likewise, the Lake Victorian basin is thought to have been completely dry 13,000 years ago (Johnson et al. 1996), yet this lake now contains an assemblage of over 300 cichlid species (Greenwood 1974; Seehausen 1997). Unfortunately, little is known about the forces that have produced so many species in such a short time.

The advent of several molecular phylogenies has begun to shed light on the selective forces driving these evolutionary radiations (Albertson et al. 1999; Kocher et al. 1995; Kornfield and Parker 1997; Meyer et al. 1990). Figure 1 illustrates the proposed phylogenetic history of Lake Malawi's cichlid species flock. The model suggests that diversification was achieved through three sequential cladogenic events, driven by distinct selective forces (Danley and Kocher, 2001). The first occurred in response to ecological pressure, establishing two distinct clades; one that occupies the sandy habitat and the other that is restricted to the rocky shoreline. The second cladogenic event occurred in response to selection on trophic biology, leading to the establishment of morphologically distinct genera. The most recent speciation event was likely in response to sexual selection, leading to diversity in reproductive behavior and male nuptial color.

This general model provides a tractable framework in which to address specific questions as to the evolution of Lake Malawi cichlid fishes.

Recent studies have emphasized the role of sexual selection as a driving and stabilizing force behind East African cichlid assemblages (Dominey, 1984; McKaye et al., 1990; McKaye, 1991; Seehausen et al., 1997). The importance of natural selection has been less thoroughly examined, despite the suggestion by Liem (1974) that the pharyngeal jaw apparatus in cichlids represents a 'critical innovation' that allowed for rapid and extensive diversification in feeding biology. I am most interested in adaptive morphological radiation and this second cladogenic event in Lake Malawi's phylogenetic history. This dissertation involves elucidating both the intrinsic and extrinsic factors that have contributed to the rise and maintenance of morphological diversity among Lake Malawi cichlids.

### Adaptive Radiation

Adaptive radiation is the evolutionary diversification of a lineage across a series of niches or adaptive zones (Futuyma 1986; Mayr 1963). Implicit to the term is that diversification occurs rapidly. One of several postulated causes of adaptive radiation is competition for food, leading to divergence in trophic morphology and resource use. Among of the best examples of extensive and replicate adaptive radiations are different groups of lacustrine teleosts, including arctic charr, the three-spine stickleback, and cichlid fishes on two continents.

Four sympatric morphs of arctic charr (*Salvelinus alpinus*) are found in Thingvallavatn, a small lake in Iceland. These incipient species have one of two basic morphologies: a benthic form with a subterminal mouth, and a pelagic form with a



terminal mouth. The morphs appear to have arisen in sympatry (Volpe and Ferguson, 1996), and differences in trophic morphology have a clear genetic basis (Skulason et al., 1989; 1996).

The marine stickleback, *Gasterosteus aculeatus*, has repeatedly invaded small coastal lakes in British Columbia (McPhail, 1994). Two species frequently arise following colonization: a small limnetic form and a larger benthic form (Ridgway and McPhail, 1984; McPhail, 1992). Schluter and McPhail (1993) suggest that ecological character displacement may have played a role in speciation. Hatfield (1997) and Peichal et al. (2001) found that relatively few genes control the stereotypical traits that distinguish these forms.

Crater lake cichlids on two continents also illustrate the importance of trophic selection in speciation. Monophyletic radiations of cichlids have occurred in three lakes in Cameroon (Schiewen et al., 1994). A pair of nascent species in Lake Ejagham, Cameroon, assortatively mate according to body size, a trait likely correlated with different feeding habitat. Several crater lakes in Nicaragua contain endemic cichlid assemblages (Midas species complex, *Amphilopus spp.*) that differ in diet, body size, head shape and pharyngeal jaw morphology (McKaye et al. 2002; Stauffer and McKaye 2002).

The vast East African cichlid assemblages endemic to the three large lakes in the region represent some of the most dramatic examples of adaptive morphological radiation (Futuyma 1986; Fryer and Iles 1972). Different trophic morphologies have arisen both rapidly (Owen et al. 1990; Johnson et al. 1996) and in parallel (Kocher et al 1993). Further, alternate feeding mechanisms correlate with feeding performance and fine-scale ecological niche partitioning (Bouton et al. 1997,1998; Liem 1974, 1980; Otten 1983; Reinthal 1990), implicating competition as the impetus of phenotypic evolution and maintenance.

## Functional Morphology of the Cichlid Head

Several studies have demonstrated the linkage between functional/morphological divergence and differences in feeding performance of cichlids (Bouton et al. 1997,1998; Liem 1974, 1980; Otten 1983; Reinthal 1990). If we assume that diversification in feeding behavior is principal in the adaptive radiation of these assemblages, then understanding the function biology of the feeding apparatus is critical in any study of cichlid evolution.

There is a large body of literature devoted to interpreting the functional morphology of the cichlid head. Three major modes of feeding have been identified: sucking, biting, and ram feeding. These three modes are easily predicted from the functional design of the cichlid head (reviewed by Liem, 1991). For instance, the most efficient design for suction feeding is a cone-shaped buccal cavity and a highly protrusible upper jaw that allows for rapid expansion of the buccal volume. On the other hand, streamlined predators have a more cylindrical buccal cavity that cannot produce much suction, but is optimal for the pursuit and overtaking of prey, also known as ram feeding (Liem, 1991).

Most cichlids employ more than one strategy of prey capture and possess skulls of intermediate design. These more 'generalized' designs allow species to feed on a variety of foods. For example, *Metriaclima zebra* has been characterized as a 'biter' (Witte, 1984), but will often employ a 'sucking' mode when feeding on plankton in the water column (McKaye and Marsh, 1983; Ribbink et al, 1983; and Reinthal, 1990). Rather than viewing individual species as specialists, we should consider the balance each has struck among conflicting structural demands (Barel, 1983; Liem, 1980).

Biting fish are characterized by shifts in anatomical points on the premaxilla, maxilla, and mandible (Otten, 1983) (Figure 2). Through extensive modeling, Otten (1983) identified seven 'hot spots' of anatomical change which distinguish species along the biting/sucking functional continuum. Relative shifts at these points affected the mechanisms of force transmission during biting. The main changes in proportion which increase biting force include:

- 1) Shortening of the premaxillary ascending arm (anatomical points 1 and 2).
- 2) Steepening of the premaxillary ascending arm (anatomical points 1, 2, and 3).
- 3) Rostrad movement of the intermaxillary ligament (anatomical point 4).
- 4) Lengthening of the maxillad process of the palatine (anatomical points 5 and 6).
- 5) Shortening of the dentary process of the lower jaw (anatomical point 7).
- 6) Dorsad shift of the adductor mandibulae 1 (mA1), resulting in a smaller eye or displacement of the eye (anatomical point 8).
- 7) Caudo-ventrad shift of the adductor tendonae 1 (A1t) on the maxilla (anatomical point 9).

Otten (1983) found that these anatomical 'hot spots' accurately predicted where species aligned on the biting/sucking continuum. In every instances species that employed a biting mode of feeding fell on one end of the continuum, while species that were predominant suction feeders fell on the opposite end.

## Developmental Units of the Cichlid Head

Since evolution in adult form occurs via modifications during development (Atchley and Hall 1991; Gould 1974), it is important to understand both the embryological origins of the teleost jaw apparatus, as well as how genotype is translated to phenotype in this character complex.

The teleost head is composed of two types of bone (DeBeer, 1985). Dermal bone has no cartilaginous precursor and is always derived from neural crest cells (ectoderm). Endochondral bone has a cartilaginous precursor and may develop from either neural crest or mesoderm (Hall, 1999). The developmental origin of various structures that constitute the teleost head is shown in table 1. The maxilla, premaxilla, and the dentary arise from separate condensations of dermal bone. The articular and the hyoid skeleton are derived from endochondral bone. The neurocranium and suspensorium are derived from both dermal and endochondral bone (Hall, 1999).

Work in the zebrafish model has provided excellent insight as to the mechanisms of teleost head and jaw development. The pharyngeal and buccal skeleton originate from a series of pharyngeal arches that develop along the lateral side of the head (Schilling, 1997). The first arch (mandibular, 1) gives rise to part of the lower jaw, the second (hyoid, 2) forms the hyoid and associated elements, and five more posterior arches (branchial, 3-7) form the gill supports. Neural crest cells, which constitute the arch primordia, arise from specific segments of the hindbrain (the rhombomeres) and migrate in three major streams: 1) mandibular, r1-3; 2) hyoid, r3-5; 3) branchial, r5-8 (Lumsden et al., 1991). It has been demonstrated that the translocation of neural crest cells from one rhombomeric segment to another will result in the reorganization of the skeletal pattern according to their new arch primordia (Noden, 1986). This pattern implicates neural crest cells as inherent organizers of anterioposterior (A/P) patterning.

Within different rhombomeric segments, A/P patterning appears to be established by differential expression of Hox genes (reviewed in Schilling, 1997). In addition, a number of novel genes involved in head patterning have been discovered in zebrafish, via random mutagenesis (reviewed in Schilling, 1997). Such genes have been found to differentially affect the migration of neural crest cells into their respective pharyngeal segment. For instance, mutation of the gene *sucker* or *schmerle*, affect both the first and second arches, while leaving the more posterior arches unaffected (Piotrowski et al. 1996). Likewise, transplantation of neural crest cells from a wild-type donor to a mutant host can rescue skeletal development in the region of the transplant (reviewed in Schilling, 1997). Again, the potential for A/P patterning seems to reside within the cells of the neural crest.

Within each pharyngeal arch, neural crest cells must also differentiate along the dorsoventral (D/V) axis. In the first arch, this patterning leads to the development of one dorsal and one ventral element. Within the second arch, there are four elements separated along the D/V axis. Finally, the branchial arches have two dorsal and three ventral cartilages. In 1987, Hall proposed that interactions between migrating neural crest and adjacent epithelial tissue might be important in D/V patterning of the head.

Endothelin-A (ET-A) is expressed in neural crest-derived ectomesenchyme of the pharyngeal arches. Initial migration of neural crest cells appears normal in endothelin-A receptor deficient mice, however an absence of ET-A ultimately results in abnormal growth and differentiation in arch development (Clouthier, et al., 2000). Recently, it has been established that the zebrafish mutant *sucker* (*suc*) encodes an endothelin ligand (ET-1) (Miller, et al., 2000). Like mouse, *suc/et-1* is expressed in paraxial mesoderm and arch epithelia. In *suc* mutants, expression of *dHAND*, *dlx-2*, *dlx-3*, *msx-E*, and *gsc* are either missing or reduced in the anterior arches, resulting in severe defects in the ventral cartilage of the first and second arch. Other zebrafish mutants that affect endoderm

formation (*casanova* and *van gogh*) also affect pharyngeal arch patterning (Alexarder et al., 1999; Piotrowski and Nusslein-Volhard, 2000). Thus, D/V patterning within each arch may be the result of interactions between post-migratory neural crest and the surrounding epithelium.

The development of the neurocranium begins along the ventral midline of the skull (basicrainium) beneath the developing brain, and proceeds along the mediolateral axis (M/L). Phenotypes of several zebrafish mutations (i.e. *chameleon*, *cyclops*, *detour*, *iguana*, *silberblick* and *you-too*) are shown to disrupt the development of the neurocranium along the M/L axis (Schilling, 1997; Kimmel et al. 2001).

Since most of the molecular players involved in craniofacial patterning in zebrafish are conserved across different vertebrate taxa, it is reasonable to assume that most are involved in regulating development and patterning of the cichlid head. To what degree the mechanisms of craniofacial development are involved in the evolution of trophic morphology will be interesting to see.

### Quantitative Genetic Studies of Complex Morphologies

A complex morphological structure is one whose final form arises from the integration of a number of different component parts (Atchley, 1993). One example is human height. Such a trait exhibits a normal distribution. In contrast to Mendel's peas, which are either round or wrinkled, human height may range from four to seven feet and include every possibility in between. The expression of a complex or "quantitative" trait is the result of the action of a number of different genes.

Mutant hunts, such as those conducted in zebrafish and other vertebrate models, have the capacity to identify genes critical to developmental pathways. Unfortunately,

these approaches have clear limitations in the realm of evolutionary biology. First, mutant screens are generally conducted in embryos, making defects in adult form difficult to infer. Further, mutant phenotypes are often dramatic (and lethal) and may provide little insight into the genes and mechanisms responsible for fine-scale adaptive changes. Hanken (1993) argues for the integration of model systems with comparative approaches to achieve a better understanding of the development and evolution of the vertebrate head.

Quantitative genetic studies are an important approach in identifying the genetic basis of complex morphologies. The genetic basis of morphological differences between populations (parental lines) can be deduced by examining the segregation of phenotype and genotype in their hybrid progeny. Recent studies have begun to identify the quantitative genetic basis for morphological differences in natural populations of several species (Bradshaw et al., 1998; White and Doebley, 1998). Considerable insight has come from experiments with *Drosophila*, in which the genetic basis for differences in bristle number (Mackay, 1996), and the shape of the male genitalia (True et al., 1997; Laurie et al., 1997; Zeng et al., 2000)) have been determined.

Studies of the murine mandible provide another excellent paradigm for work on cichlids (Atchley and Hall, 1991). Significant genetic variation for jaw size and shape can be found among inbred lines of mice (Atchley et al., 1988). Particularly interesting is the observation that elements with a common developmental origin show genetic and phenotypic correlations (Cheverud et al., 1991; Mezey et al., 2001).

## Study Species

I examined the genetic basis of differences in jaw morphology between two closely related, yet morphologically divergent rock-dwelling cichlids (locally known as mbuna) from Lake Malawi. *Metriaclima zebra* (hereafter referred to as 'MZ') is characterized by a moderately sloped head, a terminal isognathus mouth, and a swollen, horizontally directed vomer (Stauffer et al., 1997). When feeding from the substrate, MZ combs loose diatoms, algae and other detritus from filamentous algae beds while oriented perpendicular to the substrate. MZ is also one of the only mbuna species that regularly feeds in the water column with a sucking mode (McKaye and Marsh, 1983; Ribbink et al., 1983; and Reinthal, 1990; personal observation). *Labeotropheus fuelleborni* ('LF') has a large fleshy snout and an inferior-subterminal mouth that it uses to crop algae from rocks while oriented nearly parallel to the substrate (Ribbink et al., 1983). LF favors shallow water where surge is a prominent part of the environment (Ribbink et al., 1983).

McElroy and Kornfield (1993) studied the morphological differences between these two species and their F<sub>1</sub> hybrids. They scored 11 landmarks in the pre-orbital region of the head from lateral radiographs. *Labeotropheus* was found to have a significantly downturned vomer, a sharply bent dentigerous arm of the premaxilla, and a bent maxilla. These observations are consistent with the principal components analysis by Reinthal (1990), which found that MZ and LF fell at opposite ends of PC axes II and III constructed from linear measurements on the neurocranium.

The initial radiation of Lake Malawi's cichlid species flock is characterized by a functional divergence across three basic modes of – biting, sucking, and ram-feeding; a trend reiterated in many other groups of fishes (e.g. stickleback, whitefish, arctic charr). I chose LF and MZ as my study species because they representative members of a monophyletic clade (the mbuna) that lie on opposite ends of the biting sucking



continuum. Understanding the genetic bases of changes that differentiate LF and MZ should lend insight as to the genetic bases of differences along this functional/adaptive axis.

### Specific Objectives

Each of the subsequent chapters in this dissertation stands as an independent study covering seemingly disparate topics and methodologies. Taken together, each chapter represents a facet in an integrative and comprehensive assessment of adaptive radiation in Lake Malawi cichlids.

The first chapter provides a glimpse into how rock-dwelling cichlids, including LF and MZ, partition foraging habitat. Next, I quantify the specific differences in oral jaw morphology between LF and MZ. Finally, I describe a series of experiments aimed at understanding the inheritance and genetic bases of these shape differences.

For reasons delineated above, I feel that aspects of functional and developmental biology are critical components to any discussion of adaptive radiation in cichlids. Thus, wherever relevant I relate my results to the function and developmental biology of the cichlid head.

Chapter 1: Revisiting the 'Peaceful Condominium': Habitat Partitioning in Foraging Space. There is some question as to the extent to which sympatric cichlid species partition habitat in foraging space. A long-standing view states that, in spite of its tremendous size, Lake Malawi does not provide the diversity in either habitat or food for speciation to be accomplished or species diversity to be maintained (Fryer 1959; Genner et al. 1999). I challenged this perspective with data collected in the field. Dimensions in

which species partition foraging habitat were characterized and a stepwise model was postulated by which sympatric species may partition their environment in the space of foraging habitat. The goal of this chapter was to demonstrate the importance of habitat partitioning in the maintenance of species diversity, and to relate differences in trophic morphology to differences in feeding behavior.

**Chapter 2: Assessing the Morphological Differences in an Adaptive Trait: a Landmark-based Morphometric Approach.** To better understand the adaptive evolution of the oral jaw apparatus, I performed a rigorous morphological analysis on the individual skeletal elements that constitute the head in MZ and LF, as well as in their  $F_1$  hybrid progeny. I chose to employ landmark based, geometric morphometrics to better relate my results to the developmental and functional biology of the oral jaw apparatus. There were two main goals of this study. First, I wanted to see how well differences in form predict differences in feeding performance and habitat preference (as discussed in Objective 1). Secondly, I wanted to develop a phenotypic assay that maximized my power to discriminate between MZ and LF morphology. The geometric descriptors of shape difference developed in this study will be the phenotypic characters assessed in Chapter 3 and mapped in Chapter 5.

**Chapter 3: Genetic Basis of Adaptive Shape Differences in the Cichlid Head.** The effective number of genetic factors that underlie differences in the cichlid head were biometrically estimated through a comprehensive assessment of the morphological variance in MZ, LF, and their  $F_1$  and  $F_2$  hybrid progeny. The genetic correlation among individual skeletal elements was also inferred by characterizing the structural units that are inherited together in the  $F_2$ . This experiment also enables me to better estimate the power needed to detect QTL in Chapter 5.

**Chapter 4: A Genetic Linkage Map for Lake Malawi's Rock-dwelling Cichlids, the Mbuna.** A CA<sub>n</sub> microsatellite library was constructed from *Metriaclima zebra* DNA, and a mbuna linkage map was built using the F<sub>2</sub> from the MZ x LF cross. The full pedigree of all F<sub>2</sub> animals was described. The mbuna map was compared to a pre-existing genetic map for tilapia, as several molecular markers were used in both mapping experiments. Markers were identified that segregate with two Mendelian traits that segregate in the MZ x LF cross: color morphology and sex.

**Chapter 5: Genetic Determinants and Genomic "Hot-spots" in the Adaptive Radiation in Cichlid Fishes.** The culmination of this dissertation was a quantitative trait loci (QTL) analysis where shape differences between LF and MZ were mapped to specific chromosomal intervals. This experiment was performed on oral jaw dentition and eight bony elements of the head. In many instances shape differences in several elements mapped to a similar chromosomal region, suggesting a role of pleiotropy in the genetic architecture of the cichlid head.

**Table 1**  
**Developmental origin of craniofacial elements in the teleost head.** Dermal bone is always derived from neural crest cells (NCD). Endochondral bone develops from neural crest (NCD) and/or mesoderm (MDD).

Elements	Dermal	Endochondral	
	NCD	NCD	MDD
Dentary	X		
Articular		X	
Maxilla	X		
Premaxilla	X		
Neurocranium	X	X	X

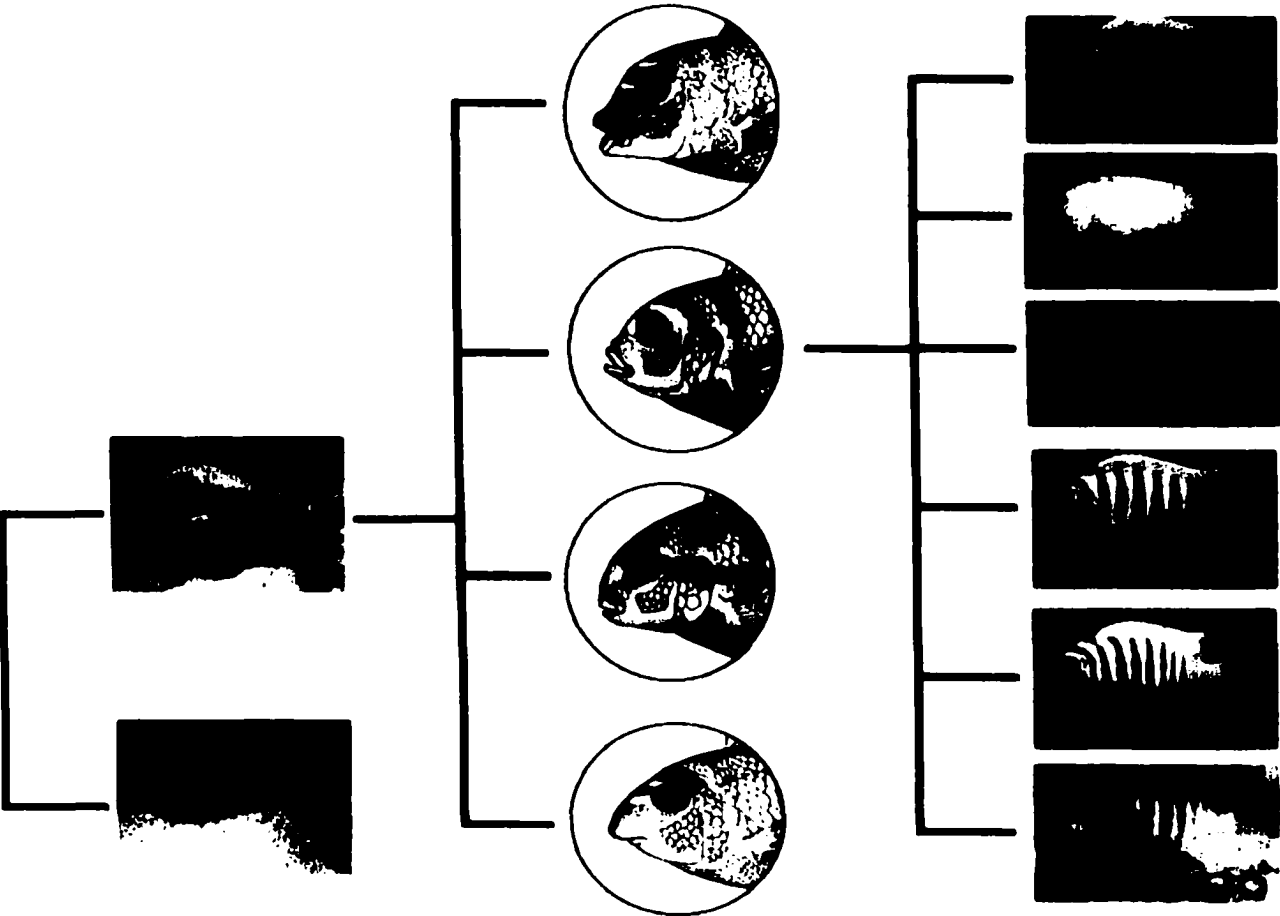
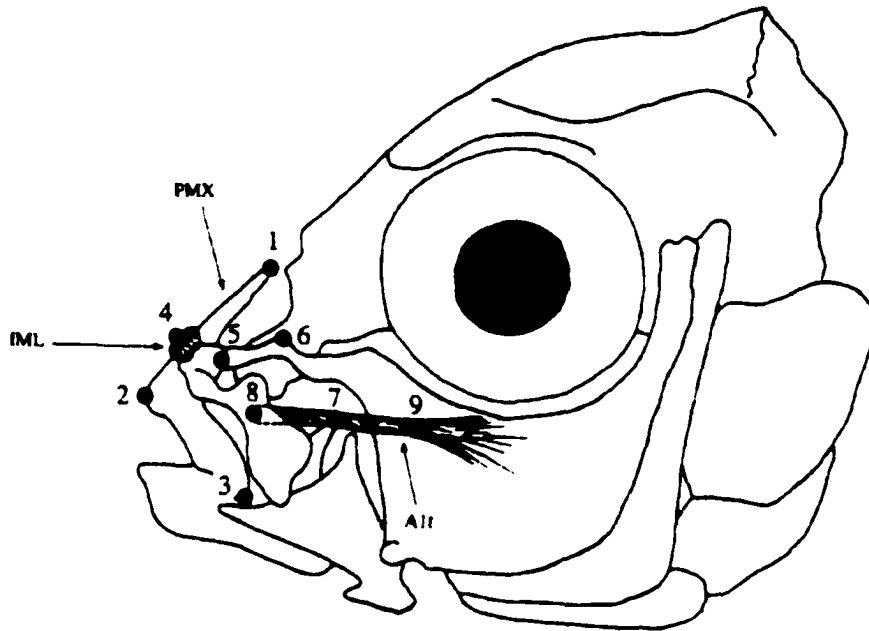


**Figure 1**

**Proposed phylogenetic history of Lake Malawi cichlid fishes.** The model is based on several molecular phylogenies and suggests that diversity was achieved via three cladogenic events in response to three distinct selective forces (after Danley and Kocher 2001).

**Figure 2**

**“Hot spots” of anatomical change.** The relative position of anatomical points reflect where species lies along the biting/sucking functional axis (after Otten 1983). PMX – premaxilla, IML – intermaxillary ligament, AIt – adductor tendonae.



## CHAPTER 1

### REVISITING THE 'PEACEFUL CONDOMINIUM': HABITAT PARTITIONING IN FORAGING SPACE

#### Abstract

The extent to which sympatric cichlid species partition their environment in foraging space is an open question. It is a long-standing view that, in spite of its tremendous size, Lake Malawi does not provide enough variety in habitat or food to maintain species diversity through partitioning of diet or foraging space. I challenge this perspective with field data collected from a highly diverse rocky community. Six microhabitat characteristics were used to define the dimension in which six sympatric species partition foraging space. All species were separated by at least one, and in most cases three or more, characteristics. Moreover, certain microhabitat characters were partitioned according to jaw morphology. Finally, I offer a stepwise model that suggests microhabitat partitioning is sufficient to maintain species diversity in complex rocky communities.

## Introduction

East African rock-dwelling cichlid communities embody several characteristics that make them attractive models for the study of ecology and evolution. Species that live over the rocky habitat tend to exhibit high levels of philopatry accompanied by low rates of dispersal. The rocky community tends to be both highly speciose and densely packed. For decades evolutionary biologists have used the rocky habitat and its associated cichlid fauna to elucidate the factors that have contributed to both the evolution and maintenance of morphological diversity among East African cichlids.

In his classic study, Fryer (1959) suggested that the rock-dwelling community represents a “peaceful condominium,” with little or no competition for resources due to an apparent superabundance of algae. To Fryer, it is this attribute of the cichlid community that explains the coexistence among species. It has also been postulated that trophic specializations among cichlid species may not be adaptive (Liem 1980). In a series of laboratory studies, Liem found that different morphological “specialists” often employ the same functional repertoire (Liem 1980 and references within). The crux of Liem’s paradox is morphological specialization without functional divergence. In his own words, he asks:

If specialists are simultaneously jacks-of-all-trades, how could they have evolved according to the pervasive ecological theory that broadening the range of usable resources prevents species from specializing on individual types (Liem 1980, p. 307)?

In contrast to these classical studies, a growing body of contemporary evidence suggests that competition is a prominent part of the rocky habitat and that morphological



specialization confers an adaptive advantage upon species. Reinthal (1990) identified four general feeding behaviors among Lake Malawi's rock-dwelling cichlids: nipping, brushing, mowing, and pelagic foraging. Moreover, he found that these four feeding behaviors broadly correlate with differences in trophic morphology, diet, and habitat. Bouton and coworkers (1997) showed that species with different oral morphologies differed in their efficiency to collect as well as process different prey items in the lab. In a complementary field study, both inter- and intraspecific differences in diet and microhabitat were shown to correspond to local and seasonal resource abundance (Bouton et al. 1998). Competition for food was implicated as playing a role in these communities since dietary overlap among species decreased with an increase in fish abundance and a decrease in resource availability. Microhabitat partitioning has also been observed among Lake Malawi's rock-dwelling cichlids (Genner et al. 1999). However, because niche differentiation was not detected among all species pairs, foraging-niche differentiation was deemed insufficient to explain coexistence.

A common theme of these studies is that fine-scale foraging-niche partitioning does occur between rock-dwelling species. Determining the biological consequence of partitioning in foraging space remains a contentious and unresolved issue. At what point is partitioning of foraging-niche sufficient to explain the coexistence among species?

This report adds to the evidence that competition does occur in the rocky community, and that it manifests itself through microhabitat partitioning in the space of foraging habitat. I also bolster the argument that morphology is adaptive, by showing that morphology predicts differences in microhabitat and feeding performance. Finally, this is the first study that demonstrates that partitioning of trophic-niche has the capacity to maintain complex rock-dwelling communities.

I examined foraging habitat, depth distribution, and mode of feeding for six sympatric rock-dwelling species, locally referred to as mbuna. Species were chosen

because they represent four different trophic morphotypes, and employ three distinct modes of feeding. I applied a stepwise, as opposed to an all-inclusive, model of habitat partitioning, which reveals patterns that facilitate the coexistence of species. Results from this study demonstrate that even species of the same morphotypic class, or those that are identical in several ecological respects, may coexist. I contend that the rocky habitat is not a “peaceful condominium,” and that competition for trophic resources has led to the establishment and maintenance of different trophic morphologies.

## Materials and Methods

### Study site

Thumbi West Island is part of Lake Malawi National Park, located in the Southern part of the Lake. Thumbi West Island is 2 km long and 500 m at its widest point. It is located 2.6 km from Domwe Island, 1.5 km from Otter Point, and less than 1 km from Chembe Beach (Figure 1.1). Its shoreline is a continuous rocky habitat with the exception of two small sand/weedy beaches. The rocks around Thumbi West are variable in size and shape.

All observations for this study were performed at the eastern most end of the Island, Mitande Cove. This area is characterized by slabs, boulders, and large, medium and small rocks. The rock-sand interface was approximately 20 m in 2001, with small pockets of sand and weeds occurring below 10 m. Most rocky surfaces were covered with a layer of sediment below 5 m. Between 40 and 50 mbuna species coexist at Mitande cove (Ribbink et al. 1983; personal observations).

### Study species

Six species within three genera were chosen for this study. *Labeotropheus fuelleborni* ('LF') forages almost exclusively from the rocks with a "mowing" mode of feeding. LF's mouth is subterminal, which allows it to crop attached algae from rocks while oriented parallel to the substrate. *Metriaclima zebra* ('MZ') will feed from rocks with a "brushing" mode, and is one of few mbuna species that regularly forages in the

water column with a sucking motion. Four members of the *Pseudotropheus tropheops* complex were chosen for this study: *red cheek* ('RC'), *lilac* ('LIL'), *orange chest* ('OC'), and *intermediate* ('INT'). All *tropheops* species have a steeply descending snout and a slightly subterminal mouth. Members of this species complex tend to feed on attached algae with a "nipping" action, while oriented approximately 45° from the substrate (Ribbink et al. 1983).

### Morphology

*Labeotropheus*, *Metriaclima* and *Tropheops* species show discrete differences in craniofacial profile and mouth orientation. More subtle differences also exist in jaw width, especially among *tropheops* species.

Differences in jaw width among species were assessed by measuring the width of the lower jaw for 120 individuals (n=20 for each species) in animals that were skeletonized by dermestid beetles. Width was measured at the dentigerous (tooth bearing) region of the lower jaw with digital calipers to the nearest 0.01 millimeter, and standardized by standard length. Differences were assessed via a multifactorial ANOVA and a subsequent Tukey's test for pair-wise differences.

### Depth Distribution

100m transects were run parallel to the shoreline down to 25 feet at 5 foot intervals. Using SCUBA, the number of males and females of each species was counted along the transect. Individuals were counted if they were on or up to 5 feet below the transect. Each length was swum three times and the number of fish was averaged and

rounded to the nearest whole number. Depth distribution was shown to violate the assumptions of homoscedasticity and normality; therefore differences in this variable were determined via Kruskal-Wallis nonparametric ANOVA (Sokal and Rohlf, 1981).

### Focal Study

Focal samples were conducted between July 25<sup>th</sup> and August 7<sup>th</sup> 2001. 20 individuals from each species were observed between 1 and 10 meters, along the same 100m stretch of rocky habitat as the depth distribution assay. All focal samples lasted 10 minutes between 7:00 and 16:00.

Bouts of feeding were observed for each fish. One bout was defined as a continuous feeding event that was interrupted by 20 or more seconds of non-feeding, a change of substrate, or a social interaction (i.e., courting, defending territory). Several microhabitat characters were scored for each bout of feeding. Differences among species for each character were assayed via a Kruskal-Wallis Nonparametric ANOVA (Sokal and Rohlf, 1981).

Rock surface size. The length and width of the rocky surface was measured in inches for each bout of feeding. The surface area, rather than the size of the rock itself, was chosen for several reasons. Animals often showed a clear preference for one particular side of a rock (i.e., top instead of bottom). Moreover, when the foraging substrate was a slab, or when many rocks were stacked upon each other, the size of the entire rock was difficult to measure.

**Slope.** The slope of each rocky surface was measured underwater to the nearest 10<sup>th</sup> degree with a protractor. Scores were from 0 to 90, with OH being given to a surface that was an overhang.

**Shelter.** The shelter offered by each rocky surface was estimated as follows. A rocky surface was given a score of one if there were no other perpendicular surfaces within twelve inches of the foraging area, two if there was one other perpendicular surface within twelve inches, three if there were two other surfaces, four if there were three, and five if an animal was effectively foraging in a cave.

**Sediments.** For each bout, the foraging area was described as being either sediment-covered or sediment-free, and the proportion of each was recorded. Note that this variable does not measure whether the rock itself was sediment-covered, just the foraging area (see below).

**Mode of feeding.** Three modes of feeding were identified during focal samples. Biting entailed foraging from the rocky surface. For this character I did not discriminate between LF “mowing,” MZ “brushing,” and *tropheops* “nipping.” Sucking involved taking prey from the water column. Sifting was a discrete action performed exclusively by INT, which entailed taking mouthfuls of sand and sediments and sifting them, presumably through the gill rakers.

## Results

### Morphology

Results from the multifactorial ANOVA revealed three discrete groupings according to lower jaw width (Figure 1.2). LF had the widest jaw relative to body length. RC and OC had very narrow jaws with distributions that could not be distinguished from one another. LIL, INT, and MZ had intermediate jaw widths with distributions that were much closer to RC and OC than to LF.

Species were assigned to one of four morphotypic classes (Figure 1.3), according to craniofacial profile, jaw rotation, and jaw width (as determined by the ANOVA): I) Subterminal/Wide - LF; II) Tropheops/Wide – LIL and INT; III) Tropheops/Narrow – RC and OC; and IV) Terminal – MZ.

### Depth distribution

Results from the Kruskal-Wallis test show a discrete split between species with respect to depth, producing one shallow- and one deep-water group (Figure 1.4). LF, RC and LIL were never found below twenty feet, and were rarely observed below ten feet of water. OC, INT and MZ were rarely observed above 10 feet, and were most abundant between 15 and 25 feet.

### Rock surface size

Species partition their habitat according to foraging surface (Figure 1.5). MZ, RC, LIL, and INT consistently foraged from small surface areas, while LF and OC foraged from larger rocky surfaces.

### Slope

Partitioning in terms of slope seems to recapitulate the depth grouping seen above (Figure 1.6). LF, RC and LIL appear to feed from surfaces with a greater slope than INT, OC and MZ. The deep-water assemblage tended to forage from flat surfaces (i.e., slope = 0) more often than the shallow-water species. Within the shallow-water group, LF fed from surfaces with a greater slope than RC or LIL. This trend is likely due to the observation that LF was one of the only species that consistently fed from rocky overhangs.

### Shelter

Species partition their habitat according to shelter offered by the foraging area (Figure 1.7). Both LF and INT tended to forage from surfaces that were highly sheltered. OC and MZ, on the other hand, fed from highly exposed rocky surfaces. OC fed almost exclusively from fully exposed surfaces. RC and LIL foraged from surfaces that offered intermediate shelter.



## Sediment

Species differed in the proportion of bouts from sediment-free versus sediment-covered substrate (Figure 1.8). INT and MZ seldom foraged from sediment-free rocks. It is noteworthy that OC did not forage from sediment-covered surfaces to the same extent as INT and MZ, in spite of occupying a depth distribution where most rocky surfaces were covered with sediments. Another notable observation is that RC fed more often from sediment-free substrate than did LIL. This is the only variable in which RC and LIL differed.

When considering only the *tropheops* species, differentiation in this microhabitat character corresponds to differences in jaw width. Of the deep-water species, OC has a narrow jaw and INT has a wide jaw. In the shallows, RC has a narrow jaw and LIL has a wide jaw. Thus, jaw width does not predict depth distribution, but rather sedimentation of the foraging habitat.

## Mode of feeding

All species examined spent some time foraging from the substrate with a biting mode of feeding (Figure 1.9). However, INT and MZ fed less from the rocky surface than did the other four species. MZ individuals spent approximately half of their time foraging in the water column. Other species were rarely, if ever, observed feeding in the water column. INT was the only species that fed by sifting sediments through its mouth. INT was also the only species that employed all three modes of feeding.

## Discussion

This study shows that rock-dwelling species partition their habitat in foraging space, and jaw morphology predicts foraging habitat. While other studies have demonstrated this pattern in Lake Victoria (Bouton et al. 1998), Tanganyika (Yamaoka et al. 1986), and Malawi (Genner et al. 1999), the relative role of foraging-niche partitioning in the maintenance of species diversity remains debated.

### Trophic morphology predicts foraging habitat

Species were grouped into four morphotypic classes based on craniofacial profile, jaw rotation and jaw width. LF has an inferior sub-terminal mouth that is both very wide and robust. The orientation of its jaw enables LF to crop attached algae from the substrate (Albertson and Kocher 2001). MZ, on the other hand, has a terminally oriented mouth, and a long lower jaw. MZ's oral jaw apparatus is typical of species that employ a sucking mode of feeding (Liem 1991; Albertson and Kocher 2001). All four *tropheops* species were similar in terms of their slightly sub-terminal jaw rotation, and steep craniofacial profile (Ribbink et al. 1983). However, they differed in the width of their jaws.

RC and OC have very narrow jaws with nearly identical phenotypic distributions, while LIL and INT have decidedly wider jaws. Thus, both the shallow and the deeper habitats have one narrow-mouth and one wide-mouth *tropheops* species. Does this observation relate to the coexistence of *tropheops* at Mitande Cove? The segregation of morphology according to the presence/absence of sediments on the foraging surface suggests that morphological differentiation facilitates co-existence among *tropheops*

species on the basis of foraging efficiency in different micro-habitats (see below). This argument would be supported by observations of the same pattern in other populations of *tropheops*; that is, jaw width segregating according to the degree of sedimentation of foraging area.

### Depth as a foraging micro-habitat

Depth is important in maintaining species diversity. At nearly every rocky habitat throughout Lake Malawi there are discrete groupings of species according to depth (Ribbink et al. 1983). Members of the *Pseudotropheus tropheops* and the *Metriaclima zebra* complex exemplify this trend. For example, *Pseudotropheus tropheops* “red cheek” and “lilac” always occupy the shallows, whereas “gracilior” is most abundant below 15 meters. At many localities *Pseudotropheus tropheops* “orange chest” has a peak distribution at an intermediate depth, between the ranges of deep and shallow water species. Perhaps most striking is the observation that wherever more than one *tropheops* species occurs, one occupies the depths and the other the shallows (Ribbink et al. 1983; Albertson, personal observation). At Mitande Cove, two deep-water and two shallow-water *tropheops* species occur.

In a survey of food resource use, Genner and coworkers (1999) did not detect foraging-niche partitioning among particular mbuna species at Nkhata Bay (~150km north of Mitande Cove). In particular, no differences were observed in the foraging behavior of two *Metriaclima* species, *M. zebra* and *M. callainos*. Genner et al. (1999) concluded that alternatives to niche theory should be considered to explain this coexistence. However, species can afford to have the same foraging behavior if they have distinct spatial (i.e., depth) distributions (Reinthal, 1990). For example, *M. zebra* and *M. callainos* also co-occur at Thumbi West Island where they have distinct depth

distributions (Trendall 1988; Albertson, unpublished data). Thus, *M. zebra* and *M. callainos* may indeed have identical feeding strategies, but they still partition their habitat according to depth. When depth distribution is included in analyses of habitat partitioning, niche theory may suffice.

### Habitat Partitioning

Slope. If depth is an important factor by which species partition their habitat, it should be correlated with other microhabitat characters. The shallow and deep-water groups were reiterated with divergence in slope. Shallow-water species tended to feed from surfaces with a greater slope than deep-water species. This may be an artifact of differences in the physical habitat. The shallows (> 15 feet) were comprised of small and medium sized rocks piled on top of one another, whereas the depths were dominated by large, interspersed rocks and slabs.

Sediments. Because deeper habitats tend to be sediment-covered to a greater extent than wave-washed rocks in the shallows, an intuitive hypothesis would be that deep water species feed from sediment-covered rocks more often than shallow water species. In general, this pattern was observed. INT and MZ tended to forage from sediment-covered surfaces to a greater extent than other species. Certainly, MZ fed more from sediment covered rocks than LF. However, when considering only *tropheops* species a more complex pattern emerges, which may be the result of a novel foraging behavior.

Within the deep-water assemblage, OC fed from sediment-free rocks to the same extent as the shallow water species. Within the shallow water assemblage, sedimentation

is the only variable in which RC and LIL differed. RC and OC were unique among *tropheops* species in that they were regularly seen foraging with species that employed a brushing mode of feeding. Members of the genus *Petrotilapia* forage from the substrate by brushing loose filamentous algae, diatoms and other detritus (e.g. sediments) that have settled onto algal beds. RC and OC would often wait until a *Petrotilapia* species “cleaned” an area from a sediment-covered rock before feeding on the attached algae beneath. Even territorial males tolerated the presence of these heterospecific individuals within their territories, which they vigorously defended from most other fish. In this way, RC and OC could forage from sediment-free substrate even if the rock itself was covered by sediments. Thus, depth is not a faithful predictor of sedimentation of the foraging habitat.

Foraging from sediment-covered substrate is, however, predicted by differences in jaw width among *tropheops* species. In general, *tropheops* species that inhabit sediment-rich areas have wide mouths, such as the aptly named *Pseudotropheus tropheops* “broad mouth” (Ribbink et al. 1983). On the other hand, shallow water species tend to have very narrow, beak-shaped jaws used to “pluck” filamentous algae from the substrate.

A wider mouth may be advantageous for species foraging in sediment-rich areas, because the nutritional value per bite may be less when feeding from sediment-covered surfaces. A wider jaw would serve to increasing the nutritional value per bite by enabling individuals to exact more sustenance. A wider jaw would also allow individuals to take other prey that is more abundant in sediment-rich areas, such as benthic invertebrates. Gut content analyses in both a broad survey over many localities (Ribbink et al. 1983) and a more focused evaluation (Reinthal 1990) showed that *tropheops* species that occur in sediment-rich areas tend to take less attached algae and more benthic invertebrates relative to species that inhabit sediment-free zones.

**Rock size.** OC tended to feed from very large rocky surfaces, boulders and flat slabs. Except for LF, other species clearly preferred smaller surfaces. Again, this preference may be an artifact of habitat composition. However, the low variances associated with mean surface areas for both shallow and deep water species (RC, LIL, INT and MZ) suggests that animals are choosing foraging areas of a particular size.

**Shelter.** Discrete groupings among species were also identified by the degree of shelter offered by the foraging habitat. OC and MZ tended to feed from exposed surfaces, while LF and INT frequently fed in cracks, caves and crevices. LF appears to be very well adapted to its environment. The inferior, subterminal orientation of its mouth allows it to forage from rocky surfaces that are effectively unavailable to species with a terminal mouth. LF can “mow” attached algae from rocks while swimming parallel to the substrate, enabling it to forage within cracks and crevices. LF is also relatively large for a rock-dwelling species. The combination of being large and foraging in a highly sheltered habitat may be in response to elevated predation pressure in the shallows due to the presence of kingfishers and otters.

### **Coexistence of species**

In all, six foraging microhabitats were considered. Species partitioned foraging habitat by at least one, and in most cases three or more characters (Figure 1.10). Previous studies of foraging-niche differentiation among East African rock-dwelling cichlids have considered all microhabitat characters simultaneously. In some cases this approach could explain the co-existence among the species examined (Reinthal 1990; Yamaoka et al.

1986). In other investigations, resource partitioning was recognized as playing a role in the organization of rock-dwelling assemblages, however among certain species partitioning was either “less obvious” (Bouton et al. 1997), or absent (Genner et al. 1999). By including depth distribution as a microhabitat variable, foraging niche partitioning appears to have the capacity to maintain species diversity.

Figure 1.11 demonstrates how interspecific co-existence may be achieved. Species first apportion their habitat according to depth, producing two discrete groups. The deep-water group then separates according to surface size and sedimentation, while the shallow-water species partition with respect to surface size, shelter and slope. The last partitioning event within the deep-water assemblage is coincident with sedimentation and mode of feeding. Both MZ and INT feed from the substrate. But MZ also employs a sucking mode of feeding, while INT actively sifts through the sediments. The last partitioning event within the shallow-water assemblage separates RC and LIL according to sedimentation of the foraging habitat.

Morphological differentiation coincides with all three levels of partitioning. Morphotypic classes I (LF) and IV (MZ) are separated with the first partitioning event. The second level of habitat divergence separates morphotype II (OC) from III (INT) and IV (MZ) in the deep-water group, and morphotype I (LF) from II (RC) and III (LIL) in the shallow group. Finally, morphotypic classes III (INT) and IV (MZ), and II (RC) and III (LIL) are separated with the last round of habitat partitioning. Thus, species of the same morphotypic class are distinguished with respect to foraging-niche microhabitat.

### Revisiting the *peaceful condominium*

Fryer (1959) viewed the cichlid rock-dwelling community as a “peaceful condominium” that violates the Gaussian principle of competitive exclusion. In contrast, my data suggest that competition does exist in the rocky habitat, and that it manifests itself as foraging-habitat partitioning.

Two general conclusions can be drawn from this study. First, depth distribution should be considered in future investigations of habitat partitioning. Species clearly partition their habitat with respect to depth. Moreover, recent evidence suggests that depth has the capacity to restrict geneflow (Kellogg and Jordan, personal communication). I also contend that a step-wise, rather than all-inclusive, model should be considered in future discussions of the maintenance of species diversity. Since several foraging behaviors and habitats can (and likely will) be correlated with one another, not all should be given the same weight. If species partition foraging-habitat in one or several key ecological characters, they can afford to be identical in others.

This study does not offer a definitive statement on foraging-niche partitioning among rock-dwelling cichlids. I examined a subset of the species present at Mitande Cove over a short period. Seasonal and temporal fluctuations have been documented among species with respect to trophic biology (Bouton et al 1997). Future studies should endeavor to assay a greater number of species over a longer period of time. Fieldwork by Bouton and coworkers (1997) in Lake Victoria provides an excellent model for future studies.

Another future direction should include a more comprehensive morphological assessment (such as in Albertson and Kocher, 2001) of *tropheops* species at Thumbi West Island. It will be important to determine whether morphological divergence among species is the result of phylogenetic history or adaptation. There is some evidence that



divergence in jaw width is not a consequence of phylogeny among *tropheops*. At a rocky habitat less than 20 km from Mitande Cove, three *tropheops* species co-occur, “red cheek”, “orange chest” and “gracilior.” *Pseudotropheus tropheops* “gracilior” typically occurs in sediment-rich areas, and is characterized by a wide mouth. A cladistic analysis using molecular markers united “orange chest” and “gracilior” (NJ algorithm - bootstrap value of 100) to the exclusion of “red cheek,” which was positioned sister to this grouping (Albertson et al. 1999). If mouth width among *tropheops* species was the result of phylogenetic history, small-mouthed species should group together. The occurrence of just the opposite merits an investigation of alternative hypotheses.

The phylogenetic relationship among other wide- and narrow-mouthed *tropheops* species should be investigated. Moreover, jaw width should be examined in the same species at multiple localities to determine whether this character varies in response to the physical habitat, or to the presence/absence of other *tropheops* competitors. In other words, can character displacement be detected? The answer to this and related questions would go a long way towards firmly putting to rest the question of whether competition for trophic resources has played a role in the adaptive radiation of this group of fish.

#### Acknowledgements

This work was supported by a NSF grant (IBN #9905127) awarded to T. D. Kocher. I thank the Malawi Government and the University of Malawi for the opportunity to conduct fieldwork in Africa. This chapter is dedicated to the memory of Amos Chamabala, whose help in collecting and identifying species was invaluable. Amos was a teacher whose experience and knowledge of Lake Malawi’s animal fauna was unsurpassed; he will be missed.

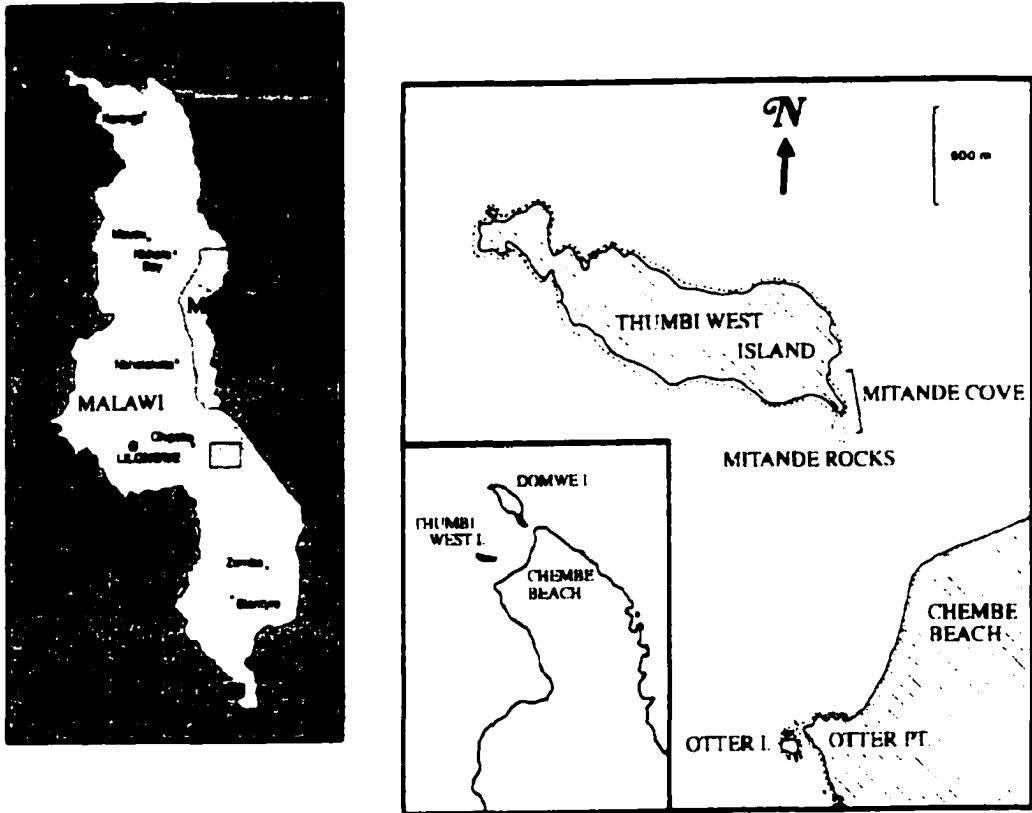
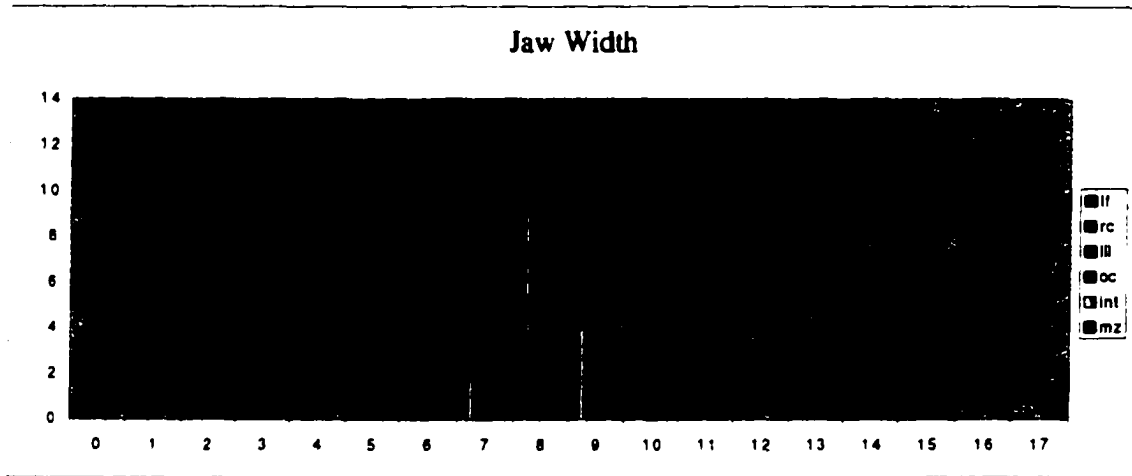


**Figure 1.1**

Map of Thumbi West Island, Lake Malawi. The collection site (mitande cove) is on the East side of the island.

**Figure 1.2**

Results from the multifactorial ANOVA for jaw width. a. Histogram of the ratio between jaw width and standard body length. The x-axis is frequency. The y-axis is standard deviation units recorded as average between-group standard deviations. b. Results of the ANOVA and Tukey's multiple comparison test. c. Graphical depiction of differences in jaw width among species. Bars indicate 95% confidence intervals.



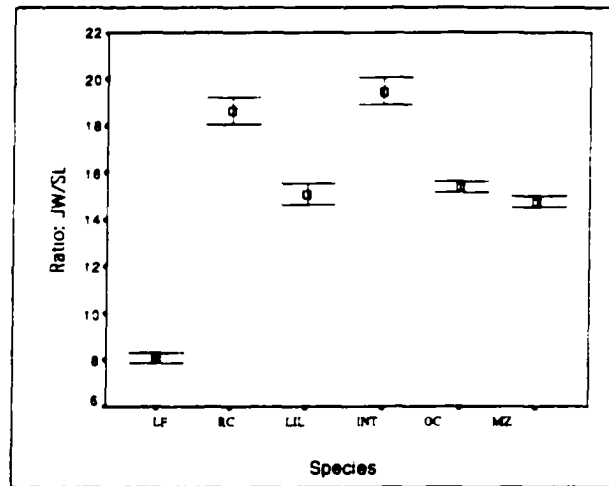
b. ANOVA

	Sum of Squares	df	Mean Square	F	Sig.
Between Groups	1654.387	5	328.861	403.668	< .001
Within Groups	90.84	114	0.798		
Total	1745.227	119			

Multiple Comparisons  
 Dependent Variable: JW  
 Tukey HSD

(i) Species	(j) Species	Mean Difference (i-j)	Sig.
LF	RC	-10.6686	< .001
	LL	-7.0108	< .001
	OC	-11.3982	< .001
	INT	-7.3271	< .001
	MZ	0.8288	< .001
RC	LF	10.6686	< .001
	LL	3.6677	< .001
	OC	-0.8308	0.048
	INT	3.2416	< .001
	MZ	-3.8793	< .001
LL	LF	7.0108	< .001
	RC	-3.6677	< .001
	OC	-4.3882	< .001
	INT	-0.3181	0.068
	MZ	0.3127	0.871
OC	LF	11.3982	< .001
	RC	0.8308	0.048
	LL	4.3882	< .001
	INT	4.0721	< .001
	MZ	-4.7008	< .001
INT	LF	7.3271	< .001
	RC	-3.2416	< .001
	LL	0.3181	0.068
	OC	-4.0721	< .001
	MZ	0.8288	0.232
MZ	LF	0.8983	< .001
	RC	-3.8793	< .001
	LL	-0.3127	0.871
	OC	-4.7008	< .001
	INT	-0.8288	0.232

c.



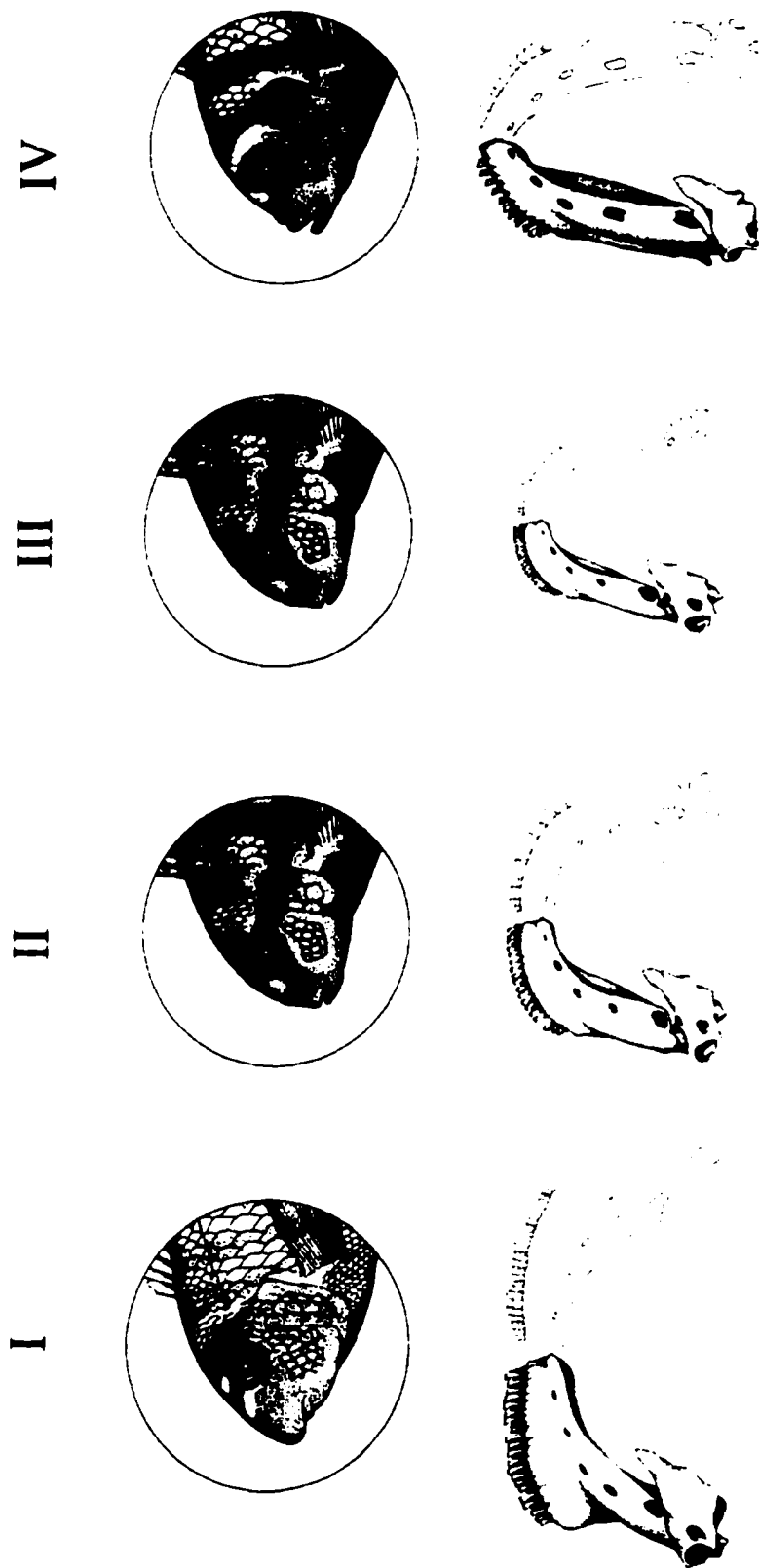


**Figure 1.3**  
 Illustration of morphotypic classes, as defined by craniofacial profile and jaw width.

**Figure 1.4**

a. Results of Kruskal-Wallis Nonparametric ANOVA for depth distribution. b. Graphical depiction of differences in depth distribution. Bars indicate 95% confidence intervals.

a. Kruskal-Wallis Test - Nonparametric ANOVA

Depth	SPP	N	Mean Rank
DEPTH	LF	52	69.07
	RC	35	86.43
	LIL	17	66.18
	INT	61	244.7
	OC	66	219.03
	MZ	115	199.19
Total		346	

Test Statistics	
Chi-Square	159.917
df	5
Asymp. Sig.	.0
Kruskal-Wallis Test	
Grouping Variable: SPP	

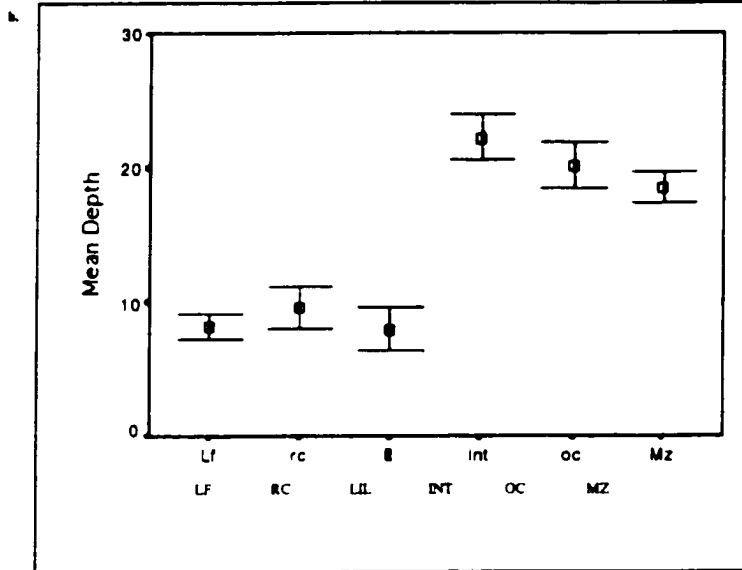


**Figure 1.5**

a. Results of Kruskal-Wallis Nonparametric ANOVA for foraging area. b. Graphical depiction of differences in foraging area. Bars indicate 95% confidence intervals.

a. Kruskal-Wallis Test - Nonparametric ANOVA

Rank	SPP	N	Mean Rank
SIZE	LF	39	362.28
	RC	34	184.44
	LIL	61	195.43
	INT	37	153.78
	OC	36	343.86
	MZ	60	191.99
	Total	307	

Test Statistics	SIZE
Chi-Square	69.426
df	5
Asymp. Sig.	.0
Kruskal-Wallis Test	
Grouping Variable: SPP	

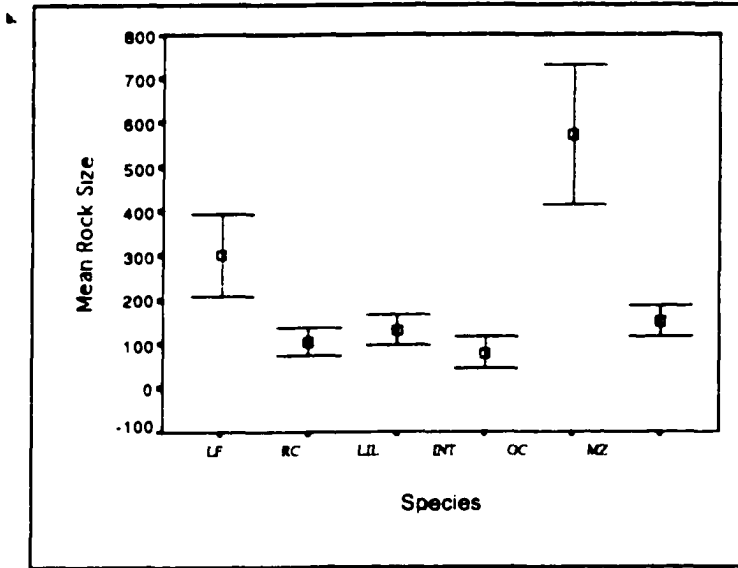
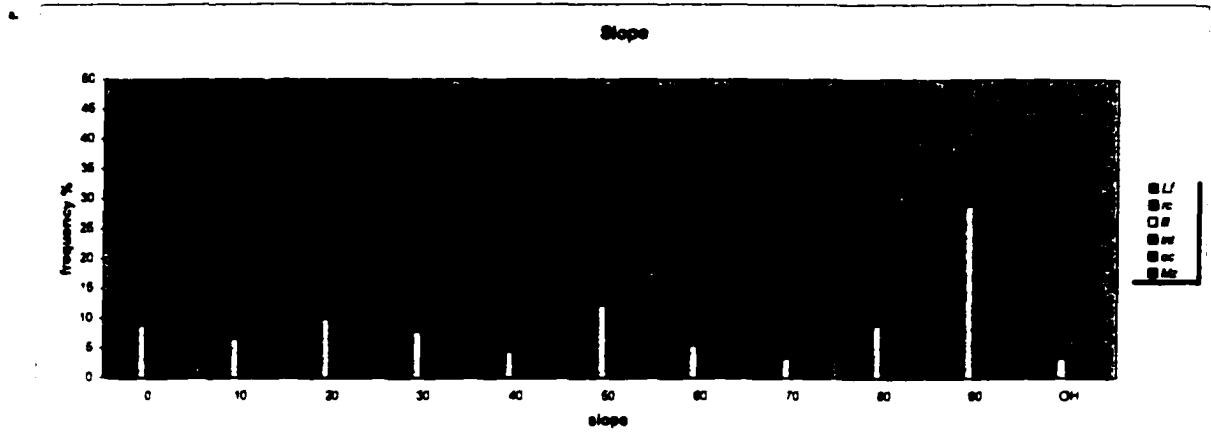


**Figure 1.6**

a. Histogram of the frequency that species foraged from surfaces with difference slopes. Slope was recorded in 10° intervals, with OH representing an over-hang. b. Results of Kruskal-Wallis Nonparametric ANOVA for slope. c. Graphical depiction of differences in slope. Bars indicate 95% confidence intervals.



b. Kruskal-Wallis Test - Nonparametric ANOVA

Ranks				Test Statistics	
SLOPE	SPP	N	Mean Rank	Chi-Square	SLOPE
	LF	100	390.59	103.834	
	RC	83	313.89	5	
	LIL	90	312.47	Asymp. Sig.	.0
	INT	75	199.19	Kruskal-Wallis Test	
	OC	70	229.94	Grouping Variable: SPP	
	MZ	67	231.52		
	Total	485			

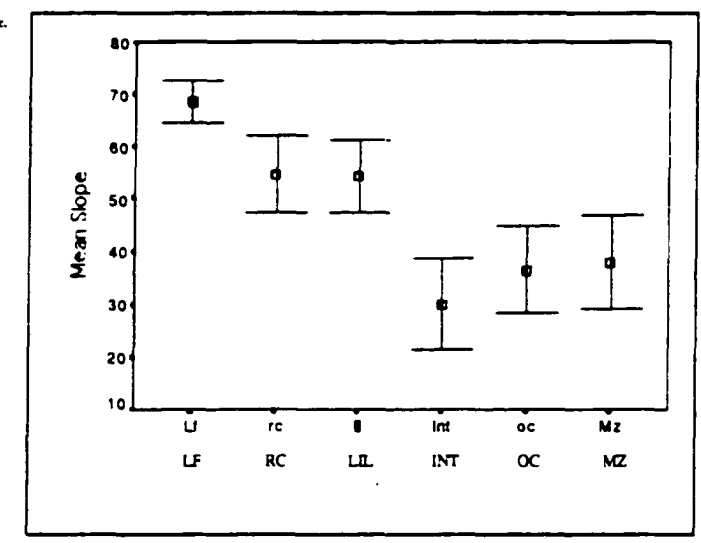


**Figure 1.7**

a. Results of Kruskal-Wallis Nonparametric ANOVA for shelter offered by foraging area. b. Graphical depiction of differences in shelter. Bars indicate 95% confidence intervals.

a. Kruskal-Wallis Test - Nonparametric ANOVA

Ranks			
SHEL TER	SPP	N	Mean Rank
	LF	51	291.57
	RC	84	212.46
	LIL	80	208.06
	INT	75	206.25
	OC	70	110.05
	MZ	52	159.83
	Total	424	

Test Statistics	
	SHEL TER
Chi-Square	126.309
df	5
Asymp. Sig.	.0
Kruskal-Wallis Test	
Grouping Variable: SPP	

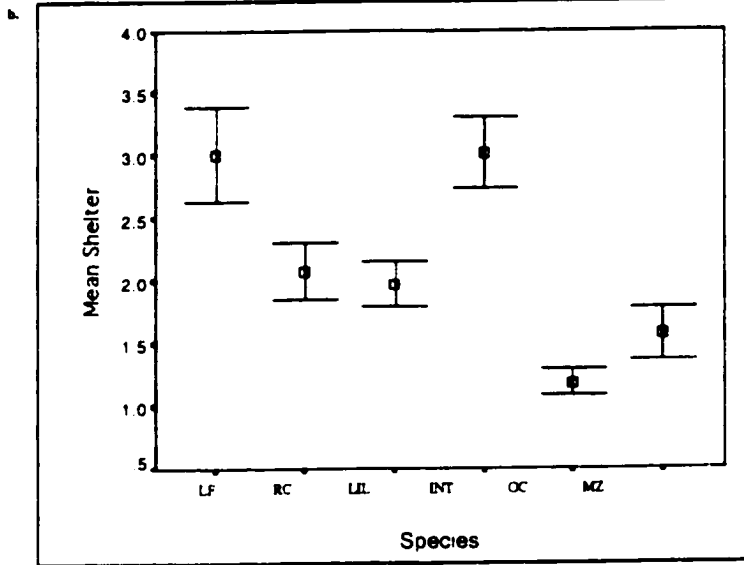




**Figure 1.8**

a. Results of Kruskal-Wallis Nonparametric ANOVA for the proportion of sediment free bouts of feeding. b. Graphical depiction of differences in bouts. Bars indicate 95% confidence intervals.

a. Kruskal-Wallis Test - Nonparametric ANOVA

Species	SPP	N	Mean Rank
Sediments	LF	20	80.94
	RC	20	82.93
	LIL	20	64.03
	INT	20	22.8
	OC	20	64.4
	MZ	8	17.77
Total		108	

Test Statistics	Sediments
Chi-Square	66.237
df	5
Asymp. Sig.	.0
Kruskal-Wallis Test	
Grouping Variable: SPP	

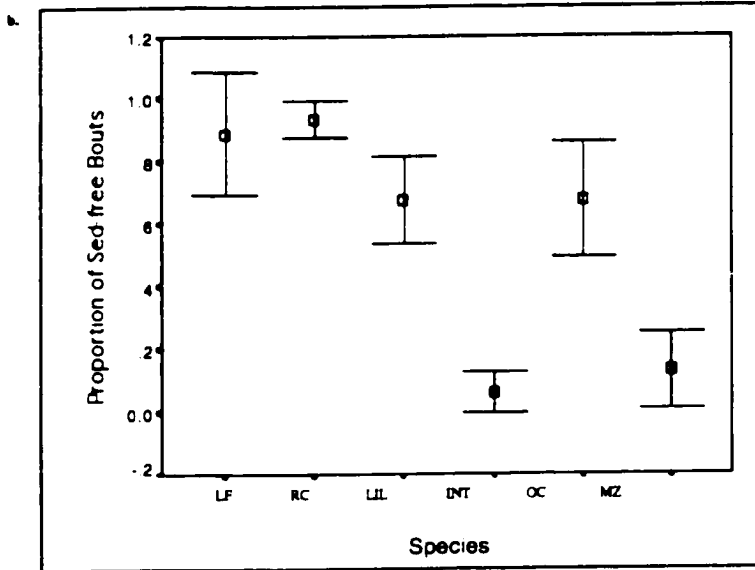


**Figure 1.9**

a. Results of Kruskal-Wallis Nonparametric ANOVA for differences among three modes of feeding: biting, sucking, and sifting. b. Histogram depicting differences in feeding mode. Stars indicate significant ( $p < 0.05$ ) differences among species.

**a. Kruskal-Wallis Test - Nonparametric ANOVA**

Ranks			
	SPP	N	Mean Rank
BITE	LF	100	247.0
	RC	84	247.0
	LIL	89	247.0
	INT	55	201.2
	OC	70	247.0
	MZ	60	155.4
	Total	458	
SUCK	LF	100	205.58
	RC	84	201.00
	LIL	89	201.00
	INT	55	209.33
	OC	70	204.27
	MZ	60	199.47
	Total	458	
SIFT	LF	100	214.30
	RC	84	214.30
	LIL	89	214.30
	INT	55	339.41
	OC	70	214.30
	MZ	60	214.30
	Total	458	

**Test Statistics**

BITE	
Chi-Square	129.009
df	5
Asymp. Sig.	.0

Kruskal-Wallis Test  
Grouping Variable: SPP

SUCK	
Chi-Square	348.887
df	5
Asymp. Sig.	.0

Kruskal-Wallis Test  
Grouping Variable: SPP

SIFT	
Chi-Square	348.887
df	5
Asymp. Sig.	.0

Kruskal-Wallis Test  
Grouping Variable: SPP

**b.**

**Feeding mode**

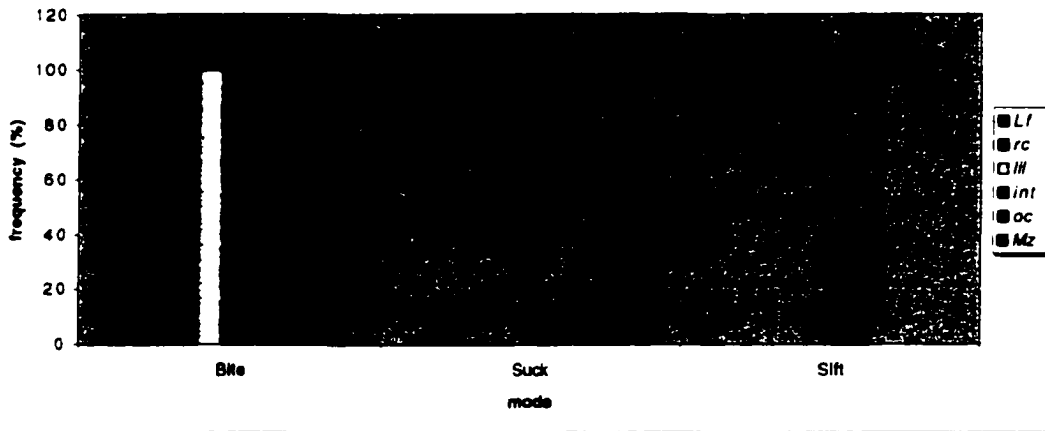
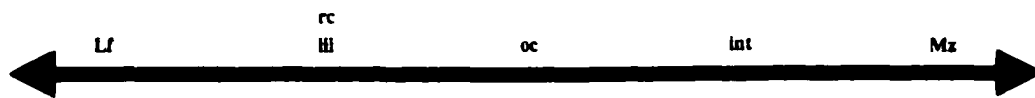


**Figure 1.10**  
 Summary of foraging microhabitat partitioning. Pairwise comparison of the microhabitat characteristics in which species differ.

	<i>L. fulleborni</i>	"red cheek"	"lilac"	"intermediate"	"orange chest"	<i>M. zebra</i>
<i>L. fulleborni</i>						
<i>Tropheops</i> "red cheek"	rock size slope shelter					
<i>Tropheops</i> "lilac"	rock size slope shelter	sediment				
<i>Tropheops</i> "intermediate"	depth rock size sediment mode slope	depth sediment mode slope shelter	depth sediment mode slope shelter			
<i>Tropheops</i> "orange chest"	depth rock size slope shelter	depth rock size slope shelter	depth rock size slope shelter	rock size sediment mode shelter		
<i>M. zebra</i>	depth rock size sediment mode slope shelter	depth sediment mode slope shelter	depth sediment mode slope shelter	depth mode shelter	rock size sediment mode shelter	



Species approximate positions in dimension of foraging habitat

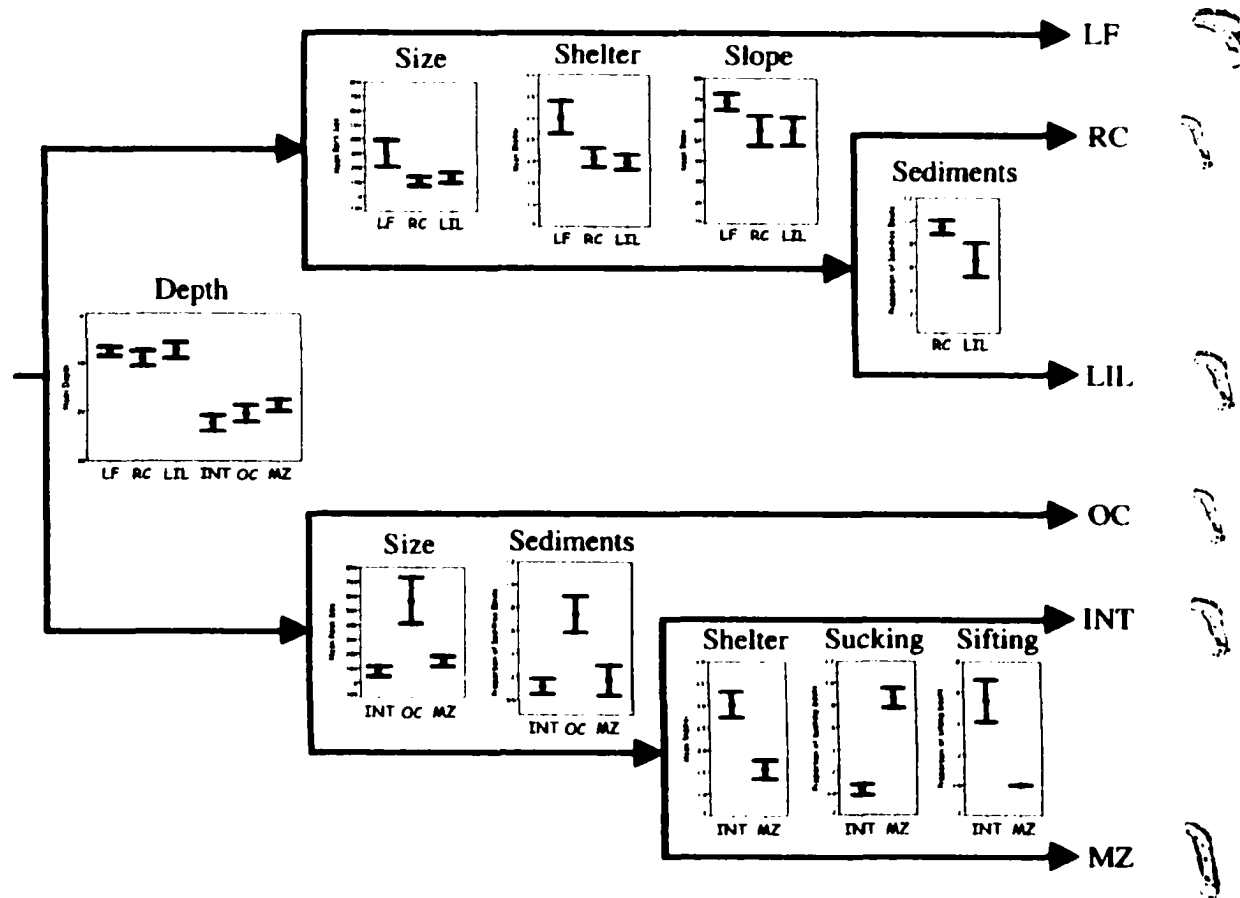


**Figure 1.11**

Proposed mechanism by which species partition their environment. Morphological differences among species are illustrated via jaw width. Both the deep and shallow water groups have one narrow and one wide mouthed *tropheops* species. This morphological difference coincides with sedimentation of the foraging habitat. Note, this is not a phylogenetic reconstruction of species at Thumbi West Island. Rather, it is a mechanism through which species may partition a locality as it is colonized.

## CHAPTER 2

### ASSESSING MORPHOLOGICAL DIFFERENCES IN AN ADAPTIVE TRAIT: A LANDMARK-BASED MORPHOMETRIC APPROACH

#### Abstract

East African Cichlid fishes have evolved a stunning array of oral jaw morphologies. To better understand the adaptive evolution of this trait, I performed a morphological analysis of the jaws of two closely related species from Lake Malawi which have very different modes of feeding. *Labeotropheus fuelleborni* forages along the substrate with a 'biting' mode of feeding, while *Metriaclima zebra* feeds in the water column with a 'sucking' mode. I analyzed each of the four skeletal elements that make up the oral jaws: the dentary, articular, premaxilla, and maxilla. In addition, I performed the same analysis on the neurocranium, an element closely associated with the oral jaws. I used the thin-plate spline method to quantify morphological differences, which allowed us to relate our results to the functional biology of the species. I find many aspects of shape change that relate directly to the functional design of the cichlid head. The same series of measurements was made on hybrids between *Labeotropheus* and *Metriaclima*.

For every character, hybrid progeny are statistically different from both parental species. These results suggest an additive mode of action of the alleles responsible for these phenotypes.

## Introduction

The cichlid fishes of East Africa are a spectacular example of evolutionary radiation. Each of the three large lakes in the region (Victoria, Tanganyika and Malawi) contains a 'flock' of several hundred cichlid species (Fryer and Iles 1972; Echelle and Kornfield 1984). Molecular and geological studies suggest that these radiations are extremely recent (Greenwood 1974; Owen et al. 1990; Meyer 1993; Kocher et al. 1995; Seehausen et al. 1997). For instance, Lake Malawi is less than 1MY old (Meyer et al. 1990), but contains a flock of well over 500 species (Ribbink et al., 1983), and much of this radiation probably occurred within the past several thousand years (Owen et al. 1990).

The morphological diversification among Lake Malawi cichlids is of a magnitude normally found only among families of teleosts (Greenwood 1974). Key to their success has been the diversification of the oral jaw apparatus, which has allowed them to evolve many different specialized modes of feeding.

In this study I assess shape differences of the individual skeletal elements of the oral jaws in two rock-dwelling cichlids from Lake Malawi, *Labeotropheus fuelleborni* and *Metriaclima zebra*, and their F<sub>1</sub> hybrid progeny. I employ geometric morphometrics, which gives us tremendous power to discriminate overall shape difference between these three groups. Moreover, a geometric approach maintains a closer relationship to true biological form than do simple linear measurements between landmarks.

## Functional morphology and adaptive radiation

There is a large body of literature devoted to interpreting the functional morphology of the cichlid feeding apparatus. Three major modes of feeding have been identified: sucking, biting, and ram feeding. These three modes are easily predicted from the functional design of the cichlid head (Liem 1991). For instance, the most efficient design for suction feeding is a cone-shaped buccal cavity and a highly protrusible upper jaw that allows for rapid expansion of the buccal volume. On the other hand, streamlined predators have a more cylindrical buccal cavity that cannot produce much suction, but are optimized for the pursuit and overtaking of prey, also known as ram feeding (Liem 1991). Biting fish require shifts in anatomical points on the premaxilla, maxilla, and mandible to increase the biting force (Otten 1983).

Most cichlids employ more than one strategy of prey capture, and possess skulls of intermediate design that will allow them to feed on a variety of foods. For example, *Metriaclima zebra* has been characterized as a 'biter' (Witte 1984), but will often employ a 'sucking' mode when feeding on plankton in the water column (McKaye and Marsh 1983; Ribbink et al 1983; and Reinthal 1990). Rather than viewing individual species as specialists, I should consider the balance each has struck among conflicting structural demands (Barel 1983; Liem 1980).

## Geometric morphometrics

A geometric approach to shape analysis is based on landmark data (i.e. anatomical points inferred to be homologous between specimens). Landmark positions are recorded



in terms of a Cartesian coordinate system, such that each point's (x, y) position can be plotted on a graph.

Geometric morphometrics offer several advantages over traditional morphometrics. First, a landmark-based approach emphasizes the geometry of a given structure, allowing shape change to be reported relative to other structures. Moreover, geometric morphometric results are basis-invariant. That is, results do not depend on arbitrary choices, such as the selection of shape variables or the baseline to be used. Finally, results can be reported via pictorial representations of the structure/organism, rather than just tables of numerical coefficients (Rohlf and Marcus 1993).

Our approach to shape analysis of the cichlid head is unique in several ways. I focus on individual skeletal elements, which allows us to examine aspects of morphology that might otherwise be hidden or confounded when viewing the articulated skeleton or external morphology. I also employ a geometric approach rather than traditional methods of shape analysis, which provides a more precise biological representation of shape differences. The union of these two approaches should offer a more comprehensive understanding of the differences in oral jaw morphology among species.

## Materials and Methods

### Animals and husbandry

Lake Malawi rock-dwelling cichlids (mbuna) are classified into 13 genera that differ primarily in trophic morphology (Moran et al. 1994). *Metriaclima zebra* and *Labeotropheus fuelleborni* (Figure 2.1), referred to as MZ and LF from here on, are two mbuna species which have evolved very different oral jaw morphologies.

MZ is characterized by a moderately sloped head, a terminal isognathus mouth, and a swollen, horizontally directed vomer (Stauffer et al. 1997). When feeding, MZ typically combs loose diatoms from filamentous algae beds while oriented perpendicular to the substrate. This species will also leave its territory in order to feed on plankton in the water column, where it uses a suction mode of feeding (McKaye and Marsh 1983; Ribbink et al. 1983; and Reinthal 1990).

LF has a large fleshy snout and an inferior-subterminal mouth that it uses to crop algae from rocks while oriented nearly parallel to the substrate (Ribbink et al. 1983). Gut analysis and direct observation reveal that the primary diet of LF is attached algae, removed from the rock surface using a biting mode of feeding (Ribbink et al. 1983; and Reinthal 1990). The orientation of its mouth allows LF to forage in shallow water where surge is a prominent part of the environment, and heterospecific competition is reduced (Ribbink et al. 1983).

Parental specimens used in this study were lab-reared F<sub>1</sub> animals generated from wild-caught stock. Hybridization, which has been observed to occur among cichlids

under no-choice conditions (Loiselle 1971; Crapon de Caprona and Fritzsich 1984; McElroy and Kornfield 1993; personal observation), was achieved by crossing male LF with female MZ in 500 gallon pools containing one male for every four or five females.

All mbuna species are mouth-brooders. Brooding females were transferred to 10-gallon tanks to incubate their clutch. Incubation in the lab averaged about three weeks for both species. Females were removed from the tank after they released their young. Fry were reared in 10-gallon tanks for approximately three months. They were then transferred to 50-gallon tanks for an additional two to three months. Finally, families were moved to 500-gallon pools where they were allowed to grow to sexual maturity (an additional six to eight months). Since the primary diet of these species in the wild is algae (Reinthal 1990), all specimens were reared on high quality spirulina flake food (Aquatic Ecosystems, FL). A diet of flake food was chosen to minimize the functional demands on the trophic apparatus.

#### Preparation of specimens

Animals were collected no earlier than 12 months of age, and more typically at 18 months. 50 specimens were used in this study, 15 of each parental species and 20 F<sub>1</sub> hybrids. Animals were sacrificed with MS222 in accord with a protocol approved by the University of New Hampshire ACUC. Specimens were then prepared for morphometric analysis using dermestid beetles, which cleaned and disarticulated skeletal elements of the head. Afterwards, elements were bleached with 10% H<sub>2</sub>O<sub>2</sub>.

Images of individual elements were captured using a SPOT digital camera (Diagnostic Instruments, Inc. ) mounted on a Zeiss SV11 dissecting scope. Images were

imported into NIH Image (version 2.1), and landmark positions scored as (x,y) coordinates. Descriptions of landmarks are found in Table 2.1.

### Superimposition of landmark data

Superimposition of landmark data was performed using a Procrustes generalized least-squares fit (GLSF) algorithm (Gower 1975; and Rohlf and Slice 1990) in Morphometrika 7.0 (Walker 1999). A least-squares approach will superimpose configurations so that the sum of squared distances between corresponding landmarks is minimized. This is achieved by scaling, translating, and rotating specimens with respect to a mean consensus configuration. A potential disadvantage to this approach arises when the difference between forms is localized to one or few landmarks. In this situation, GLSF may distribute localized variance over multiple landmarks, making the way variance is allocated to individual landmarks an artifact of the method. Procrustes generalized resistant-fit (GRF) superimposition compensates for this problem by using a more complex, and computationally expensive, approach of regression using repeated medians (Rohlf and Slice 1990). Since LF and MZ differ dramatically over the entire structure for most elements, I used GLSF rather than the GRF algorithm. The only possible exception to this trend is found in the neurocranium, where LF and MZ differ most dramatically in the anterior region of the skull. I performed both GLSF and GRF superimposition for this structure and found no difference in the results (not shown).

### Thin-plate spline analysis

Thin-plate spline (TPS) analysis was performed in Morphometrika 7.0 (Walker, 1999). The TPS technique rigorously implements D'Arcy Thompson's concept of Cartesian grid deformations (Thompson 1917). A thorough description of the technique may be found in Bookstein (1989, 1991). In short, TPS models the form of an infinitely thin metal plate that is constrained at some combination of points but is otherwise free to adopt the target form in a way that minimizes bending energy. In morphometrics, this interpolation is applied to a Cartesian coordinate system where deformation grids are constructed from two landmark configurations (Bookstein 1991).

Thin-plate spline analysis is valuable for several reasons. First, the TPS technique is independent of any anatomical frame of reference. That is, the position of each landmark is evaluated relative to all other landmarks rather than to a single point. This method also allows for the objective generation of deformation grids. Finally, the total deformation of the thin-plate spline can be decomposed into geometrically orthogonal components based on scale (Yaroch 1996; Rohlf and Marcus 1993). These components (partial warps) can be localized to describe precisely what aspects of shape are different. Partial warp scores are also the shape variables used in multivariate analyses.

### Multivariate analysis of TPS data

For each skeletal element a discriminant function analysis was performed using SPSS (version 6.0 for Macintosh) on all shape variables (partial warp scores, including the uniform component). Results from this test were used to assess group differences for

each skeletal element, and to estimate the magnitude of shape difference between the parental species. Since the first Canonical Variate axis best represents interspecific shape differences, results are only presented for CV1.

To estimate the relative contribution of each shape variable in the discriminant function analysis, a multivariate regression was performed for each skeletal element using TPSregr (Rohlf 1999). Regression analysis was used to assess the relationship between shape variables and scores on the Canonical Variate axis. In terms of partial warps, the model follows:

$$\text{Shape (PW1x, PW1y, PW2x, PW2y, ...PW0x, PW0y)} = \text{Constant} + (m)\text{CV1 score}$$

Furthermore, TPSregr allows for the deformation of shape, as interpreted by each canonical variate axis, to be visualized as a deformation grid or associated vector displacements, allowing for a more exacting biological interpretation of the discriminant function analysis.

## Results

A multivariate analysis of variance (MANOVA) showed that mean differences among LF, MZ, and F1 along the CV axis were unlikely due to chance, Wilk's  $\Lambda = .00433$ ,  $F(12, 72) = 85.2$ ,  $p < 0.0001$ . Likewise, univariate F-tests for each element revealed significant mean differences among groups ( $p < 0.0001$  in every case).

Disarticulated skeletal elements are shown in Figures 2.2 – 2.7. Below, results are described both qualitatively as landmark variation after superimposition, and quantitatively as deformations after the multivariate analysis of shape variables (Figures 2.9 – 2.14). Table 2.2 lists: 1) the variation explained by the first canonical variate axis; 2) the number of standard deviation units which separate the parental species along CV1; and 3) the relationships between shape variables and CV1.

### Lower Jaw (lateral view)

After GLSF superimposition (Figure 2.8b), landmark variation around the consensus configuration is distributed over most landmarks in the lateral view of the lower jaw. However, variation around landmarks one and four describes most interspecific difference.

The lower jaw in teleosts is composed of two ontogenetically distinct elements. The anterior portion that bears the teeth is the dentary, while the more posterior region that articulates with the suspensorium is the articular. These two bones are both

developmentally and functionally discrete. Differences revealed by the first canonical variate axis (Figure 2.8c and d) deal with relative shape differences between these two elements. In MZ, the height of the articular is reduced relative to the length of the dentary, which is dramatically elongated. There is also a pronounced and localized lengthening of the ventral process of the suspensorial articulation facet relative to the rest of the articular. On the other hand, LF is characterized by a dramatic increase in the height of the articular relative to a pronounced shortening of the dentary.

#### Lower Jaw (ventral view)

Landmark variation is distributed over landmarks one, two, and five in the ventral view of the lower jaw (Figure 2.9b). Variation around landmarks one and two, which represent the mandibular symphysis and the lateral-most point of the dentary, captures variation in the width of the dentary. Along the antero-posterior axis, most variation is observed at landmark five, which is the rostral tip of the couler process.

The first canonical variate axis characterizes equivalent aspects of interspecific shape change (Figure 2.9c and d). The major aspect of shape change deals with the width of the lower jaw. There is a dramatic increase in the width of the lower jaw in LF relative to MZ. However, other more subtle aspects of shape difference are revealed by the analysis. For example, the most extreme difference in jaw width is localized to the dentary, with difference in the width of the articular being less pronounced. In LF, an increase in the width of the dentary is accompanied by a relative lengthening of the couler region of the articular. There is also a pronounced and localized shortening of the ventral process of the suspensorial articulation facet in LF. In MZ, the width of the



dentary is reduced, the ventral process of the suspensorial articulation facet is elongated, and the couler process is shortened.

### **Maxilla**

After GLSF superimposition (Figure 2.10b), landmark variation is distributed in the maxilla over landmarks one, two, and three. Most of this variation is along the medio-lateral axis (the palatine process is taken as lying along the medio-lateral axis). Landmarks two and three lie on opposite ends of this process. Variation in landmark two is slightly skewed towards the antero-posterior axis. This variation captures not only the length of the palatine process, but also the bending of the entire maxilla. Little variation is observed at landmark four.

The first canonical variate axis emphasizes two aspects of shape difference in the maxilla (Figure 2.10c and d). The first deals with the length of the palatine process, and the second with the curvature of the entire maxilla. In MZ, there is a shortening of the palatine process relative to the length of the entire element, while in LF the same process is dramatically elongated. In addition, the maxilla is virtually straight in MZ, as opposed to LF where it is distinctly bent.

### **Premaxilla**

Landmark variation around the consensus configuration is distributed over most landmarks in the premaxilla (Figure 2.11b). There is considerable variation around

landmarks one and five along the antero-posterior axis, reflecting the length of the dentigerous arm. Variation around landmark two is largely along the dorso-ventral axis, but it is also slightly skewed toward the antero-posterior axis. This pattern captures both the length of the ascending arm, and the angle formed by the two arms of the premaxilla. There is also variation along the dorso-ventral axis at landmarks three and four associated with the height of the maxillad spine.

The deformation of the premaxilla along CV1 emphasizes several aspects of interspecific shape change (Figure 2.11c and d). In MZ, the rostral portion of the ascending arm is elongated relative to the more distal region of the same arm, with localized shortening of both the ascending and maxillad spines. The dentigerous (tooth bearing) arm is also elongated in MZ relative to the ascending arm. In contrast, the rostral portion of the ascending arm is shortened in LF relative to the distal portion, and both the ascending and maxillad spines are elongated. The dentigerous arm in LF is also shortened relative to the ascending arm. Finally, the angle formed by the two arms of the premaxilla is obtuse in LF and acute in MZ.

### Neurocranium

Landmark variation (Figure 2.12b) reveals three aspects of shape variation in the neurocranium. Change in vomer rotation is captured by variation at landmark one. Difference in the length of the preorbital region is identified by variation at landmark two. Finally, variation in the height of the supraoccipital crest is reflected by variation at landmark four.

Deformation of the neurocranium (lateral) along CV1 captures two aspects of interspecific shape change (Figure 2.12c and d). The first is vomerine position, and the second preorbital length. LF has an expanded preorbital area relative to the rest of the skull, while in MZ this area is more attenuated. There is also a horizontal rotation of the vomerine process relative to the rest of the ethmoidal region of the skull in MZ. In LF, the vomerine process is rotated ventrally relative to the ethmoidal region. Deformation as a function of CV1 does not implicate height of the supraoccipital crest as a major source of interspecific shape difference.

### Vomer

After GLSF superimposition (Figure 2.13b), landmark variation occurs along both the antero-posterior and medio-lateral axis of the vomer. Variation at landmark two reflects shape change in the width of the vomer, while variation at landmark one identifies change in the length of the vomer. The relative distance between landmarks two and three also varies. This aspect of shape change captures the distance between the vomerine notch (landmark two) and the vomerine palatinad articulation facet (landmark three). There is little variation at landmark four.

The deformation of the vomer as a function of CV1 (Figure 2.13c and d) shows that LF and MZ differ in terms of both the width and the roundness of the vomer. The vomer is shown to be wider in MZ than LF. Moreover, in MZ the vomer is expanded (laterally) at the vomerine notch relative to the palatinad articulation facet, while in LF there is no difference in width between these two structures. Thus, interspecific change in the width of the vomer occurs at the vomerine notch, not the palatinad articulation

process. Finally, **MZ** has a blunt vomerine process relative to **LF**, which has a more rounded vomer.

## Discussion

During the early radiation of Lake Malawi's cichlids, an important functional divergence probably occurred between the three basic modes of feeding – biting, sucking, and ram-feeding (Albertson, et al. 1999). This same trend has been observed repeatedly in many fishes from post-glacial lakes, including stickleback (*Gasterosteus aculeatus* complex), whitefish (*Coregonus* complex), and arctic charr (*Salvelinus alpinus* complex) (reviewed in Schluter and McPhail 1993). I chose MZ and LF because they are closely related species which lie on opposite ends of the biting/sucking continuum. I find many aspects of interspecific shape difference that relate directly to the functional biology of these organisms. Several morphological characters have been identified in the cichlid head which predict feeding performance (Otten 1983; Liem 1991). A subset of these, which pertain to MZ and LF, are listed in Table 2.3, and described in greater detail below.

### Form and Function

One important difference between MZ and LF involves the ascending process of the articular. This process is where the second adductor mandibulae inserts, and is an important lever in the action of jaw adduction (Otten 1983). LF has a substantially higher articular process, suggesting greater force transmission of the adductor mandibulae and therefore a stronger bite. The height of this lever also has major consequences in the

speed of jaw rotation. The implications of a shorter articular process in MZ is that this species has a faster jaw closing motion (greater angular rotation).

Both the width and length of the lower jaw differ dramatically between LF and MZ. In LF the jaw is short, wide, and U-shaped. In MZ it is narrow, elongated, and V-shaped. The U-shaped lower jaw of LF is part of a square-shaped buccal cavity, better for taking large bites of algae. In fact, LF has developed pronounced lateral expansions (\*\* in Figures. 2.3 & 2.4), just dorsal to the reentrant angle of the articular, which bear teeth and dramatically expand biting surface area. The V-shaped lower jaw of MZ is part of a more attenuated buccal cavity, better for sucking plankton from the water column.

These species also differ in the shape of the suspensoriad articulation facet, which is where the lower jaw articulates with the suspensorium. In MZ the ventral lip of this facet is long, while in LF it is quite short. Since MZ feeds with a sucking action, this long ventral process may be used to support the lower jaw during mouth opening.

The maxilla is more robust in LF than in MZ, presumably because it endures greater force during biting. The first adductor mandibulae inserts into the buccal side of the maxillary shank. This muscle is larger and shifted dorsally in LF. The maxilla may be more robust in LF to support the action of this larger muscle.

LF also has a much longer and wider palatinad wing of the maxilla. The intermaxillary ligament inserts on the rostral face of this structure. A longer palatinad wing may allow the maxilla to articulate more securely with the premaxilla. Likewise, a larger wing provides greater surface area for the intermaxillary ligament to insert.

The most noticeable difference in the premaxilla involves the relative lengths of the ascending and dentigerous arms. A longer ascending arm in LF facilitates the ventral rotation of the oral jaw (see below). The length of the ascending arm is also correlated with the length of the maxillad spine. This process is much longer in LF than in MZ.

The maxillad spine is associated with the maxilla as well as the rostral cartilage. A longer maxillad spine in LF may simply be a consequence of a longer ascending arm.

Alternatively, this process may serve to maintain a more effective articulation with both the maxilla and rostral cartilage.

An obtuse angle formed by the ascending and dentigerous arms of the premaxilla allows for greater force transmission during biting (Otten 1983). This angle is obtuse in LF, and acute in MZ. Again, LF has a more efficient design for biting.

The premaxilla in LF is an excellent example of how a species evolves under opposing structural and functional demands. How can LF have an inferior-subterminal mouth, yet employ a highly specialized biting mode of feeding? A subterminal mouth allows LF to feed while swimming nearly parallel to the substrate. This orientation allows LF to forage in shallow, wave-swept habitats where competition with heterospecifics is minimized. Structurally, this orientation is accomplished by rotating the vomerine process ventrally, and elongating the ascending arm of the premaxilla. However, a *shorter* ascending arm of the premaxilla will increase force transmission during biting (Otten 1983). A shorter arm increases biting efficiency, in part, because the distance between the intermaxillary ligament and the rostral tip of the premaxilla is a determinant of biting force: the shorter the distance the greater the biting force (the intermaxillary ligament lies below the interprocess edge of the premaxilla – landmark 3) (Otten 1983). Although LF has a longer ascending arm than MZ, the distance from the interprocess edge and the rostral tip of the premaxilla (landmarks one and three) is actually shorter in LF than in MZ. The length of the ascending arm in LF is increased by lengthening the ascending spine, not the entire arm. In other words, LF has a long ascending arm to facilitate the ventral rotation of the lower jaw, however this species also manages keep the load-bearing region of the arm short and robust.

The robust load-bearing area of the ascending arm in LF correlates with an enormous intermaxillary ligament. Species in the genus *Labeotropheus* are characterized by a large fleshy "nose" which wraps around the rostral tip of the upper jaw. This "nose" consists predominantly of the intermaxillary ligament. This massive ligament is presumably needed to resist the considerable force applied as the maxillary shank is pulled posteriorly by the adductor mandibulae during biting.

Interspecific shape difference in the neurocranium is limited to two aspects of morphology: vomer position, and length of the preorbital region of the skull. MZ, like other species that feed with a sucking mode, has a terminal mouth and a large, horizontally directed vomer. This orientation facilitates jaw protrusion during suction feeding. During suction feeding, the ascending arm of the premaxilla slides along the vomerine process by way of the rostral cartilage, allowing the upper jaw to distend. Upper jaw protrusion serves to increase the volume of the buccal cavity. LF, like other species with a subterminal mouth, has a vertically directed vomer. I also find that MZ has a short, attenuated preorbital region of the skull, while LF has an expanded preorbital region. These shape differences clearly reflect different modes of feeding.

The supraoccipital crest is where the epaxial musculature inserts on the skull. Epaxial muscles are important in head lifting, a critical aspect of suction feeding (Lauder 1979; Liem 1980). Dorso-ventral compression of the supraoccipital crest is thought to occur within cichlid species that maintain close contact with the substrate (Greenwood 1978; Barel 1983). One might expect that the supraoccipital crest would be higher in MZ than in LF. However, I found no difference in this trait between MZ and LF (see Figure 2.14). Rather, this element is the source of considerable intraspecific variation. This result is supported by Reinthal (1990) who found that crest height showed a great deal of



intraspecific variation among mbuna, and was not a good character to distinguish among species.

The neurocranium is a large and functionally dynamic structure; it is associated with the oral jaws via the ethmoidal region of the skull, the pharyngeal jaws by way of the pharyngeal apophysis, and the epaxial musculature via the supraoccipital crest. Interestingly, differences in skull shape between MZ and LF, which have widely disparate jaw morphologies, are limited to the ethmoidal region. That is, shape differences are limited to the region of the skull directly associated with the oral jaw apparatus.

The lateral aspect of the ethmoidal region is much more important in distinguishing MZ and LF than is the ventral aspect of the same region. LF and MZ differ by over 21 standard deviations in the lateral view of the skull, while in the ventral view, they are only separated by 5.5 standard deviations.

These results parallel Reinthal's observation (1990) that MZ and LF can be easily distinguished by vomer rotation, but not vomer width. Rock-dwelling cichlids can be separated into two broad groups based on vomer shape. The first group includes species that have enlarged, horizontally directed vomers, terminal mouths, and feed primarily on plankton either by sucking them from the water column or by brushing them from beds of algae. The second group includes species that have thin, vertically directed vomers, inferior mouths, and feed primarily on attached algae (Reinthal 1990). MZ fits well into the first group. However, LF does not fit well into either group, because it has a ventrally directed vomer like species in the second group, and an enlarged vomer like species in the first group.

The width of the vomer at the vomerine notch is independent of width at the palatinad articulation facet. There is no difference in the width of the vomer between MZ

and LF where the palatine articulates. Rather, shape difference in the width of the vomer is limited to the vomerine notch, which is associated with the maxilla. Here again, only aspects of shape associated with the oral jaws are different in the skulls of LF and MZ.

There are several general conclusions to be drawn from the results of this morphological study. First, aspects of morphological change between LF and MZ support field observations that these species employ different modes of feeding. Liem (1991) argues that a biting design is merely an “exaggeration” of a suction design. For instance, both designs are characterized by an attenuated cone-shaped buccal cavity and a relatively small mouth gape (Barel 1983). However, biting fish also generally have shorter and more robust jaws. The major trend between LF and MZ, is that LF elements are both shorter and more robust. Finally, when examining a structure that is not part of the oral jaw apparatus (e.g. the neurocranium), only those aspects of shape associated with the jaws differ between LF and MZ. This supports the idea that cichlid diversification is expressed mainly in their trophic biology, while the rest of their body remains relatively conserved (Fryer and Iles 1972; Greenwood 1974; and Liem 1991).

### The geometric approach

The primary objective of this study was to demonstrate the power and utility of geometric morphometrics in describing overall shape change in a complex structure. A major advantage of a geometric approach is that the analysis is not constrained by focusing on particular shape features *a priori*. Rather, the method identifies differences in any direction of shape space, providing a more comprehensive and biologically meaningful result.

I do not contend that a geometric approach is best for quantifying specific functional differences between species identified *a priori* (e.g. the length of a specific moment-arm). Clearly, if this were the goal, direct measures of functionally meaningful characters would be most useful. However, when describing shape change as a whole, it is difficult to relate a series of linear measures to the biology of an organism, especially if any of these measures are correlated. Moreover, many functionally relevant characters have no reliable landmarks.

It was not the goal of this study to quantify these specific differences. Rather, based on mode of action, prey choice, and habitat preference in the wild, I assume that MZ and LF differ in terms of feeding performance (McKaye and Marsh 1983; Ribbink et al. 1983; and Reinthal 1990). Given these differences, I ask what aspects of morphology facilitate these adaptive differences? Once overall shape change is defined, one may wish to formulate and test more specific hypotheses. For example, based on the differences identified above, I would predict that LF has a stronger bite and that MZ is a better suction feeder. These hypotheses could be tested by quantifying the magnitude of difference in biting and suction performance between these two species.

### Genetics

LF and MZ could be distinguished from one another in every analysis. Moreover, for every skeletal element,  $F_1$  morphology could be distinguished from both parental species (Figure 2.14). This trend suggests an equal contribution of parental alleles to hybrid morphology, and I would predict an additive mode of action for most genes responsible for the morphological differences between LF and MZ. There does,

however, seem to be a slight dominance component involving both the premaxilla and the vomer. In both cases  $F_1$  morphology is skewed towards that of MZ, and there is considerable overlap in their distributions (Figure 2.14). Therefore, certain MZ alleles underlying the premaxilla and vomer may be dominant to LF.

Definitive answers of the genetic architecture and inheritance of these traits are beyond the scope of this study. A thorough examination of  $F_2$  morphology will shed light on the number and mode of action of genes responsible for differences in the oral jaw apparatus. However, detailed knowledge of the genetic architecture of this trait must be based on linking  $F_2$  morphology to molecular markers, and genetically mapping these traits in a quantitative trait loci (QTL) analysis.

#### Acknowledgements

This work was done in collaboration with T. D. Kocher. I thank A. Ambali, the University of Malawi, and the Malawi Government for assistance with collection of specimens and M. Zelditch, K. Liem, J. Bolker, P. Danley and T. Streelman for technical advice, discussion and critical reading of the manuscript. Dermestid beetles were housed by M. Scott. All illustrations were done by R. Craig Albertson. This work was supported by the NSF.

**Table 2.1**

Descriptions of the anatomical landmarks used for morphometric analysis.  
Anatomical terms follow Barel et al. (1976).

Element	Landmarks	Descriptions (after Barel et al. 1976)
Lower Jaw (lateral)	1	rostral tip of the dentary
	2	tip of the rostral process of the articular
	3	dorsal tip of the coronoid (dentary) process
	4	dorsal tip of the primorial (articular) process
	5	dorsal process of the suspensoriad articulation facet
	6	postarticulation process (of the suspensoriad articulation facet)
	7	retroarticular process
	8	rostral process of the coultter area
Lower Jaw (ventral)	1	lateral-most point of the dentigerous area
	2	oral-most point of the symphyseal facet
	3	rostral process of the coultter area
	4	postarticulation process (of the suspensoriad articulation facet)
	5	lateral-most point of suspensoriad articulation facet
Maxilla	1	medial process of the premaxillad wing
	2	medial process of the palatinad wing
	3	lateral process of the palatinad wing
	4	shank process
Premaxilla	1	rostral-most point of the dentigerous arm
	2	dorsal process of the ascending spine
	3	ventral-most point of the interprocess edge
	4	dorsal process of the maxillad spine
	5	caudal process of the dentigerous arm
Neurocranium	1	rostral tip of the vomer
	2	caudal-most point of the preorbital ridge
	3	tip of preorbital process
	4	dorsal tip of the supraoccipital crest
	5	ventral process of the vertebrad concavity
	6	pharyngobrachiad apophysis
	7	tip of postorbital process
	8	caudal-most point of the vomerine-palatinad articulation facet
Vomer	1	rostral tip of the vomer
	2	rostral edge of the vomerine notch
	3	rostral edge of the vomerine-palatinad articulation facet
	4	doral crest of the parasphenoid, on the line connecting the preorbital processes

**Table 2.2**  
 Characteristics of the first canonical variate axis identified from the discriminant function analysis, and results from the regression of shape variables (partial warps) on CV1.  
 The number of partial warps given for each analysis is k-3, where k is equal to the number of landmarks.

Element	% Variance Explained by CV1	#stdev units between parental species	Significant ( $p > 0.01$ ) regression coefficients demonstrating the relationship between shape variables and CV1											
			x1	y1	x2	y2	x3	y3	x4	y4	x5	y5	x0	y0
Lower Jaw (lateral)	71	13.2	0.4897	0.2363	0.2474	0.3238	0.3534	0.2378	0.7129	0.9523	0.0839	0.8262	0.2603	0.933
Lower Jaw (ventral)	90	16.1	0.5746	0.1969	0.9724	N/S							0.8167	0.8827
Maxilla	85	10.3	0.809	0.0785									0.9438	0.8923
Premaxilla	84	11	0.8683	0.5376	0.9352	0.8328							0.4375	0.7584
Neurocranium	55	21.3	0.5923	0.2878	0.1409	0.7167	0.787	0.1696	0.8404	0.5501	0.4834	0.6059	0.8969	N/S
Vomer	58	5.5	0.0812	0.6973									0.7068	0.596

**Table 2.3**

Functional differences in feeding performance predicted from differences in form.

Functional differences predicted by differences in form		
Suction-feeding	Lf	Mz
long ventral process of the suspensoriad articulation facet		X
attenuated buccal cavity		X
attenuated neurocranium (Liem '90)		X
abbreviated preorbital region of the skull (Liem '90)		X
enlarged, horizontally directed vomer (Liem '90)		X
Biting		
Short ascending arm of the dentary (Otten '83)	X	
wide, robust lower jaw (Liem '90)	X	
curved, robust maxilla (Otten '83; and Liem '90)	X	
long palatinad wing of the maxilla	X	
obtuse angle formed between two arms of the premaxilla (Otten '83)	X	
short load-bearing region of the ascending arm of the premaxilla (Otten '83)	X	

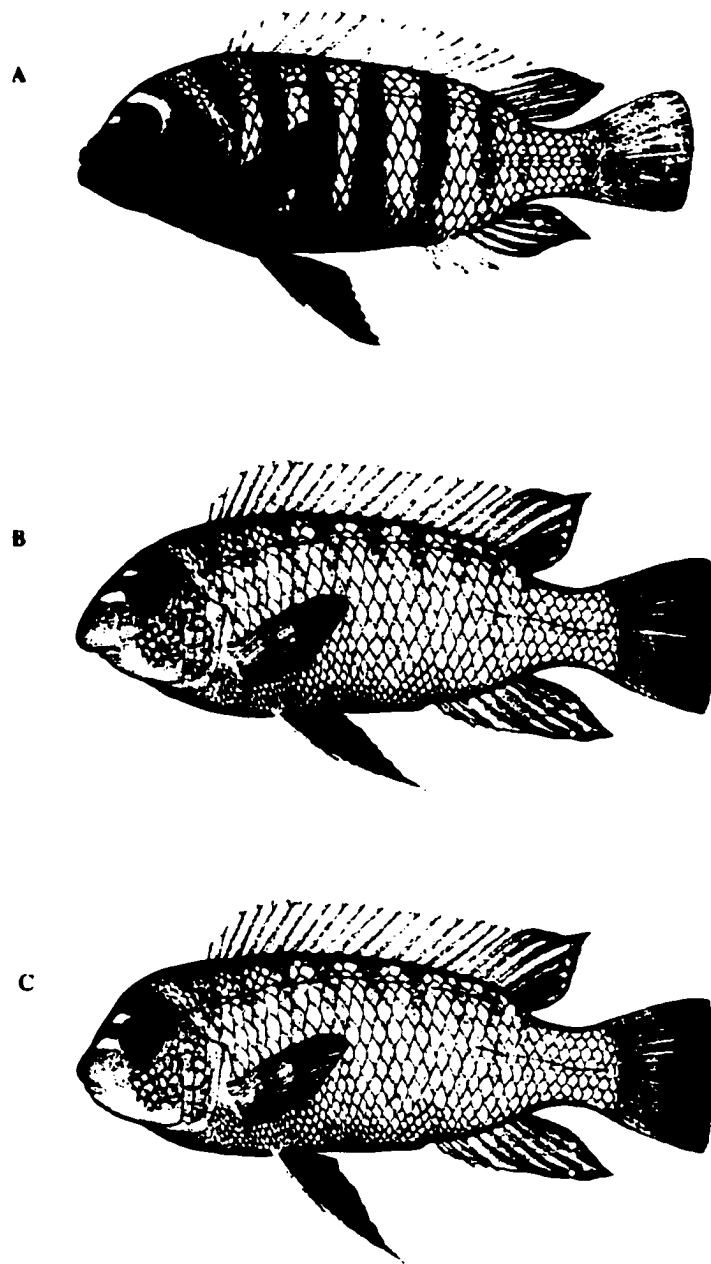


**Figure 2.1**

Specimens used in morphometric study. A. *M. zebra* B. *L. fuelleborni* C.  $F_1$  hybrid.



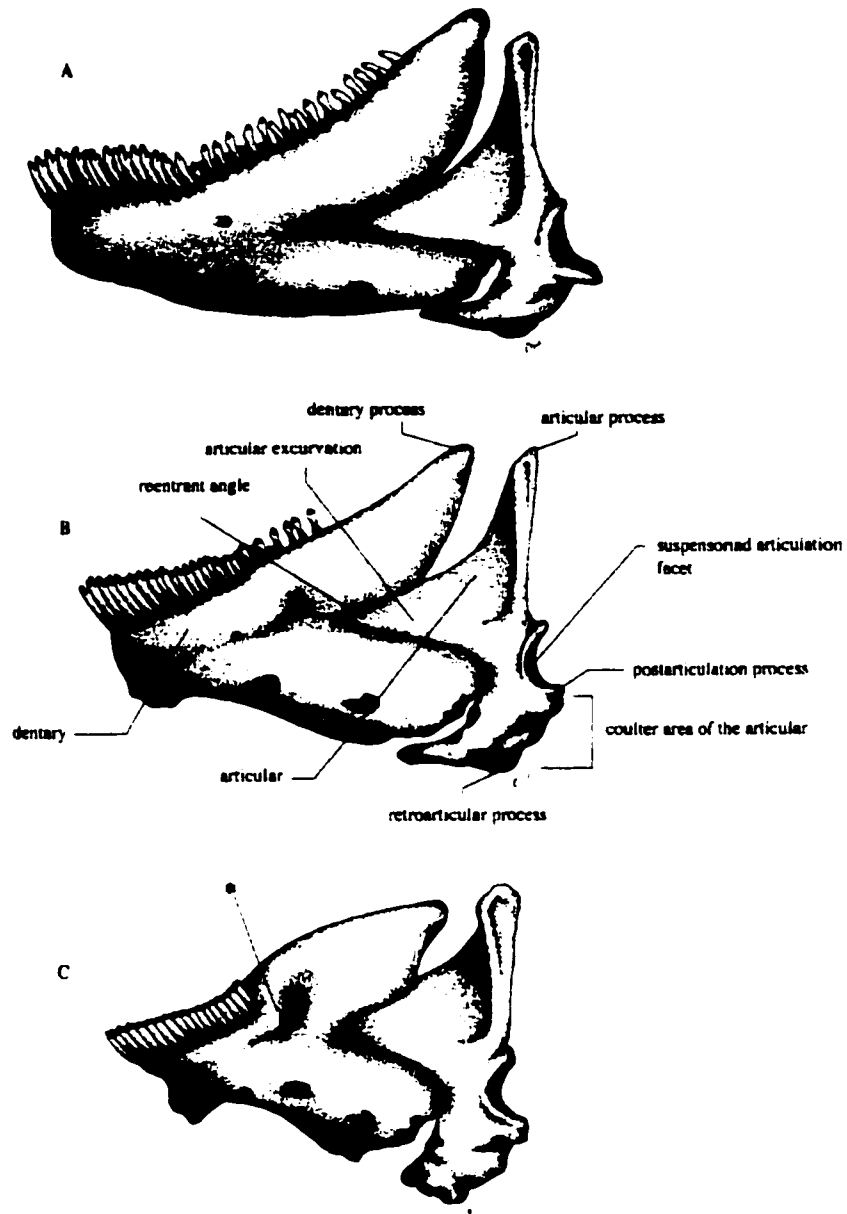


**Figure 2.2**

**Lower jaw, left lateral view.** The lower jaw is composed of two skeletal elements, the dentary and the articular. A. *M. zebra* B.  $F_1$  hybrid C. *L. fuelleborni*. Anatomical terms follow Barel et al. (1976).

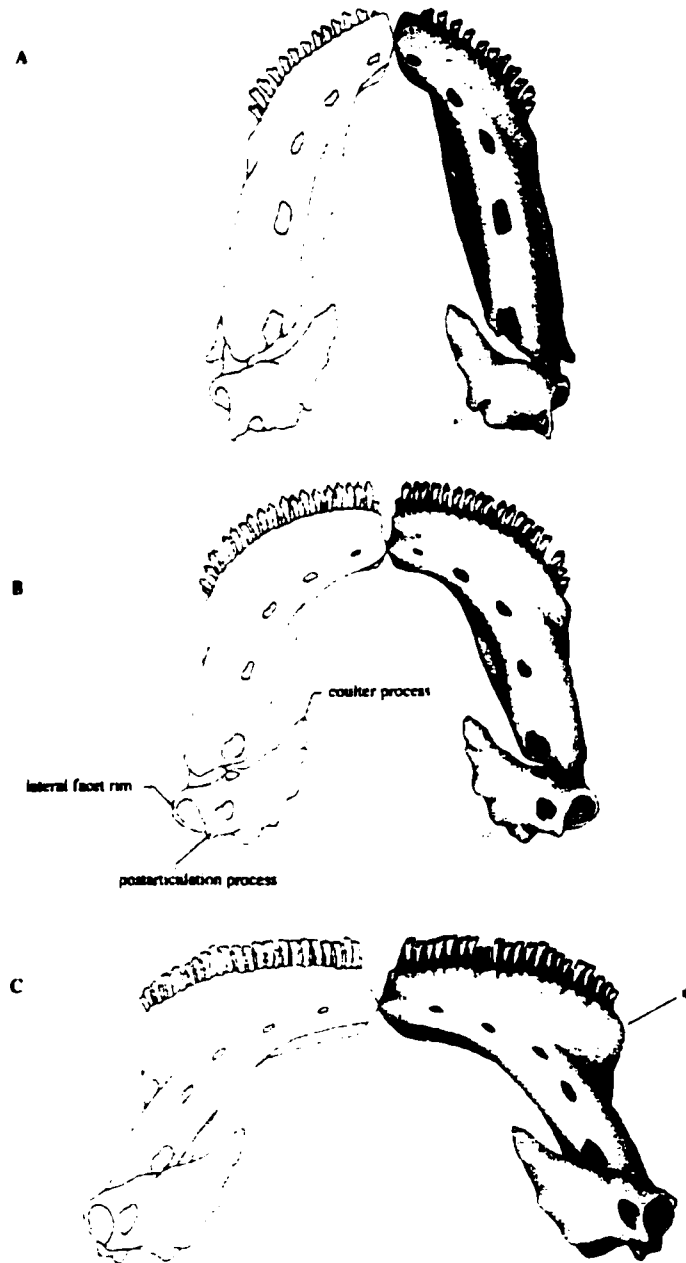


**Figure 2.3**

**Right and left halves of the lower jaw in the ventral view. A. *M. zebra* B.  $F_1$  hybrid C. *L. fuelleborni*. Anatomical terms follow Barel et al. (1976). (\*) Note the lateral expansion of the dentary in *L. fuelleborni*.**

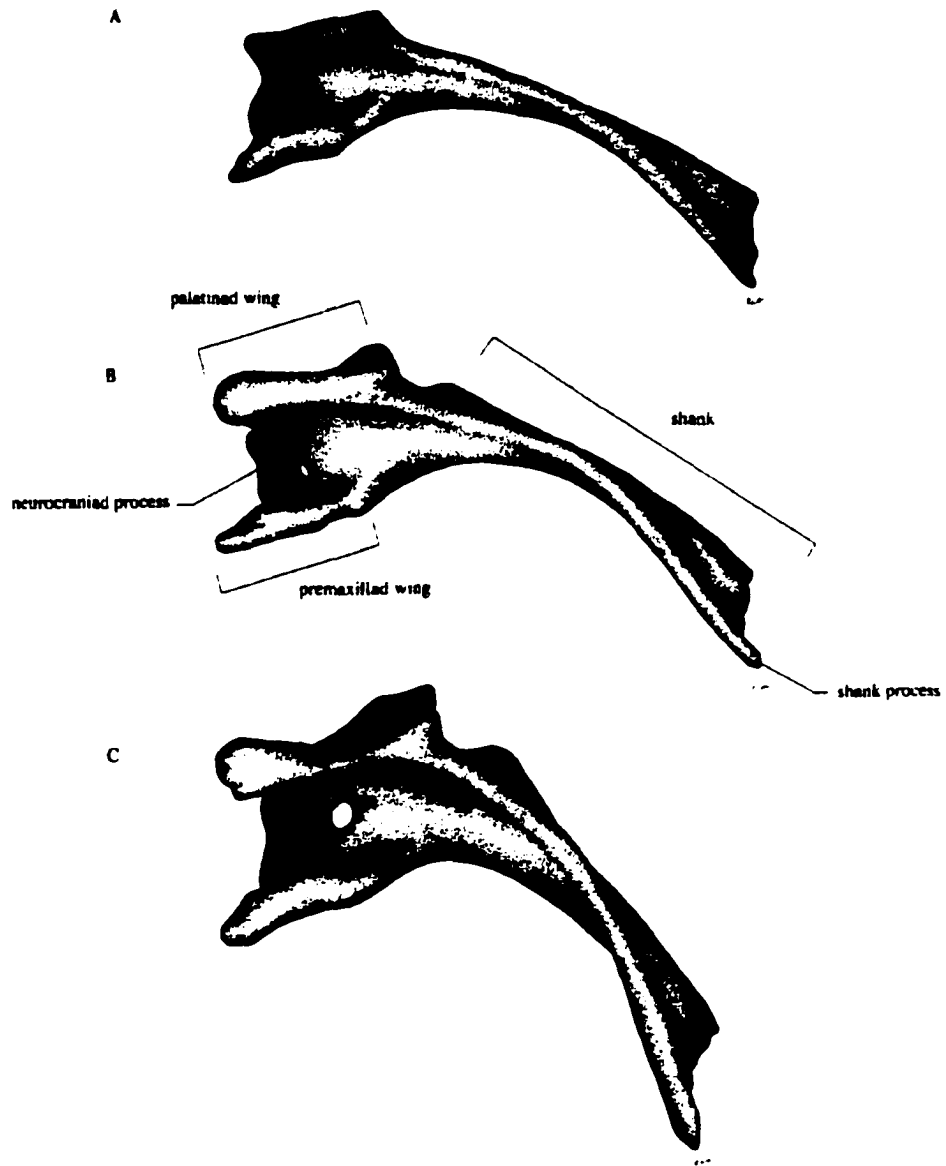


**Figure 2.4**  
**Maxilla in the right rostral view. A. *M. zebra* B.  $F_1$  hybrid C. *L. fuelleborni*.**  
 Anatomical terms follow Barel et al. (1976).

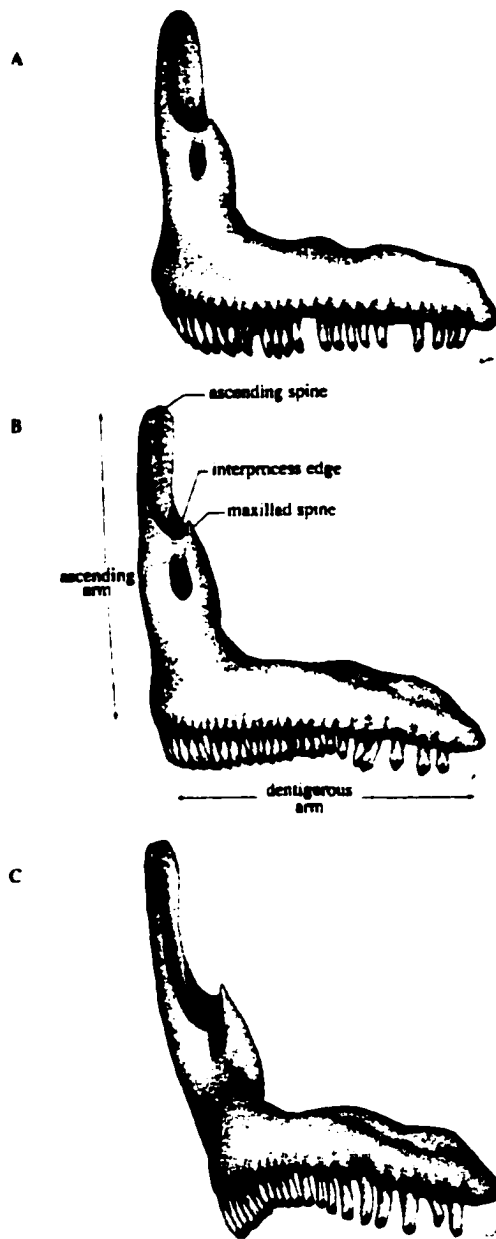


**Figure 2.5**  
**Premaxilla in the left lateral view. A. *M. zebra* B.  $F_1$  hybrid C. *L. fuelleborni*.**  
 Anatomical terms follow Barel et al. (1976).

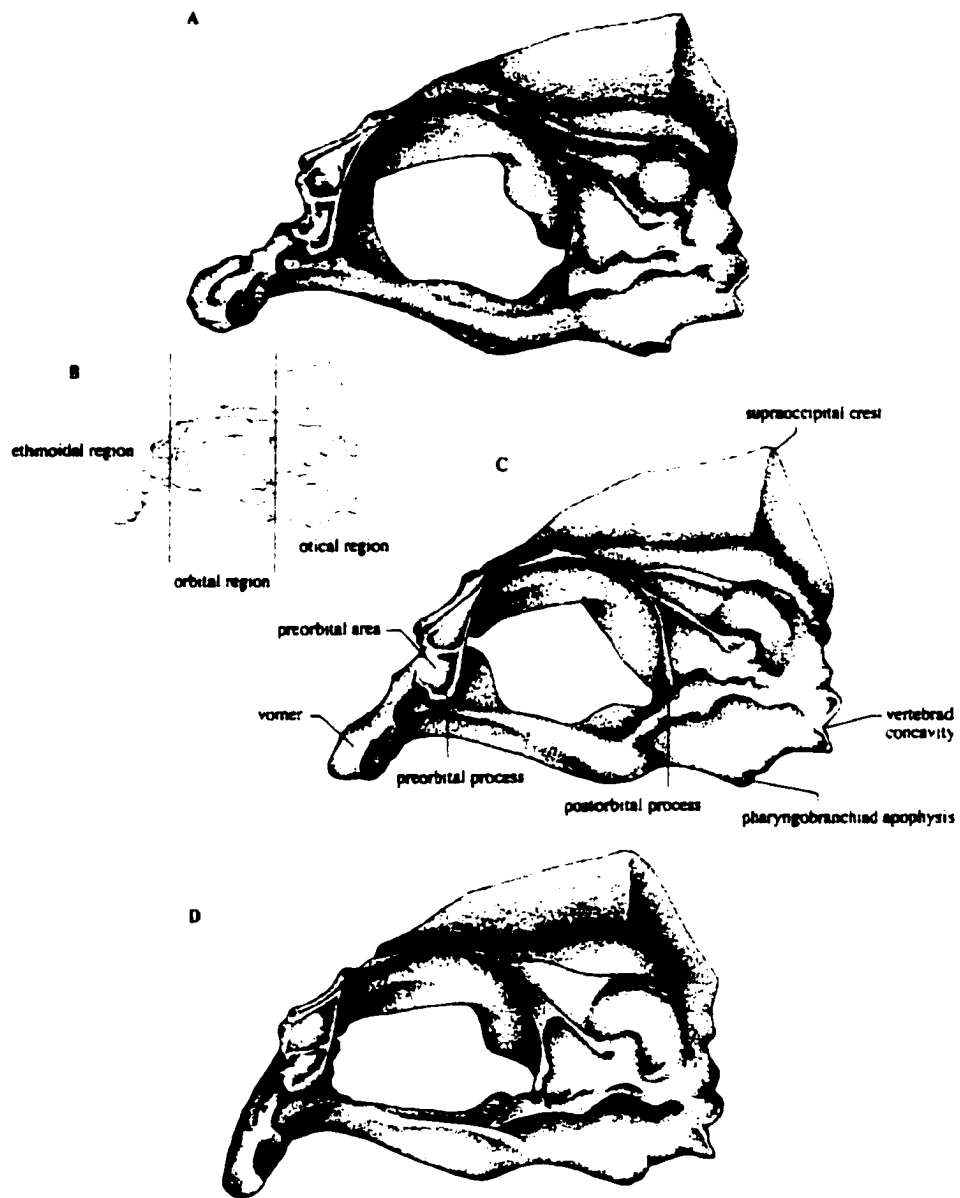


**Figure 2.6**

**Neurocranium left lateral view.** A. *M. zebra* B. Generalized line drawing, showing three regions of the neurocranium. C.  $F_1$  hybrid D. *L. fuelleborni*. Anatomical terms follow Barel et al. (1976).

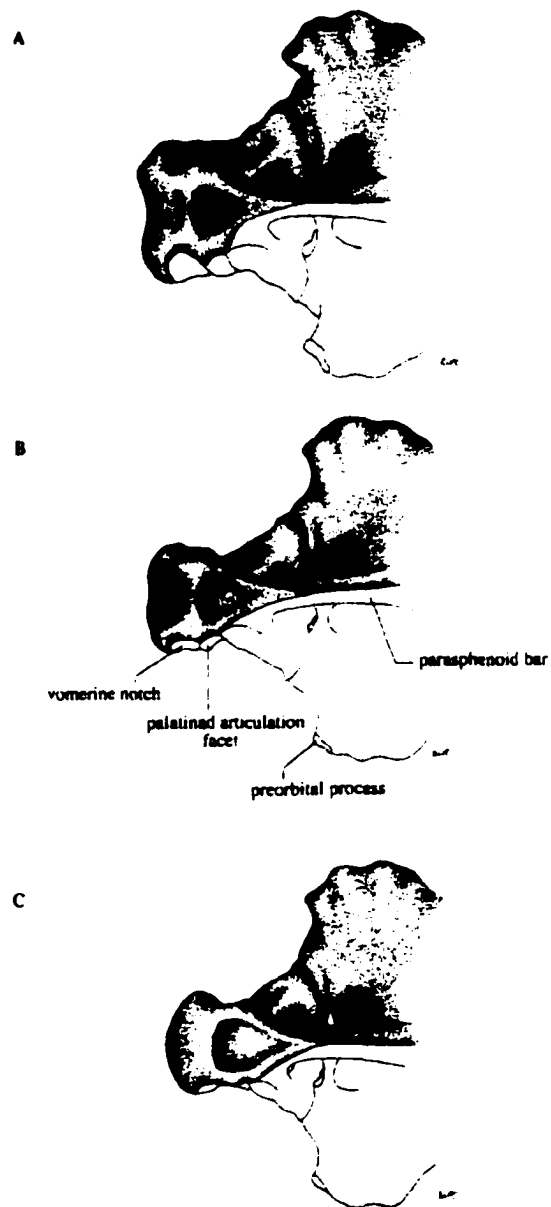
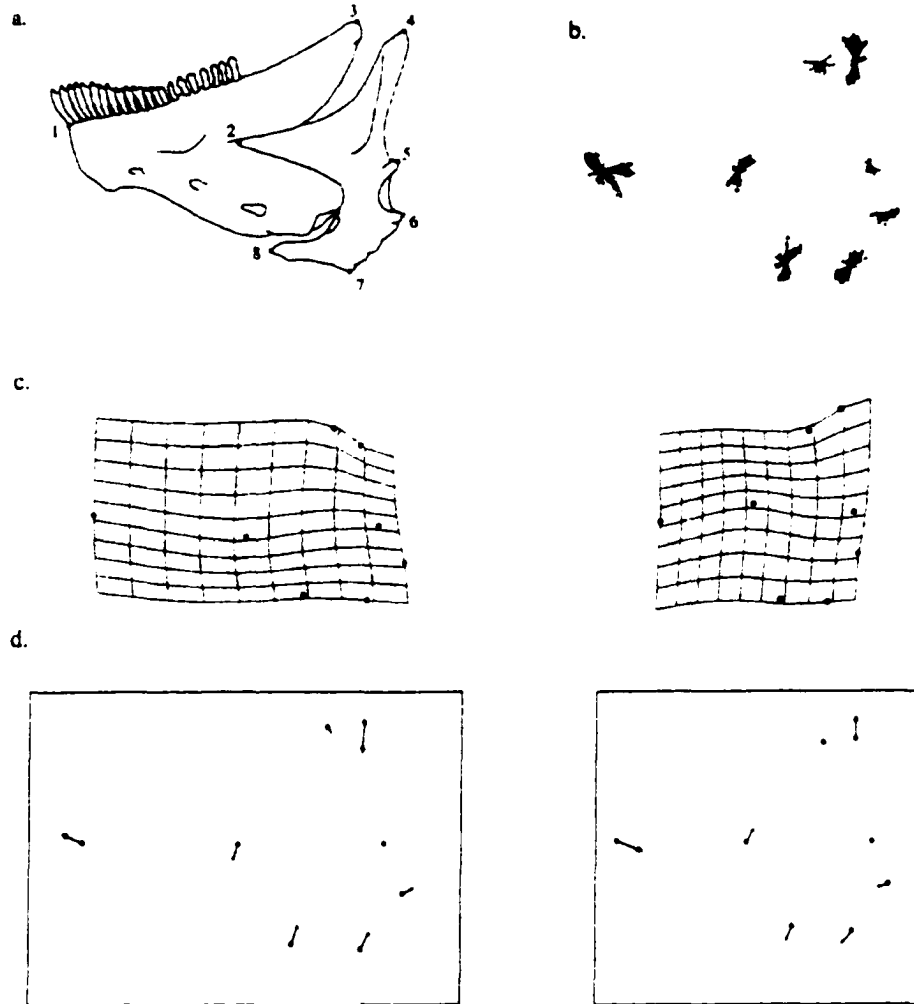


Figure 2.7

**Ethmoid region of the skull showing the vomer in the ventral view. A. *M. zebra* B.  $F_1$  hybrid C. *L. fuelleborni*. Anatomical terms follow Barel et al. (1976).**



**Figure 2.8**

a. Landmark position on the lower jaw in the lateral view. b. Landmark variation around the consensus configuration after a generalized least-squares fit superimposition. c. Deformation grids as a function of the first canonical variate axis. The figure on the left represents the deformation when the mean form of *M. zebra* is the target. Likewise, the figure on the right represents the deformation when the mean form of *L. fuelleborni* is the target. d. Vector displacements which correspond to the deformation grids.

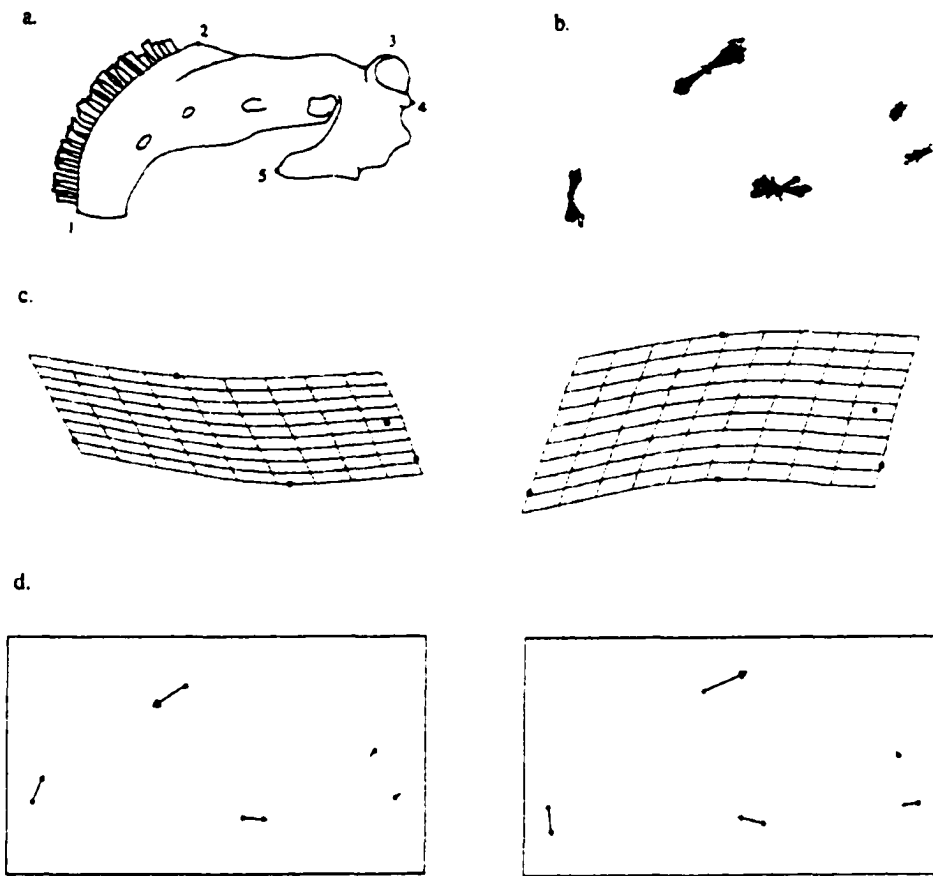


**Figure 2.9**

a. Landmark position on the lower jaw in the ventral view. b. Landmark variation around the consensus configuration after a generalized least-squares fit superimposition. c. Deformation grids as a function of the first canonical variate axis. The figure on the left represents the deformation when the mean form of *M. zebra* is the target. Likewise, the figure on the right represents the deformation when the mean form of *L. fuelleborni* is the target. d. Vector displacements which correspond to the deformation grids.



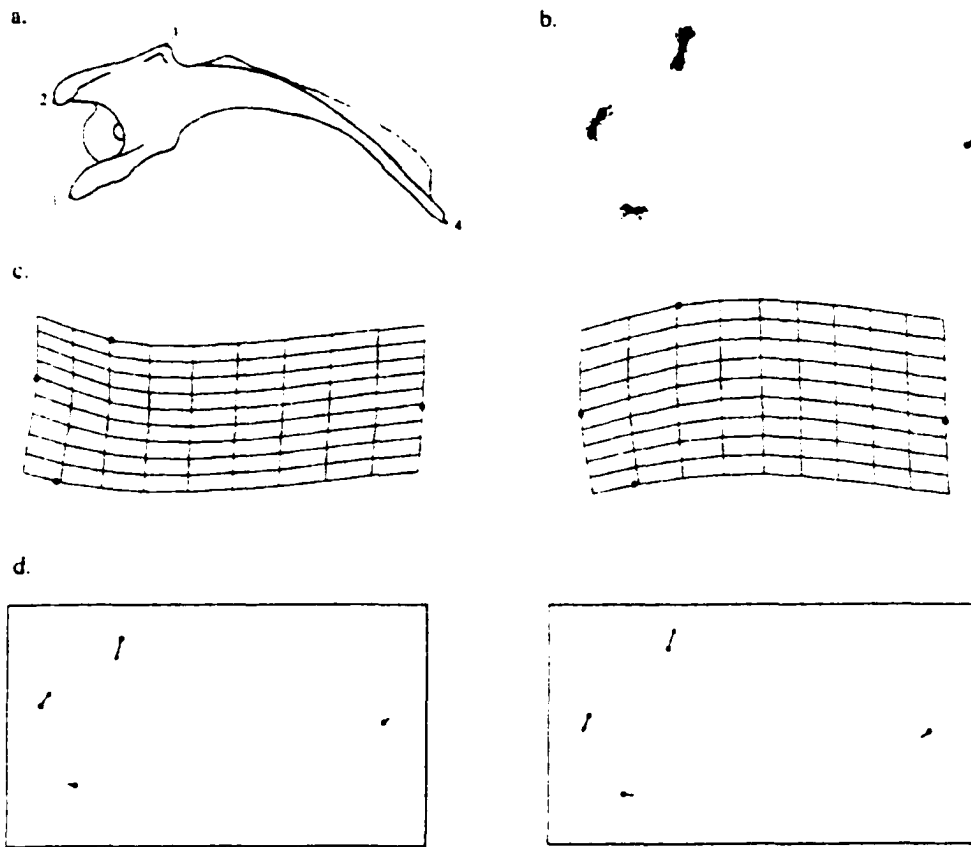


**Figure 2.10**

a. Landmark position on the maxilla. b. Landmark variation around the consensus configuration after a generalized least-squares fit superimposition. c. Deformation grids as a function of the first canonical variate axis. The figure on the left represents the deformation when the mean form of *M. zebra* is the target. Likewise, the figure on the right represents the deformation when the mean form of *L. fuelleborni* is the target. d. Vector displacements which correspond to the deformation grids.

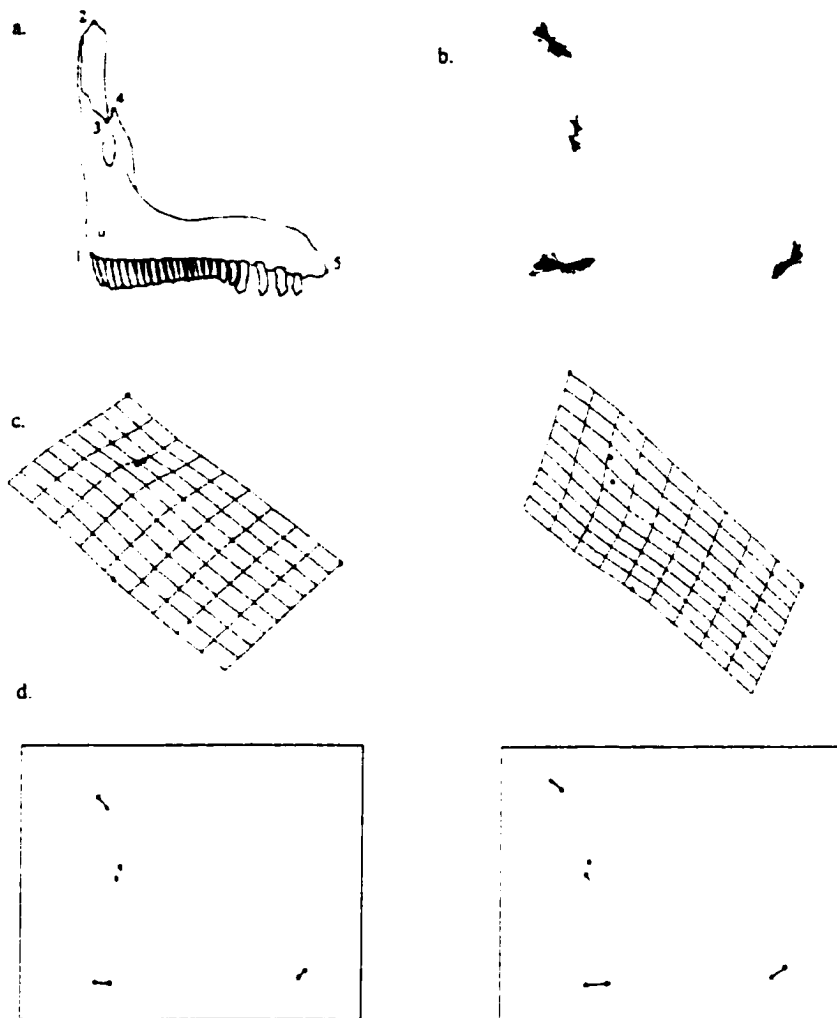


**Figure 2.11**

a. Landmark position on the premaxilla. b. Landmark variation around the consensus configuration after a generalized least-squares fit superimposition. c. Deformation grids as a function of the first canonical variate axis. The figure on the left represents the deformation when the mean form of *M. zebra* is the target. Likewise, the figure on the right represents the deformation when the mean form of *L. fuelleborni* is the target. d. Vector displacements which correspond to the deformation grids.

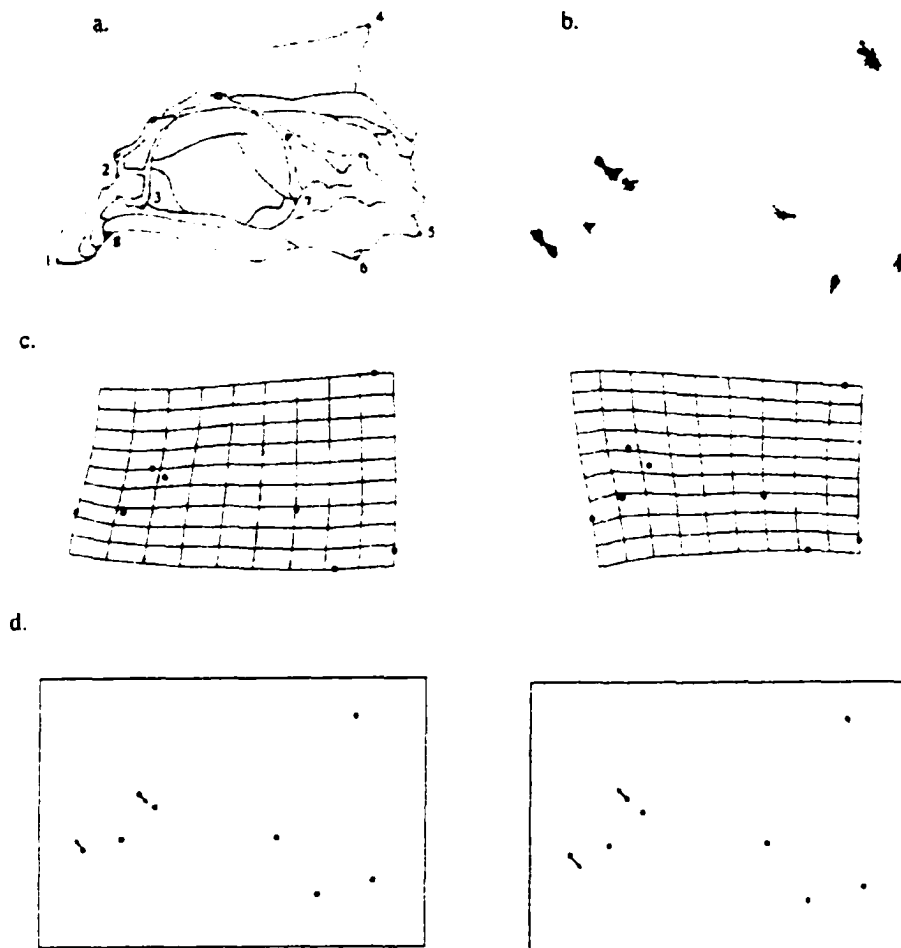


**Figure 2.12**

a. Landmark position on the neurocranium. b. Landmark variation around the consensus configuration after a generalized least-squares fit superimposition. c. Deformation grids as a function of the first canonical variate axis. The figure on the left represents the deformation when the mean form of *M. zebra* is the target. Likewise, the figure on the right represents the deformation when the mean form of *L. fuelleborni* is the target. d. Vector displacements which correspond to the deformation grids.

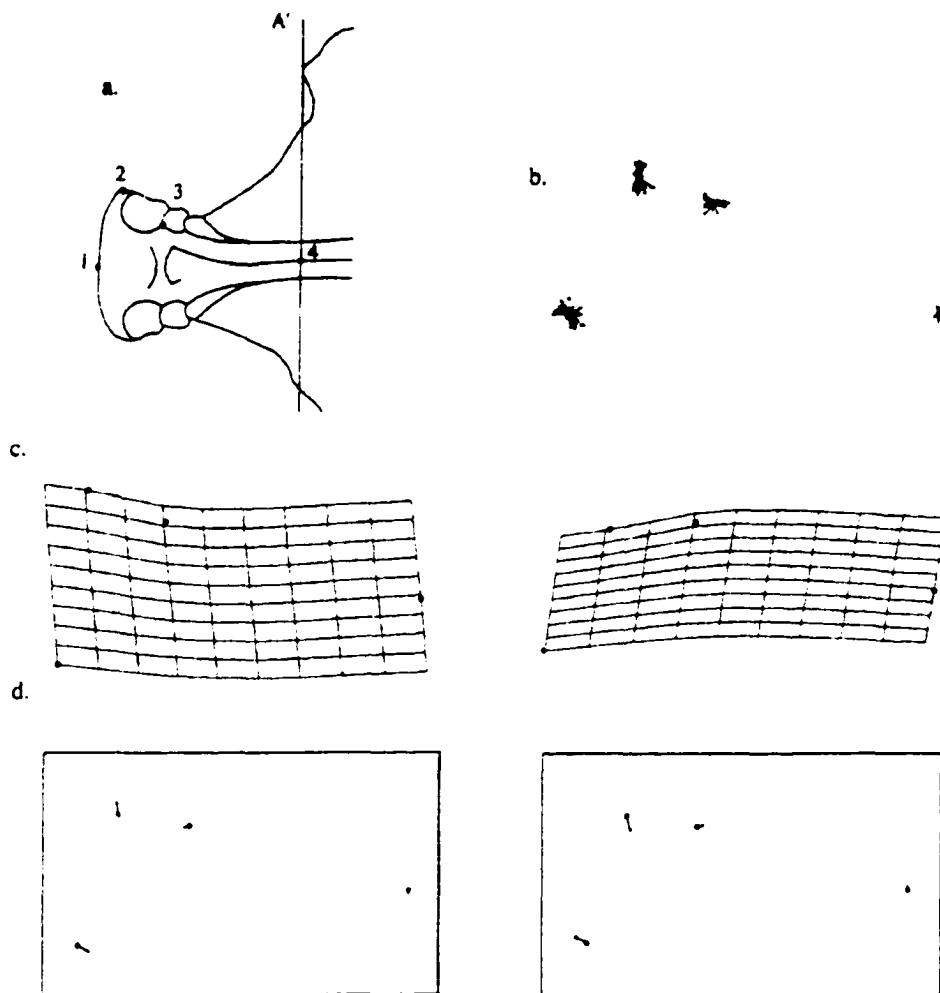
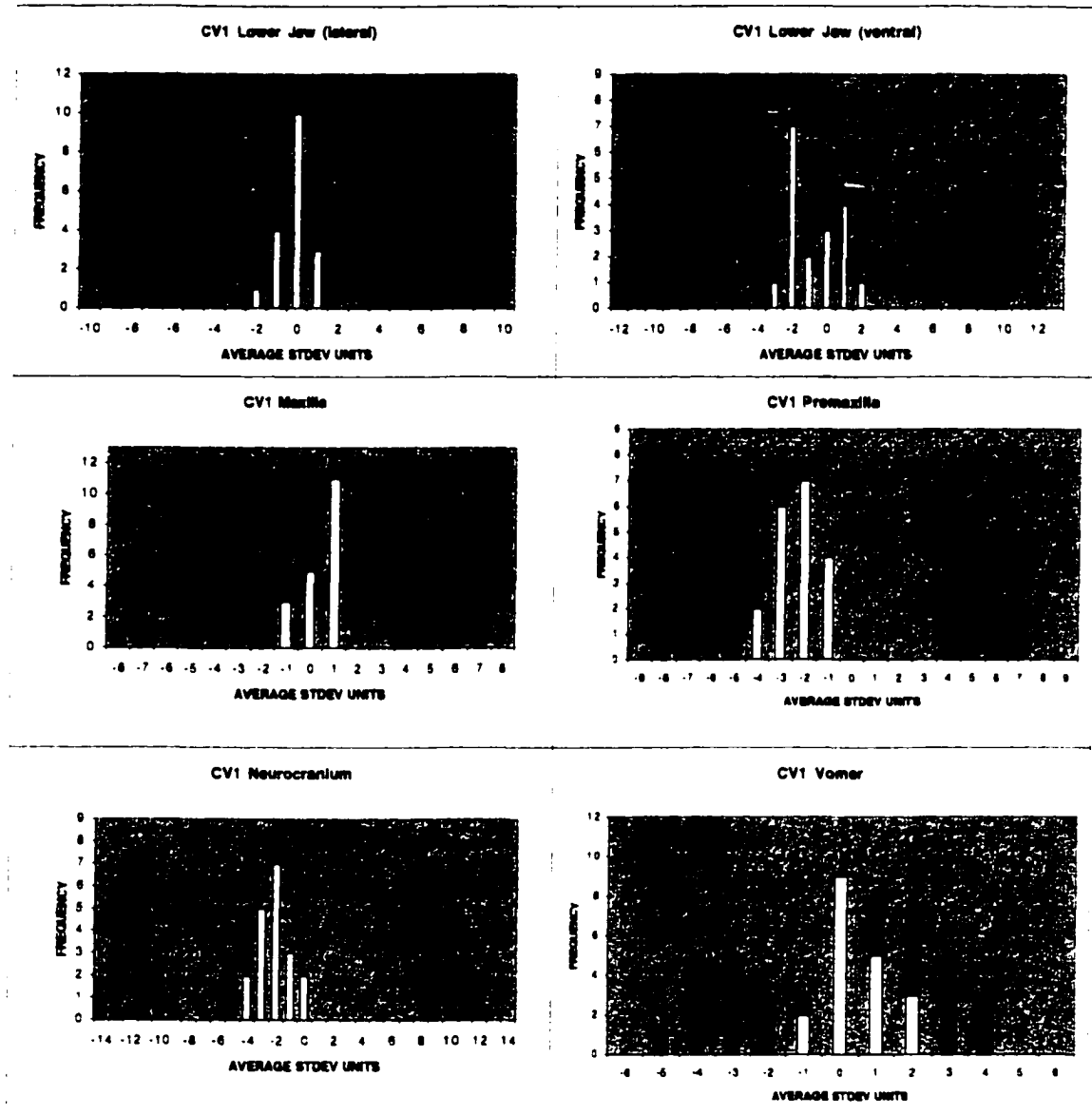


**Figure 2.13**

a. Landmark position on the vomer in the ventral view. Here, A' is the line which connects the preorbital processes. b. Landmark variation around the consensus configuration after a generalized least-squares fit superimposition. c. Deformation grids as a function of the first canonical variate axis. The figure on the left represents the deformation when the mean form of *M. zebra* is the target. Likewise, the figure on the right represents the deformation when the mean form of *L. fuelleborni* is the target. d. Vector displacements which correspond to the deformation grids.

**Figure 2.14**

Histograms showing the position of *M. zebra*, *L. fuelleborni*, and their hybrid progeny along the first canonical variate axis. Since canonical variate loadings are arbitrary units, the x-axis is recorded in terms of average within-species standard deviation units.



## CHAPTER 3

### GENETIC BASIS OF ADAPTIVE SHAPE DIFFERENCES IN THE CICHLID HEAD

#### Abstract

East African cichlids exhibit an extraordinary level of morphological diversity. Key to their success has been a dramatic radiation in trophic biology, which has occurred rapidly and repeatedly in different lakes. In this report I take the first step in understanding the genetic basis of differences in cichlid oral jaw design. I estimate the effective number of genetic factors that control differences in the cichlid head through a comprehensive morphological assessment of two Lake Malawi cichlid species and their  $F_1$  and  $F_2$  hybrid progeny. I estimate that between one and eleven factors underlying shape difference of individual bony elements. Interestingly, I show that many of the skeletal differences in the head and oral jaw apparatus are inherited together, suggesting a degree of pleiotropy in the genetic architecture of this character complex. Moreover, I find that shape differences segregate according to developmental rather than functional units.

## Introduction

There is mounting evidence that selection on trophic morphology plays a strong role in the speciation of certain groups of vertebrates. This trend has been documented in Galapagos finches (Grant and Grant 1997; Sato et al. 2001), North American salamanders (Adams and Rohlf 2000), arctic charr (Skulason et al. 1989, 1996), three-spine stickleback (McPhail 1992, 1994), whitefish (Schluter and McPhail 1993), as well as cichlids on two continents (Albertson et al. 1999; Martin and Bermingham 1998; McKaye et al. 1998; Schliewen et al. 1994). These and other studies (e.g. Echelle and Kornfield 1984; Nagelkerke et al. 1994; Tichy and Seegers 1999) suggest that selection on trophic morphology, if not causative, at least closely accompanies divergence. Unfortunately, the genetic basis of such morphological differences is poorly understood. To paraphrase a question posed by Orr and Coyne (1992): How many genes underlie the adaptive differences between species?

East African cichlids are a textbook example of adaptive morphological radiation (Futuyma 1986). The rapidity and extent of morphological divergence in this group is unparalleled among vertebrates. The most dramatic changes seem to involve the oral jaw apparatus. Freed from the constraints of prey-processing, the oral jaws have evolved highly specialized modes of food collection (Liem 1973), setting the stage for the stunning radiation in trophic biology we see in each of the three East African Great Lakes (Victoria, Tanganyika and Malawi). Molecular and geological studies suggest that these radiations are extremely recent (Greenwood 1974; Kocher et al. 1995; Meyer 1993;

Owen et al. 1990), and remarkably similar trophic morphologies have evolved convergently in different lakes (Kocher et al. 1993).

This report takes the first step in elucidating the genetic architecture of the cichlid oral jaw apparatus. I first evaluate differences in the craniofacial skeleton between two cichlid species that employ different modes of feeding. Our morphometric analysis includes four skeletal elements that constitute the oral jaws (articular, dentary, maxilla, and premaxilla), two bony elements associated with the oral jaw apparatus (suspensorium and neurocranium), as well as oral jaw dentition. I then quantify morphological variance in hybrid generations, and employing the Castle-Wright Estimator, biometrically estimate the number of genetic factors that underlie differences in shape. Finally, I infer the genetic correlation among skeletal elements by identifying structural units inherited together in the  $F_2$ . Our results provide critical insight as to the total number of determinants that underlie shape differences in this adaptively significant character complex.



## Materials and Methods

### Species

*Labeotropheus fuelleborni* ("LF") and *Metriaclima zebra* ("MZ") are two rock-dwelling species from Lake Malawi which shared a common ancestor less than one million years ago (Meyer 1993). Although both species forage on algae, they employ different modes of feeding (Ribbink 1990), occupy different microhabitats (Ribbink et al. 1983), and are characterized by very different oral jaw morphologies (Albertson and Kocher 2001; see Figure 3.1). MZ has a moderately sloped head, a large horizontally-directed vomer, and a terminal, isognathus mouth (Stauffer et al. 1997). It feeds on diatoms and loose algae by brushing these items from algal beds or by sucking them from the water column (McKaye and Marsh 1983; Reinthal 1990; Ribbink et al. 1983). LF has a large fleshy snout, a vertically directed vomer, and a robust inferior-subterminal mouth. The orientation of its mouth allows LF to bite attached algae from rocks while swimming nearly parallel to the substrate (Ribbink et al. 1983).

### Preparation of specimens

Parental specimens used in this study were lab-reared F<sub>1</sub> animals generated from wild-caught stock. Hybridization between the species occurs readily under no-choice conditions (Crapon de Caprona and Fritzsich 1984; Loiselle 1971; McElroy and Kornfield

1993). I obtained hybrids by crossing MZ females with LF males in a 500 gallon pool. Second generation hybrids were generated from four parental animals; two sires and two dams. 160 specimens were used in this study, 20 of each parental species, 20 F<sub>1</sub> hybrids, and 100 F<sub>2</sub> hybrids. MZ, LF and their hybrids reach sexual maturity by 10 to 12 months. Animals were examined no earlier than 12 months of age, and more typically at 18 months. Animals were sacrificed with MS-222 following a protocol approved by the University of New Hampshire ACUC. Specimens were then prepared for morphometric analysis using dermestid beetles, which cleaned and disarticulated skeletal elements of the head. I collected each of the four elements that make up the oral jaws (the dentary, articular, premaxilla, and maxilla), as well as the neurocranium and suspensorium. Images of individual skeletal elements were captured using a SPOT digital camera (Diagnostic Instruments, Inc.) mounted on a Zeiss SV11 dissecting scope. Images were imported into NIH Image (version 2.1), and landmark positions scored as (x, y) coordinates.

#### Morphometric technique: oral jaw morphology

I assessed differences in oral jaw morphology via landmark-based morphometrics. Landmarks used in this study are described in Albertson and Kocher (2001). Superimposition of landmark data was performed using a Procrustes generalized least-squares fit (GLSF) algorithm (Gower 1975; and Rohlf and Slice 1990) in Morphometrika 7.0 (Walker 1999). A least-squares approach superimposes configurations so that the sum of squared distances between corresponding landmarks is minimized. This is achieved by

scaling, translating, and rotating specimens with respect to a mean consensus configuration.

Thin-plate spline (TPS) analysis was performed in Morphometrika 7.0 (Walker 1999). The TPS technique rigorously implements D'Arcy Thompson's concept of Cartesian grid deformations (Thompson 1917). A thorough description of the technique may be found in Bookstein (1989, 1991). In short, TPS models the form of an infinitely thin metal plate that is constrained at some combination of points but is otherwise free to adopt the target form in a way that minimizes bending energy. In morphometrics, this interpolation is applied to a Cartesian coordinate system where deformation grids are constructed from two landmark configurations (Bookstein 1991). The total deformation of the thin-plate spline can be decomposed into geometrically orthogonal components based on scale (Rohlf and Marcus 1993; Yarooh 1996). These components (partial warps) can be localized to describe precisely what aspects of shape are different. Partial warp scores are the shape variables used in all subsequent analyses.

TPS analysis was performed on all animals (LF, MZ, F<sub>1</sub> and F<sub>2</sub>). Thus, all specimens were evaluated, and partial warp scores calculated, relative to the same mean consensus configuration. A principal component analysis was performed in Morphometrika 7.0 (Walker 1999) on partial warp scores (including the uniform component) of parental animals to identify the major axis of variation that distinguished LF from MZ. In all cases this was PC1. Principal component scores were then calculated for hybrid animals by multiplying hybrid partial warp scores by the parental eigenvectors in the space of partial warps. Thus, segregation of hybrid progeny was assessed in the dimension that distinguished parental species. A full justification for my experimental design is presented in figure 3.2.

### Assessing tooth morphology

F<sub>2</sub> dentition is a continuum between the fully bicuspid dentition of MZ and the fully tricuspid dentition of LF. Fourteen teeth in the first row of both the upper and lower jaw (seven on either side of the mandibular symphysis) were given a score between 2 and 3 (in 0.25 intervals) for 20 F<sub>1</sub> and 100 F<sub>2</sub> individuals. Tooth scores were meant to evaluate the relative height of the third cusp. A score of 2 was given to fully bicuspid dentition (MZ), while a score of 3 was given to fully tricuspid dentition, with even cusp heights (LF). The average tooth score for each element was used for subsequent analyses.

### Calculation of effective number of factors

The number of genetic factors that underlie morphological differences was estimated by applying the Castle-Wright Estimator (Lynch and Walsh 1998) to PC1 or tooth scores:

$$\hat{n}_e = \frac{(\bar{X}_{LF} - \bar{X}_{MZ})^2 - \sigma_{X_{LF}}^2 - \sigma_{X_{MZ}}^2}{8(\sigma_{F_2}^2 - \sigma_{F_1}^2)}$$

where  $n_e$  is the effective number of genetic factors,  $X_{LF}$  and  $X_{MZ}$  are the parental means,  $\sigma_{X_{LF}}^2$  and  $\sigma_{X_{MZ}}^2$  are the variances of the parental means, and  $\sigma_{F_1}^2$  and  $\sigma_{F_2}^2$  are the variances of the hybrid means.

The Castle-Wright method assumes that loci are unlinked, alleles are of equal effect, genes with positive and negative influence are fixed in alternate lines, and most critically, that alleles have an additive effect on phenotype. Violations of one or more of

these assumptions will generally lead to an underestimate of the number of effective factors (Zeng et al. 1990; Zeng 1992).

Analysis of line crosses enables one to estimate the relative contribution of additive, dominance, and epistatic effects on the inheritance of the trait(s) in question. I used weighted least-square regression to compare observed and expected means and standard errors of  $P_1$ ,  $P_2$ ,  $F_1$  and  $F_2$ . This approach enables one to estimate the parameters of an additive (A) and additive-dominance (AD) model of gene action. Formally called a joint-scaling test, the interested reader can refer to Lynch and Walsh (1998, chapter 9) for specific details. Briefly, I estimated the expected mean phenotype of the  $F_2$  ( $\mu_0$ ), the composite additive effect ( $\alpha_i^c$ ) for the A model, as well as the composite dominance effect ( $\delta_i^c$ ) for the AD model.

For the A model I tested the null hypothesis of purely additive gene action with a  $X^2$  test statistic with degrees of freedom equal to the number of lines minus the number of estimated parameters. Next, I evaluated the AD model to test for any contribution of dominance. The difference between the test statistics,  $X^2_A$  and  $X^2_{AD}$  is equivalent to a likelihood-ratio test statistic, and is denoted,  $\Delta$ , with degrees of freedom equal to the difference between the degrees of freedom in the A and AD models. The likelihood-ratio test statistic provides a test for the hypothesis that dominance explains a significant proportion of the variance.

Epistasis could not be evaluated via a joint-scaling test because there were not enough line means available (e.g. no backcross lines). But I could evaluate epistasis with a simple t-test:

$$\Delta = z_{F_2} - \left( \frac{z_{P_1} + z_{P_2}}{4} \right) + \left( \frac{z_{F_1}}{2} \right)$$

In the absence of epistasis, the expected value of  $\Delta$  is zero because at each locus the  $F_2$  should be 25% P1P1, 50% P1P2, and 25% P2P2. The variance of the test statistic is:

$$\sigma_{\Delta}^2 = \sigma_{F_2}^2 + \left( \frac{\sigma_{F_1}^2}{4} \right) + \left( \frac{\sigma_{P_1}^2 + \sigma_{P_2}^2}{16} \right)$$

Under the assumption that the sampling distribution of  $\Delta$  is normal, the ratio:

$$\frac{|\Delta|}{\sqrt{\sigma_{\Delta}^2}}$$

provides the t-test for epistasis. If the ratio is greater than 1.96, the null hypothesis of no epistasis can be rejected at the 95% confidence level (Lynch and Walsh 1998).

Finally, to identify skeletal elements that are inherited together in the  $F_2$ , I performed a Pearson correlation analysis on PC1 scores for each structure.

## Results

### Skeletal morphology

Detailed descriptions of the differences in skeletal morphology between LF and MZ are presented in Albertson and Kocher (2001). Major aspects of shape difference reflect differences in feeding performance (see Figure 3.2). For example, based on its morphology I predict that LF is better adapted for a biting mode of feeding. Morphological adaptations include 1) a short, robust, U-shaped oral jaw to optimize biting surface area; 2) a relatively high articular process, suggesting greater force transmission of the adductor mandibulae when biting; 3) a robust maxilla; 4) a long ascending arm of the premaxilla; 5) an obtuse angle formed by the two arms of the premaxilla; 6) an expanded preorbital region of the skull; and 7) a down-turned vomer, similar to other species with an inferior subterminal mouth. On the other hand, oral jaw morphology and feeding performance in MZ suggests it is better adapted for a suction mode of feeding. Relevant aspects of morphology include 1) a longer, narrower lower jaw; 2) a short articular process, suggesting a more rapid jaw closing motion (greater rate of angular rotation); 3) a thin maxilla; 4) a long dentigerous arm of the premaxilla; 5) an acute angle formed between the arms of the premaxilla; and 6) a swollen, horizontally directed vomer, similar to other suction feeding species. F<sub>1</sub> hybrid morphology is typically intermediate between parental species (Albertson and Kocher 2001), implying a generally additive mode of action of alleles responsible for shape differences.

### Tooth morphology

As with oral jaw morphology, differences in oral jaw dentition reflect different modes of food collection (see Figure 3.3). LF has a row of closely spaced tricuspid teeth on both the upper and lower jaws. Moreover, cusp height is approximately equal. This dentition resembles the cutting edge of shearing scissors and is common for species that crop filamentous algae from the substrate. MZ has a row of intermittently spaced bicuspid teeth on both jaws. Cusp height is uneven in MZ, with the dominant cusp being closer to the mandibular symphysis. MZ dentition resembles the teeth of a comb and is common for species that feed on loose algae and diatoms. Both species have a posterior row (or rows) of smaller tricuspid teeth.  $F_1$  tooth morphology is roughly intermediate between MZ and LF.  $F_1$  hybrids have three cusps like LF; however, the middle cusp is large and resembles the dominant cusp in MZ and the third cusp is generally smaller than either of the other two cusps.  $F_2$  dentition is generally the same as that of the  $F_1$ ; however, there is much greater variation in the height of the third cusp. Indeed, some  $F_2$  teeth are truly tricuspid, like those of LF, while others are truly bicuspid, like MZ. This variation is found both between and within  $F_2$  individuals (see below).

### PCA of partial warp scores

Results of the principal components analysis are presented in Figure 3.4. The PC axis that separates the parental species (in all cases this is PC1) accounts for 81% of the variance between MZ and LF for the lower jaw in the lateral view, 94% for the lower jaw



in the ventral view, 90% for both the maxilla and premaxilla, 71% for the suspensorium, and 69% and 65% for the neurocranium and vomer, respectively. The lower values associated with the skull are not altogether unexpected, as neurocranial characters are known to show high levels of intraspecific variation in cichlids (Reinthal 1990). It is also important to note that shape differences in the neurocranium are restricted to the anterior (ethmoidal) region of the skull (Albertson and Kocher 2001).

Depending on the element, parental species are separated along the PC axis by 5 to 13 environmental standard deviation units (since all  $F_1$  animals should be genetically identical, environmental standard deviation units are taken as  $F_1 \sigma$  for each structure). For every skeletal element, the  $F_1$  and  $F_2$  distributions falls between the parental species, suggesting an additive mode of inheritance.  $F_2$  morphology also exhibits much greater variance relative to the  $F_1$ . Indeed, for several elements parental morphology is regenerated in the  $F_2$  (see Figure 3.4).

### Inheritance

I find no evidence to reject the additive model of gene action for either oral jaw morphology or dentition. In all cases the chi-square statistic is not sufficient to reject the additive model (A). I therefore accept the null hypothesis of no difference between observed and expected means. For each element, the test statistic ( for the additive-dominance (AD) model is also not significant, so there is no statistical support for any contribution of dominance in the data. Finally, for every skeletal element I accept the null hypothesis of no epistasis. In all, these data suggest that the assumption of additive gene action for the Castle-Wright Estimator is appropriate in our study (data not shown).

### Castle-Wright Estimator

I find that shape differences between LF and MZ for each bony element are determined by fewer than 11 factors (see Figs. 3, 4). For example,  $n_e$  is 7.7, 9.1, and 10.5 for the premaxilla, maxilla, and lower jaw respectively. Of the approximately 10 factors that control differences in the lower jaw (lateral view), 9 are responsible for differences in the articular, while differences in the dentary are controlled by only one. I estimate that 4.5 factors control shape differences in the suspensorium, 4.0 affect the neurocranium in the lateral view, and 5.6 affect the vomerine process in the ventral view. Finally, cusp number seems to be determined by only one factor.

Considering the standard errors associated with our estimates, most bony elements appear to be controlled by a similar number of loci (4 - 10). There are, however, some notable exceptions. For example,  $n_e$  is close to one for both the dentary and tooth shape. These elements seem to have substantially lower estimates than other bony elements of the head. There also does not seem to be a direct relationship between the size of elements or the number of landmarks used to evaluate shape and the estimated number of genetic factors that contribute to morphological differences. The neurocranium and suspensorium were two of the largest structures examined in the analysis, with 8 and 6 landmarks used to describe shape change, respectively. These structures also had two of the lowest estimates of any bony element: 4.0 and 4.5, respectively. The maxilla, on the other hand, was one of the smallest structures examined, with 4 landmarks used to capture shape. The maxilla also has the second largest value of  $n_e$ , 9.1.

### Correlation among characters in the F<sub>2</sub>

The primary objective of our correlation analysis was to gain insight as to the total number of determinants that underlie shape differences in the cichlid head. When each bony element is considered independently, the number of genetic determinants appears to be small (<11), however, the sum of the independent estimates for each structure is much larger (>50). Results from the correlation analysis show that shape of many bony elements are inherited together. We, therefore, expect that some loci will affect shape differences in multiple structures, and the total number of determinants that distinguish LF and MZ will be less than the sum of the independent estimates.

Twenty-three of the fifty-five possible associations are statistically significant. Many of these correlations are conceptually intuitive, such as the strong, positive correlations between the upper and lower jaw dentition ( $p < 0.001$ ), the lower jaw in the lateral and ventral view ( $p < 0.001$ ), and the maxilla and premaxilla ( $p < 0.01$ ). Interestingly, tooth shape is not associated with the shape of either the dentary or premaxilla (elements within which teeth develop), but is correlated with both the articular and suspensorium ( $p < 0.05$ ). The two skeletal subunits of the lower jaw, the dentary and articular, are not correlated with one another, but the articular is correlated with virtually every other bony element in the head. The neurocranium in the lateral and ventral view is not correlated. The neurocranium does, however, show a strong positive correlation with the lower jaw in the lateral view ( $p < 0.001$ ).

## Discussion

### Biometrically estimating the genetic basis of adaptation

The Castle-Wright Estimator has been employed to evaluate the genetic basis of adaptation in several evolutionary model systems, including stickleback (Hatfield 1997) and *Bicyclus* (Wijngaarden and Brakefield 2000). While several assumptions underlie this estimator, recent modeling (Otto and Jones 2000) as well as quantitative trait locus (QTL) analyses (Peichel et al. 2001; Westerbergh and Doebley 2002) suggests that the method performs quite well. In all cases the estimator is taken as a minimum number of genetic factors. When the actual number of genetic factors is small ( $\leq 20$ ) (Otto and Jones 2000), or when the assumptions are met (Westerbergh and Doebley 2002), the difference between various approaches (e.g., Castle-Wright versus QTL) is quite small.

I use the Castle-Wright Estimator to take the first steps in understanding the genetic basis of differences in oral jaw morphology among cichlid fishes. During the early radiation of Lake Malawi's cichlids, an important functional divergence probably occurred between the three basic modes of feeding - biting, sucking, and ram-feeding (Albertson, et al. 1999; Greenwood 1974; Liem 1991) - a trend observed in many other groups of fishes (McPhail 1992, 1994; Schluter and McPhail 1993; Skulason et al. 1989, 1996). I examined MZ and LF because they are members of a monophyletic clade that lie on opposite ends of the biting/sucking continuum.

I find that the number of factors that underlie shape differences along this continuum is relatively small. For example, interspecific differences in dental cuspidness

are determined by approximately one gene. This is supported by the Castle-Wright Estimator as well as the roughly trimodal distribution of tooth shape observed in the  $F_2$ . Dentition features prominently in discussions of adaptive radiation in cichlid fishes (Greenwood 1974; Futuyma 1986; Ribbink et al. 1983; Ruber et al. 1999), because it tracks extremely well with feeding performance, making it a good indicator of trophic niche. Moreover, differences in tooth shape have been detected both between sister taxa (Ruber et al. 1999), and among different populations of the same species (Streelman, in prep). The observation that major differences in tooth shape (i.e. cusp number) may be controlled by as little as one gene suggests that this character has the potential to respond to selection extremely quickly.

Other notable observations include the estimated number of factors for the dentary and articular. Collectively, these two bones constitute the lower jaw. Our estimates suggest that the dentary and articular have very different capacities for morphological change. The dentary is controlled by one factor, suggesting that it, like tooth shape, has the potential to quickly respond to changes in the environment. On the other hand, the articular seems to be under the control of several loci, suggesting that morphological divergence in this character may require coordinated change at multiple loci.

The skull is a large and dynamic structure. Unlike the pharyngeal skeleton, which develops entirely from cranial neural crest cells, the neurocranium is derived from both neural crest and paraxial mesoderm. Functionally, the skull is associated with the oral jaw apparatus via the ethmoidal region of the skull, the pharyngeal jaws by way of the pharyngeal apophysis, and the epaxial musculature via the supraoccipital crest. Given the developmental and functional complexity of this structure, it is noteworthy that differences in skull shape between MZ and LF may be explained by as few as 4 genetic

factors. The ascertainment that shape difference is limited to the anterior-most region of the neurocranium (Albertson and Kocher, 2001) may help in explaining this observation.

### Phenotypic correlations

Many of the associations (or lack thereof) among elements in Figure 3.5 make sense in the context of recent molecular and developmental advances in several model organisms. For example, several mutant phenotypes in mouse have been characterized that affect tooth development. While at least two (*dlx1* and *dlx2*) affect upper and lower jaw dentition independently, the majority result in tooth defects on both the upper and lower jaws (i.e. *msx1*, *msx2*, *pax9*, *fgf8*, *pitx2*). Therefore, it is not surprising that I find tooth shape in the upper and lower jaws to be highly correlated ( $r = 0.95$ ). I expect that the same locus (loci) will affect cusp number in the upper and lower jaw of cichlids.

Tooth shape is not inherited with the bone within which teeth develop (dentary and premaxilla), but it is correlated with both the articular and suspensorium. These results suggest that the same loci may have a pleiotropic effect on tooth shape and the shape of the articular and suspensorium. These two elements develop from cartilagenous precursors within the first pharyngeal arch. Both tooth morphogenesis and chondrogenesis involve antagonistic signaling between FGFs (fibroblast growth factors) and BMPs (bone morphogenetic proteins; Peters and Balling 1999). For example, BMP4 soaked beads implanted into Meckel's cartilage explants induce exogenous cartilage formation (Semba et al. 2000), while mouse mutants lacking an FGF receptor will develop longer vertebrae (Crossley and Martin 1995). Similarly, Noggin (a BMP4 antagonist) beads implanted in developing incisors are responsible for a transformation of

tooth identity (Tucker et al 1998). Thus, FGFs as well as BMPs may be good candidates for the genetic determinants of size and shape in both teeth and bone which develops from cartilagenous precursors.

The articular and suspensorium are correlated with one another. A significant phenotypic correlation suggests that a common set of loci underlies form in these two elements. Thus, selection on one element will have an effect on the other.

Developmentally, the articular and suspensorium are derived from the dorsal and ventral cartilagenous sub-units of the first pharyngeal arch. Several zebrafish mutants are known (i.e. *suc*, *she*, *stu*, *hoo*) that disrupt the development of these elements (Piotrowski et al. 1996; Schilling et al. 1996).

The maxilla and premaxilla are correlated with one another. Both of these elements are dermal bone (bone that develops without a cartilagenous ascendant) that likely originate from mid-brain neural crest cells (Köntges and Lumsden 1996). Maxillary and premaxillary osteocytes also precipitate at approximately the same time (Albertson; unpublished data). Since most existing zebrafish mutants are lethal by 5 days post-fertilization, which is approximately a day before dermal bones appear, the developmental players involved in this process remain largely a mystery.

The lower jaw in the lateral view is highly correlated with the lower jaw in the ventral view, suggesting that a common set of loci affect both jaw length and jaw width. The lower jaw in the lateral view is also highly correlated with the neurocranium. The lower jaw and the skull are not adjacent to one another, and it seems difficult to imagine that this association is a result of steric or functional interactions. The cartilagenous precursors of both the lower jaw and neurocranium are among the first head structures to be seen in the developing teleost embryo, and a multitude of zebrafish mutants have been

described (i.e. *low, fla, bab, vgo, dol, cyc*) that affect both the jaw and the anterior region of the skull (Kimmel et al. 2001; Piotrowski et al. 1996; Schilling et al. 1996).

The dentary is not correlated with the articular ( $r = 0.02$ ). Functionally, the dentary fuses to the articular early in development to form the functioning lower jaw. Developmentally, however, these two elements are quite distinct. The dentary is a dermal bone that originates from mid-brain neural crest cells. The articular is endochondral and develops from both mid- and hindbrain cranial neural crest (Köntges and Lumsden 1996). The articular also appears 4 days earlier than the dentary in cichlid development (Albertson unpublished data). Like the masseteric and alveolar regions of the mouse mandible (Cheverud 2001), the articular and dentary clearly show that different developmental units are inherited separately.

## Conclusion

Our results lend support for the hypotheses that differences in the cichlid oral jaw apparatus are controlled by relatively few genes, and that pleiotropy figures prominently in the genetic architecture of the cichlid head. Moreover, I find that patterns of phenotypic correlation correspond to developmental rather than functional units. A number of genes involved in craniofacial development have been characterized in model organisms, most of which seem to have been conserved over vertebrate evolution. It remains to be seen whether these same players are also implicated in fine-scale adaptive variation among species.

The breadth of diversity that characterizes lacustrine cichlid assemblages make them ideal systems within which to study adaptive radiation and the evolution of feeding



mechanisms. Important future directions should include a more comprehensive dissection of the genetic and developmental architecture of the cichlid head. This knowledge will help identify the fundamental units upon which natural selection acts, as well as better facilitate an understanding of how the oral jaw apparatus responds to selection. A formal test of integration (i.e. – morphological (as in Liem 1980; Zelditch 1987), genetic (as in Cheverud 1982, 2001; Leamy et al. 1998), or developmental (as in Mezey et al. 2000)) would go a long way toward this goal. Also, given the estimated number of genes identified here, it appears feasible to conduct an experiment to map loci underlying these quantitative traits. An experiment with approximately 200 F<sub>2</sub> should have the power to detect most, if not all, of the genetic determinants of shape difference between MZ and LF (Beavis 1998).

#### Acknowledgements

This work was performed in collaboration with J. Todd Streebman and Thomas D. Kocher. I thank A. Ambali, the University of Malawi, and the Malawi Government for assistance with collection of specimens and J. Hanken, K. Liem, P. Wainwright, K. Carleton and J. Bolker for technical advice, discussion and critical reading of the manuscript. Dermestid beetles were housed by M. Scott. All illustrations were done by R. Craig Albertson. This work was supported by a National Science Foundation Grant (IBN 9905127) awarded to T. D. Kocher.

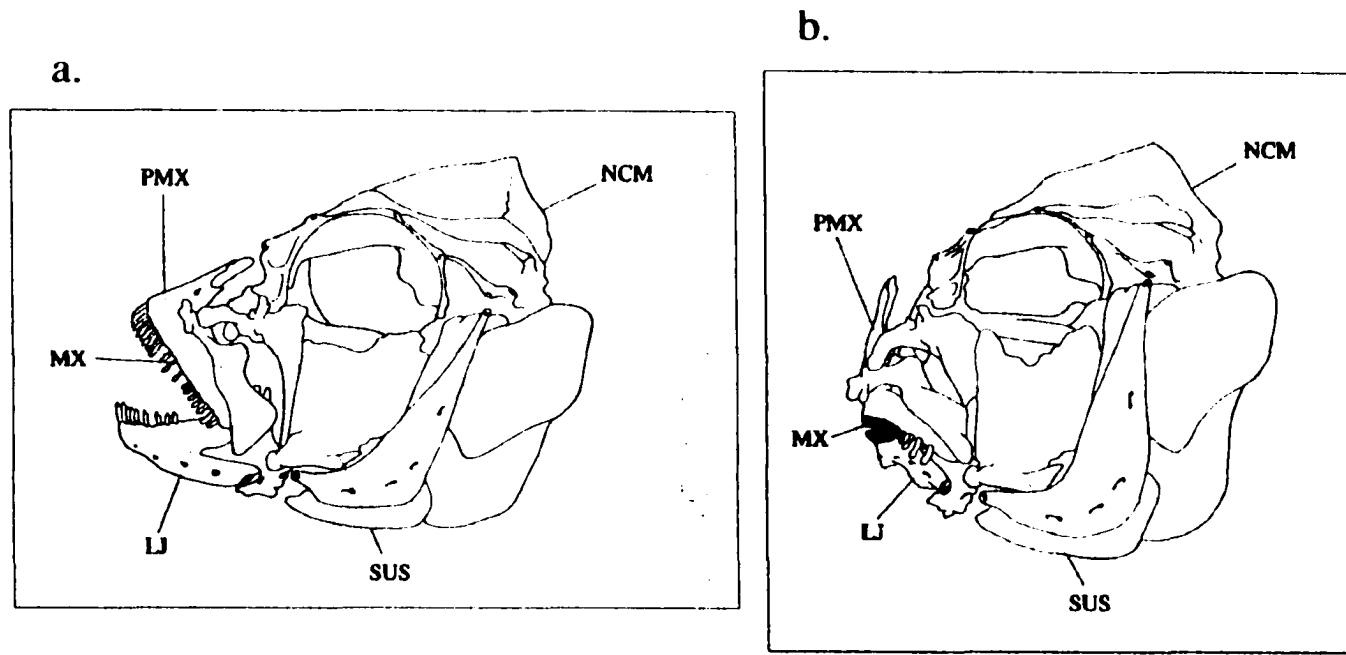


**Figure 3.1**

Craniofacial skeletal morphology of *Metriaclima zebra* (A) and *Labeotropheus fuelleborni* (B). LJ – Lower Jaw, MX – Maxilla, NCM – Neurocranium, SUS – Suspensorium, PMX – Premaxilla

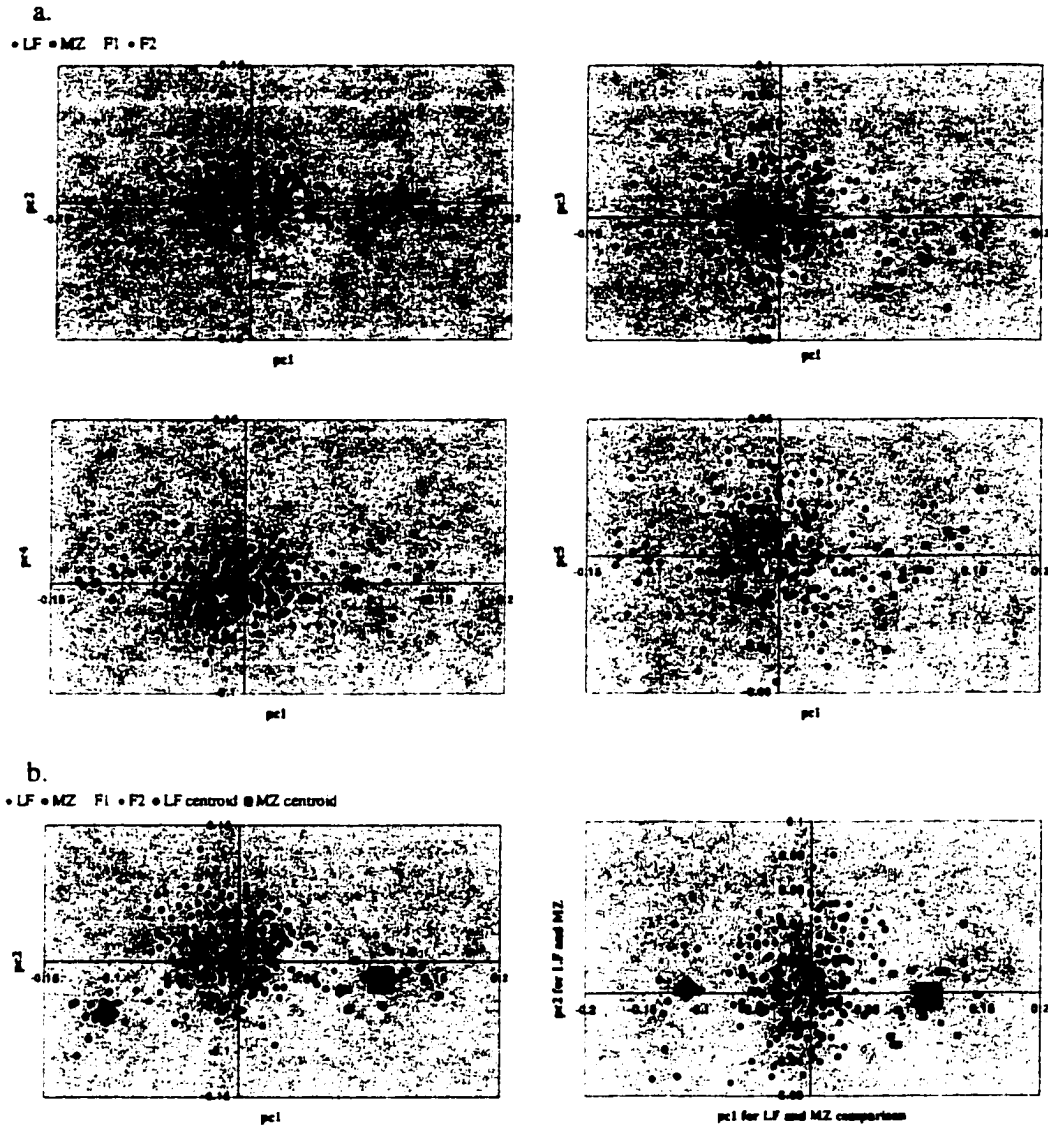


**Figure 3.2**  
 Explanation of experimental design. a. Graphical representation of principal components 1 through 5 for the articular, which collectively accounted for >90% of the variance. Note that virtually all of the interspecific variation is on pc1, whereas pc2 through pc5 account for within group variance. Thus, the genetic basis of difference along pc1 is sought. Every other skeletal element showed the same pattern of variance partitioning. b. Since pc1 did not intersect the centroids of LF and MZ when all groups were included, a principal component analysis was performed on the parental species, then hybrids were assessed relative to parental axes 1 and 2 by multiplying hybrid partial warp scores by parental eigenvectors.

*Metriaclima zebra*

*Labeotropheus fuelleborni*

Dentary  
0.64 ± 0.5



Articular  
9.0 ± 5.2



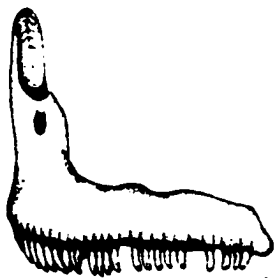
Lower Jaw  
(lateral)  
10.5 ± 6.1



Lower Jaw  
(ventral)  
8.9 ± 3.8



Premaxilla  
7.7 ± 3.8



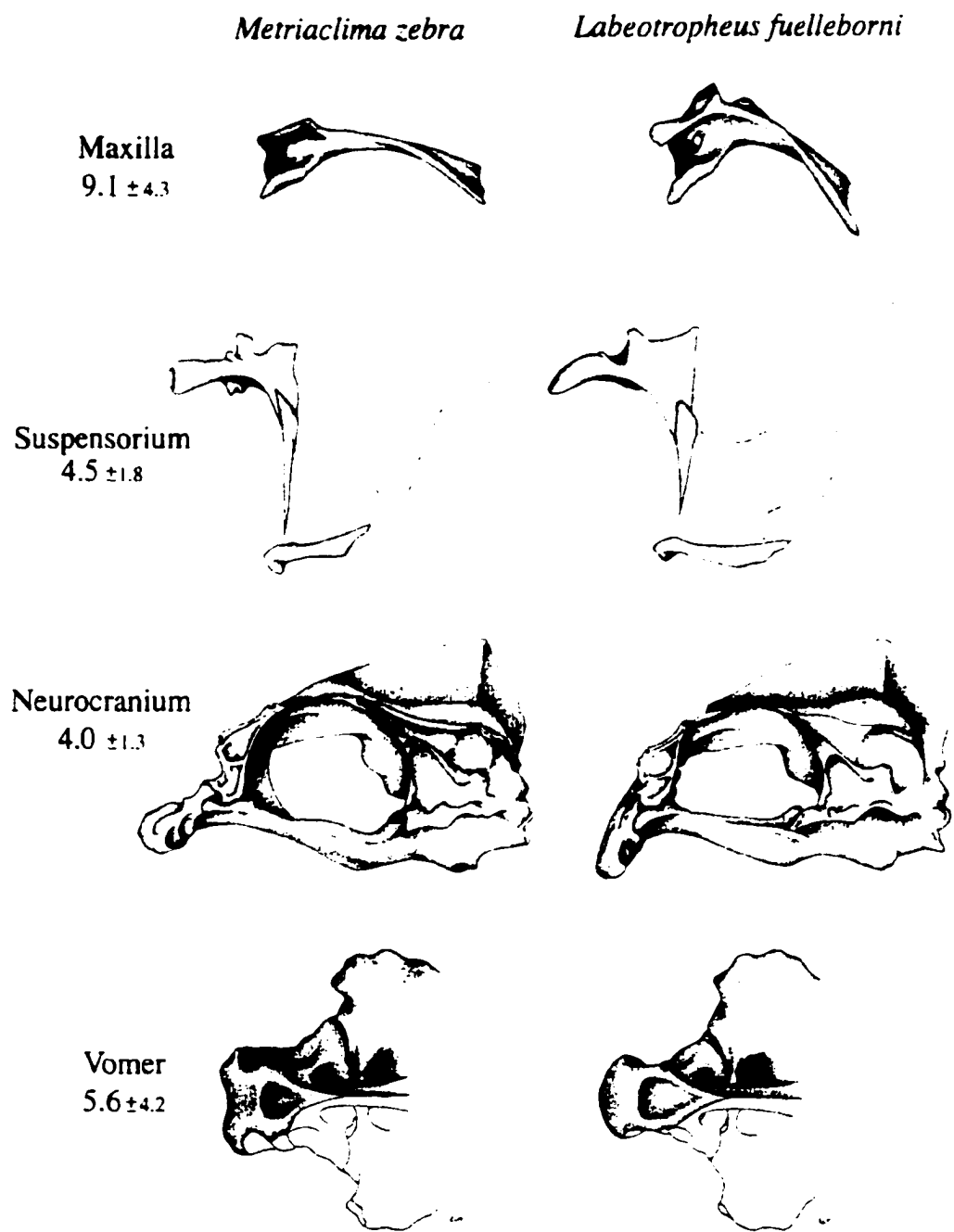


**Figure 3.3**

Number of genetic factors that underlie geometric shape differences between MZ and LF.

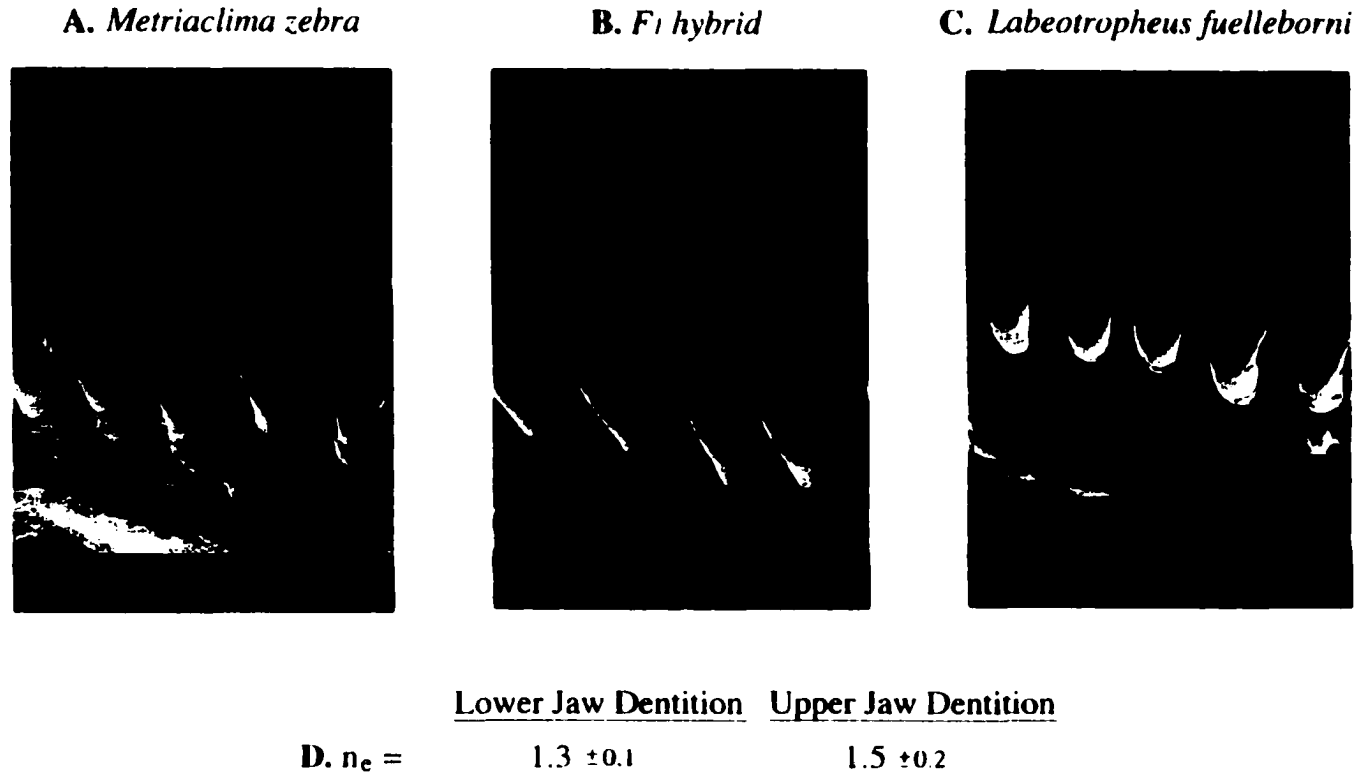


**Figure 3.4**

(A-C) SEM images of lower jaw dentition in MZ,  $F_1$ , and LF. \* is the third cusp in hybrid animals that tends to vary in size. (D) estimated number of factors that underlie upper and lower jaw cuspidness.

**Figure 3.5**

Distribution of craniofacial characters for parental species and both hybrid generations. Note the regeneration of parental morphology in the F2 for several characters. The y-axis is frequency and the x-axis is environmental standard deviation units, taken as the standard deviation of the F1 generation for each element.

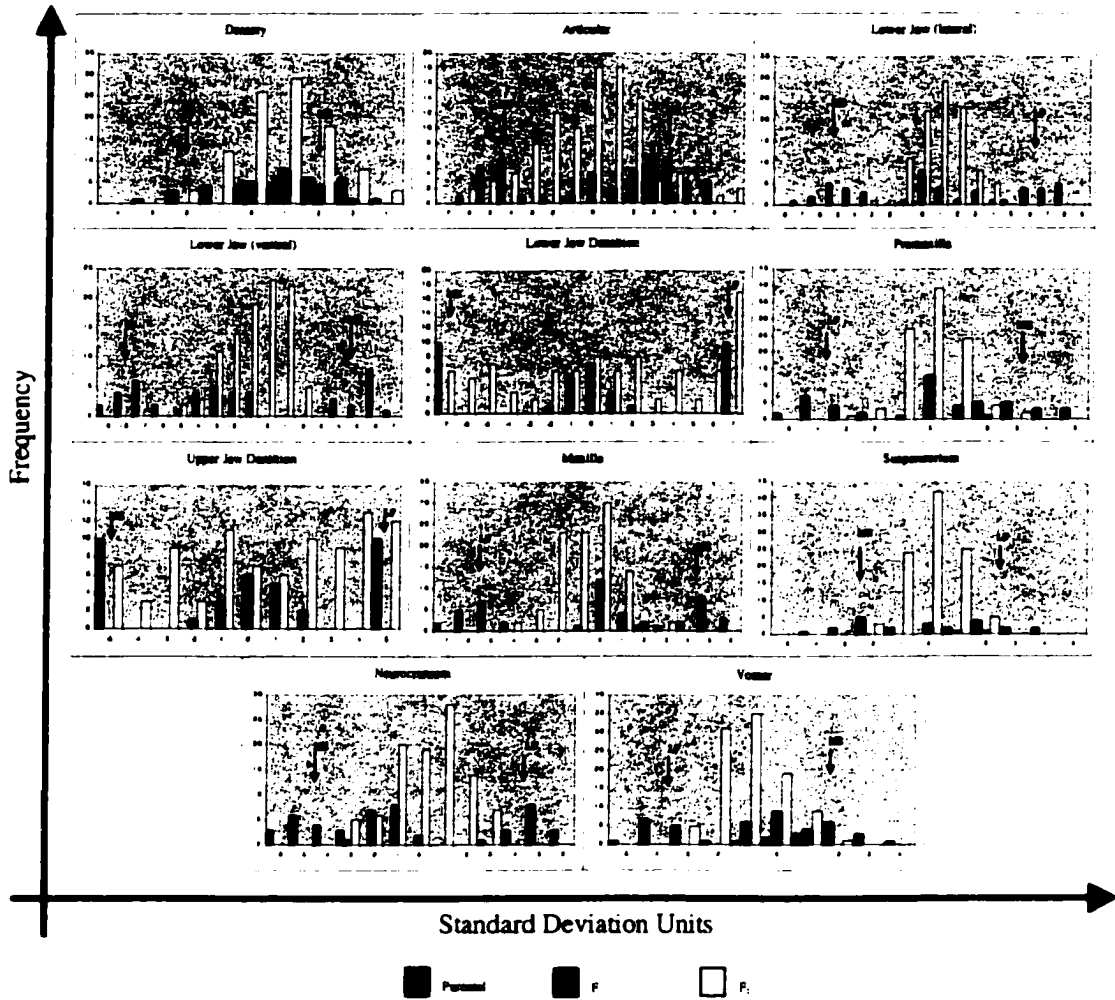


**Figure 3.6**

Pearson correlation between oral jaw characters. 23 of the 55 possible associations are significant. A. Matrix of numerical coefficients of r. B. Conceptual rendering of correlation matrix. DNT - dentary, ART - articular, LJJ - lower jaw in the lateral view, LJV - lower jaw in the ventral view, LJD - lower jaw dentition, PMX - premaxilla, UJD - upper jaw dentition, MX - maxilla, SUS - palatine region of the suspensorium, NCM - neurocranium, VM - vomer.

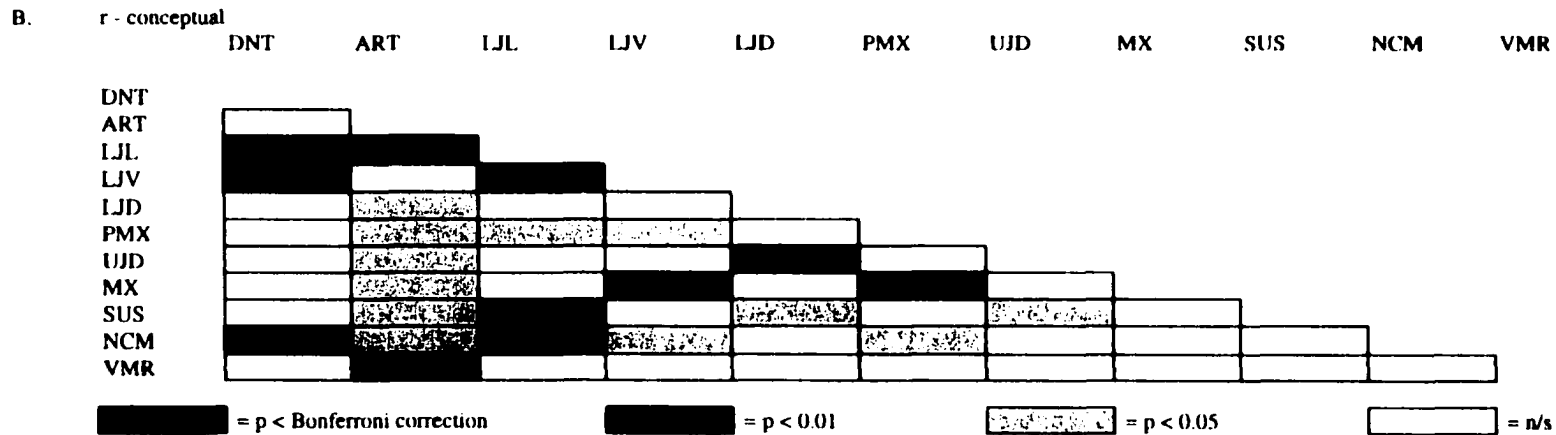
A. pearson r

	DNT	ART	LJJ	LJV	LJD	PMX	UJD	MX	SUS	NCM	VMR
DNT	1.00										
ART	0.02	1.00									
LJJ	0.62 ***	0.31 **	1.00								
LJV	0.46 ***	0.12	0.61 ***	1.00							
LJD	0.00	0.21 *	0.11	0.05	1.00						
PMX	0.11	0.21 *	0.22 *	0.20 *	0.05	1.00					
UJD	0.03	0.23 *	0.11	0.03	0.95 ***	0.03	1.00				
MX	0.00	0.20 *	0.07	0.29 **	0.04	0.29 **	0.01	1.00			
SUS	0.09	0.22 *	0.29 **	0.16	0.21 *	0.12	0.20 *	0.15	1.00		
NCM	0.30 **	0.21 *	0.47 ***	0.25 *	0.12	0.22 *	0.18	0.14	0.04	1.00	
VMR	0.01	0.29 **	0.12	0.12	0.08	0.09	0.10	0.11	0.12	0.12	1.00

\*\*\* = p < Bonferroni correction

\*\* = p < 0.01

\* = p < 0.05





## CHAPTER 4

### A GENETIC LINKAGE MAP FOR LAKE MALAWI'S ROCK-DWELLING CICHLIDS, THE MBUNA

#### Abstract

A genetic map for Lake Malawi rock-dwelling cichlids was constructed using molecular markers. Segregation at 130 microsatellite loci and six genes was studied in 173 F<sub>2</sub> hybrids derived from an intergeneric cross between two Lake Malawi rock-dwelling species. Two sires and two dams were used to produce two F<sub>1</sub> families. F<sub>2</sub> hybrids were generated via brother-sister matings of the F<sub>1</sub>. Linkage was detected among 126 markers. The map spans 838 cM over 24 linkage groups, with an average interval size of 6.6 cM. I compared this linkage map to a genetic map of another cichlid fish, the tilapia (*Oreochromis niloticus*). Markers were identified that segregate with two simple traits: color and sex.

## Introduction

East African cichlid fishes are paramount examples of rapid (Owen et al. 1990; Johnson et al. 1996), replicative (Kocher et al 1993), and extensive evolutionary radiation (Futuyma 1986; Fryer and Iles 1972). For close to a century scientists have endeavored to understand the mechanisms involved in the rise and maintenance of species diversity in lacustrine cichlid assemblages. Both sexual selection of male nuptial color and natural selection on feeding morphology have been implicated as contributing forces to cichlid diversity, but the genetic basis of these fitness related traits remain unknown.

The construction of a genetic linkage map for Lake Malawi cichlids is the starting point for mapping experiments aimed at characterizing the genetic architecture of adaptive radiation and speciation in these remarkable fishes. To demonstrate the utility of this resource, the Malawi linkage map was compared with the genetic map for tilapia, and the segregation of two simple traits were characterized and mapped to specific chromosomal regions.

## Materials and Methods

### Species

*Labeotropheus fuelleborni* (referred to as “LF” from here on) and *Metriaclicma zebra* (“MZ”) are haplochromine cichlids endemic to Lake Malawi. LF and MZ are members of the rock-dwelling assemblage, locally known as mbuna, which employ very different modes of feeding. LF is optimally designed to crop attached algae from the substrate, whereas MZ feeds both from the substrate and the water column.

### Experimental cross

Hybridization was achieved by placing two male LF in a 500-gallon pool with five MZ females. Both LF and MZ are mouth-brooding species, which means females incubate embryos in their mouths until they are free swimming (~21 days). Females holding a clutch were easily identified by their enlarged buccal pouch. Brooding females were removed from the breeding pool and placed in ten-gallon tanks until fry were released. Two F<sub>1</sub> families derived from two male LF and two female MZ were used to produce F<sub>2</sub> families via brother-sister mating.

### Genomic DNA extraction

Dorsal fin clips were taken from adult animals. Clips were stored in 90% EtOH at -20°. Tissue was washed with sterile distilled water and placed into individual sterile 1.5 ml microcentrifuge tubes containing 500 µl extraction buffer (10 mM Tris pH 8.0, 2 mM EDTA pH 8.0, 10 mM NaCl, 1% SDS, 8 mg/ml DTT, 0.4 mg/ml proteinase K). Tubes were placed at 37° overnight. Two phenol/chloroform/isoamyl alcohol (25:24:1) and one chloroform extraction were performed. DNA was precipitated with NaCl in 100% EtOH at -80° for two hours. Pellets were washed with 70% EtOH, and resuspended in 0.1 TE buffer.

### Microsatellite Markers

An enriched *Metriaclima zebra* genomic DNA library was constructed following (Lee and Kocher 1996), and screened with a CA<sub>16</sub> probe. 480 clones were sequenced, and primer pairs flanking 208 microsatellites with ten or more dinucleotide repeats were designed.

### Genes

Six genes were typed in the F<sub>2</sub>: *bmp4*, *cski*, *wtl*, *ins*, *prl*, and *clc5*. Every gene except *bmp4* had a microsatellite in an intron and LF and MZ differed in the number of repeat units. Using degenerate primers, genomic *bmp4* was sequenced in LF and MZ. A silent SNP was identified in the coding region of *bmp4*. Specific primers were designed

to amplify 147bps around the SNP. A restriction digest using Hpy CH4V produced restriction fragment length differences that were used to map *bmp4* in the LF x MZ cross.

### Tilapia microsatellites

The tilapia, *Oreochromis niloticus*, is a cichlid fish native to African lakes and rivers (Trewavas, 1983). Tilapia have been introduced around the globe as an important aquaculture species. Current world production of tilapia is ~ 2 million metric tons per year (FAO Fisheries Statistics 1999), the majority of which consists of the species *Oreochromis niloticus*.

A linkage map for *O. niloticus* exists that consists of > 500 microsatellite markers distributed over 1200 cM and 24 linkage groups. Since this species diverged from Lake Malawi cichlids approximately 10 million years ago, I tested 248 tilapia-specific microsatellites in the LF x MZ cross. Mapping tilapia markers in a cross among Malawi cichlids provides an opportunity to compare both genetic maps.

### Typing of microsatellites

Microsatellite genotypes were obtained with an ABI 377 (PE Applied Biosystems) automated sequencer, which sized fluorescently labeled alleles amplified by PCR. I used 20 µl PCR reactions containing 5 µM of each primer, 20 ng DNA, 16 mM dNTPs, 50 mM MgCl<sub>2</sub>, and 1 unit Taq polymerase. Primer pairs were multiplexed up to three ways whenever product size and the color of the fluorescent label allowed. When

multiplexing, primer concentrations were 2.5  $\mu\text{M}$ . Cycling conditions were: 94° for 2 min; 30-35 cycles of 94° for 30 sec, 52° for 30 sec, 72° for 30 sec; 72° for 5 min.

For genotypic analysis 1  $\mu\text{l}$  of PCR reaction was added to 0.24  $\mu\text{l}$  GeneScan 500 TAMRA size standard (PE Applied Biosystems) and 2.0  $\mu\text{l}$  formamide loading buffer. The solution was denatured and loaded on a 4% acrylamide gel. ABI GeneScan software (ver. 3.1.2) was used to analyze genotypes.

### Linkage analysis

A linkage map was constructed using JoinMap 3.0 (van Ooijen and Voorrips 2001). The locus file consisted of genotypes for 173  $F_2$  hybrid progeny at 136 microsatellites. The grouping module of JoinMap assigned 126 of 136 marker loci to 24 linkage groups using a LOD score threshold of 4.0. The mapping module of JoinMap built the genetic map for each linkage group using Kosambi mapping function, a LOD threshold of 1.0, a recombination threshold of 0.450, and a jump threshold of 5.0. A ripple function was performed after each marker on a linkage group was added to ensure optimal map order.

### Phenotypic traits

Two simple traits were scored in the  $F_2$  progeny: color morphology and sex. Natural populations of LF and MZ have two general color morphologies: a blue body with black vertical stripes (BB, for black bars) and an orange body with black blotches (OB, for orange blotched). The BB color morph is the more typical color pattern, and

occurs in both sexes. The OB morph is less common and occurs almost exclusively in females (though, OB males of both species are observed rarely). F<sub>1</sub> family 2 was produced by crossing a BB LF male with an OB MZ female. F<sub>2</sub> animals from this sibship were scored as either BB or OB.

Cichlids do not have obvious sex chromosomes, and sex is determined by one (or several) sex-determining loci. The existence of sex-reversal genes (Lande et al. 2001), and homoplasmy of sex-determination among closely related species (Crapon de Caprona and Fritzsich 1984), make issues of sex complex and largely theoretical, particularly in haplochromine cichlids. Mapping sex determining factors in different cichlid species is the key to unraveling this mystery. F<sub>2</sub> progeny were scored for sex using external diagnostic characters, including vent size, shape, and position.

### Mapping of phenotypic characters

Color and sex were analyzed with MapQTL 4.0 (van Ooijen et al. 2002) using the nonparametric mapping method. This approach employs the Kruskal-Wallis rank sum test, which is described in detail by van Ooijen et al (1993). The Kruskal-Wallis test is performed on one locus at a time, and makes no assumption about the distribution of the phenotypic data. The test ranks all individuals according to their phenotypic value, and then sorts them by marker genotype. A QTL of large effect segregating with a marker locus will result in large differences in the average rank of marker genotypic classes. Under the null hypothesis of no segregating QTL, the Kruskal-Wallis test statistic (K) is distributed approximately as a chi-square distribution where degrees of freedom are equal to the number of genotypic classes minus one. Since the test is performed on many linked

and unlinked loci, I only reported associations between marker loci and QTL with a p-value less than 0.0001.



## Results

### Pedigree

Two LF males and two MZ females were used to produce two F<sub>1</sub> sibships (figure 4.1). In total, 14 F<sub>2</sub> families were used in this experiment: 2 from sibship one, and 12 from sibship 2. F<sub>2</sub> family sizes were smaller than those for LF, MZ, and F<sub>1</sub> hybrids. F<sub>2</sub> family sizes ranged from 10-20 individuals, whereas LF, MZ and F<sub>1</sub> families were typically between 20-40 individuals. F<sub>2</sub> mortality was observed from early embryonic development throughout the life of animals, and was not distinctly correlated with any one developmental stage. Thus, smaller F<sub>2</sub> family sizes might be the result of recessive lethals acting at various points in development, or segregation of traits affecting general fitness (i.e. growth rate, aggression, disease resistance, vigor).

### Genotypes

A total of 173 F<sub>2</sub> hybrids from the LF x MZ cross were typed for 462 molecular markers. Of the 208 Malawi cichlid derived markers typed, 119 (57%) amplified strong bands and 90 (44%) were polymorphic. Of the 248 tilapia markers tested, 146 (59%) amplified robust bands and 39 (16%) were polymorphic. All six genes mapped in tilapia were also mapped in the Malawi cross. The final data set consisted of 136 marker genotypes for 173 F<sub>2</sub> progeny.

### Linkage map

126 (93%) of the markers typed in the F<sub>2</sub> showed detectable linkage to another marker: 6 (100%) genes, 37 (95%) tilapia microsatellites, and 83 (91%) Lake Malawi microsatellites. The final genetic map spanned 838 cM (figure 4.2) over 24 linkage groups. The average marker interval was 6.6 cM. Linkage group size ranged from 4 to 91 cM (average = 34.9 cM). The number of markers per linkage group varied from 2 to 16 (average = 5.1).

### Comparative mapping

22 mbuna linkage groups contained at least one tilapia marker; 14 of these had two or more. Marker positions were used to identify syntenic regions between tilapia and mbuna. In every instance, marker order was conserved. In all but three instances one mbuna linkage group corresponded to one tilapia linkage group. Mbuna linkage group 2 corresponded to tilapia linkage groups 17 and 18, whereas tilapia linkage groups 1 and 2 corresponded to mbuna linkage groups 5 and 11, and 7, 13 and 18, respectively (table 4.1).

### Segregation distortion

Because this was an intergeneric cross and F<sub>2</sub> hybrids showed increased mortality, I was concerned about segregation distortion due to markers being linked to deleterious alleles. Observed segregation was tested against the expected genotypic ratios with a  $\chi^2$ -test in JoinMap 3.0 (van Ooijen and Voorrips 2001). A total of 10 (7.9%) markers

showed significant ( $<0.05$ ) segregation distortion. Markers UNH2112, UNH2120, and UNH2173 mapped to linkage group 13, and markers UNH2032 and UNH2117 mapped to within one cM of each other on linkage group 1. The remaining 5 loci map to different linkage groups.

### Segregation of Color and Sex

Linkage between sex and color morphology breaks down in LF x MZ hybrids. Of the 41  $F_1$  progeny in sibship 2, 9 (22%) were OB males, 11 were BB males (27%), 9 (22%) were OB females, and 12 (29%) were BB females. Thus, sex and color are segregating independently in the  $F_1$ .  $F_2$  progeny tended to express the phenotype of their  $F_1$  parents (table 4.2). All BB x BB matings produced either BB males or BB females. OB x OB pairings produced 16 OB males, 16 OB females, 2 BB males, and 2 BB females. One OB male x BB female pairing produced 4 OB males, 1 OB female, 1 BB male, and 3 BB females. BB male x OB female matings generated 8 OB males, 24 OB females, 19 BB males and 11 BB females.

Color segregates with *cski* ( $K=42$ ,  $p<0.0001$ ) and UNH2139 ( $K=32$ ,  $p<0.0001$ ) on linkage group 12 (figure 4.3). Sex segregates with UNH2095 ( $K=31$ ,  $p<0.0001$ ), UNH2086 ( $K=36$ ,  $p<0.0001$ ) and UNH2031 ( $K=33$ ,  $p<0.0001$ ) on linkage group 1 (figure 4.3).

## Discussion

### Comparative mapping

To date, most comparative genomic studies have been limited to analyzing syntenic blocks among widely divergent taxa (Amid et al 2001; Bagheri-Fam et al 2001; Kappen and Salbaum 2001; Santagati et al 2001). Few investigations have examined genome evolution at higher taxonomic levels (although see, Lillo et al 2002; Wong et al 2002 for exceptions in microbes). The rising field of comparative genomics would benefit greatly by comparing more closely related genomes. Genome evolution is of particular interest in cichlids with respect to identifying alterations that may be associated with speciation.

I find good concordance between tilapia and mbuna genetic maps. Whenever three or more tilapia markers mapped to an mbuna linkage group the order is preserved, consistent with the hypothesis that chromosome evolution is slow among these cichlids (Kornfield 1984).

The ancestral karyotype for teleosts is thought to consist of 24 pairs of chromosomes (Gold 1979). Since most cichlids species examined ( $n = 70$ ) also have 24 chromosomes pairs, the ancestral condition among cichlids is believed to be  $n = 24$  (Kornfield 1984). Among Old World cichlids, chromosomal characterization has been largely limited to different tilapine species. The karyotype of *Oreochromis niloticus* represents the norm for tilapia,  $n = 22$  (Arai and Koite, 1980). Only one karyotype exists for a lamprologine cichlid; *Lamprologus leleupi*, from Lake Tanganyika, had  $n = 24$  (Post, 1965). The only haplochromine karyotypes come from three Lake Malawi

endemics. *Melanochromis auratus* had  $n = 23$  (Thompson, 1981), while both *Metriaclima zebra* and *Labeotropheus fuelleborni* had  $n = 22$  (Kornfield et al 1979).

The karyotypes of MZ and LF differed from *Melanochromis* in having two less subtelocentric chromosomes, but were indistinguishable from one another. Both were characterized by one large pair of subtelocentric chromosomes, a series of 15 smaller pairs of subtelocentric chromosomes, one large pair of submetacentric chromosomes, and four smaller pairs of metacentric/submetacentric chromosomes (Kornfield et al 1979).

The phylogenetic relationship among these three cichlid families place tilapines as most ancestral and haplochromines most derived (Kocher et al. 1995). Assuming an ancestral condition of  $n = 24$ , two hypotheses can be formulated regarding chromosomal evolution in Old World cichlids. Either (1) chromosomal reduction occurred early, with the lamprologine going through a subsequent expansion in chromosome number, or (2) chromosomal reduction occurred in tilapines and haplochromines independently, with lamprologines representing the ancestral state. Results presented above offer support for the later hypothesis.

The observation that one haplochromine linkage group corresponds to two tilapia linkage groups, while two tilapia linkage groups correspond with at least four haplochromine linkage groups, suggests that chromosome number was reduced independently in tilapia and haplochromines. Linkage maps for many other cichlid species need to be investigated before a clear picture of genome evolution in Old World cichlids comes to light.

## Segregation of Sex and Color

OB in natural populations. The OB/BB color polymorphism occurs in several rock-dwelling species in both Lake Malawi and Lake Victoria. OB color is linked to a female determining factor in every species that it occurs. In both Lake Malawi and Lake Victoria cichlids, the OB locus seems to affect the deployment and patterning of melanocytes during larval and juvenile development (Seehausen et al 1999; Albertson unpublished data). These observations suggest that a similar gene, if not the same locus, may be involved.

The OB color polymorphism does not occur among Lake Tanganyika cichlid species, and appears to be specific to haplochromine cichlids. The OB locus may have arisen in the ancestor of Malawi and Victoria cichlids. Alternatively, OB color could have evolved in parallel in each assemblage.

Line cross analysis in species from Lakes Malawi (Holzberg 1978) and Victoria (Seehausen et al. 1999) that have the OB color polymorphism suggest that OB is sex-linked rather than sex-limited. Thus, OB males that occur in natural populations may represent recombinants between the OB and sex-determining loci. Alternatively, Holzberg (1978) suggests that OB males are the result of an unusually high concentration of male-determining factors on the autosomes. Regardless of which mechanism produces them, OB males seem to have extremely low fecundity.

Male and female OB MZ do not readily breed in captivity (M.C. Kidd, personal communication). Moreover, only 3 of 27 embryos survived when off-spring from an OB x OB MZ cross were reared artificially (Holzberg 1978). These observations implicate pre- and post-mating barriers in eliminating the OB-male allelic combination from natural populations.

OB and sex in the LF x MZ cross. Color and sex segregated independently in the  $F_1$  of LF and MZ. Further,  $F_2$  animals tended to resemble the phenotypes (sex/color) of their  $F_1$  parents (table 4.2). These observations are consistent with the hypothesis that OB is a sex-linked trait.

I have identified chromosomal regions that segregate with the MZ OB locus, and the LF male-determining locus. Two general conclusions can be drawn from our results. First, the OB and sex-determining locus are different in LF and MZ. Second, the MZ OB allele is dominant, and the LF male-determining factor is dominant.

In separate experiments, the segregation of sex and OB within MZ has demonstrated that female MZ are the heterogametic sex and the OB allele is dominant (Holzberg 1978; Kocher unpublished data). The difference in genetic sex-determination between MZ and LF could be as simple as WZ and XY, where the relative strength of alleles are:  $Y > W > X > Z$ . This is supported by the observation that when the LF x MZ cross is performed in the opposite direction (i.e., MZ males x LF females) all  $F_1$  hybrids are female ( $n = 35$ ). More extensive intraspecific breeding and mapping experiments must be performed in LF and MZ to verify the map positions of sex determination and color in each species. Specifically, segregation of sex and color should be assessed in LF to test the hypotheses that the OB locus is recessive, and LF males are heterogametic.

OB hybrids from the LF x MZ cross were generally uniform in their degree of blotching (i.e., the percentage of the body covered with black blotches). Although this trait was not quantified, several  $F_2$  were identified that had either excessive blotching or virtually no blotching. In every instance, individuals with reduced blotching were female ( $n = 7$ ). Likewise, with only one exception, individuals with profuse blotching were male ( $n = 10$ ). It has been suggested that individuals with little or no blotching in nature represent homozygotes at the OB locus (Holzberg 1978; Seehausen et al. 1999). In these

individuals, the OB color patterns also develops earlier than in OB heterozygotes. Interestingly, all but one F<sub>2</sub> with reduced blotching were MZ homozygotes at the *c-ski* locus. Whether OB color develops early in *c-ski*<sub>MZ</sub>/*c-ski*<sub>MZ</sub> F<sub>2</sub> remains to be seen.

It has also been postulated that an OB modifying locus is linked to the male determining factor in Lake Victoria cichlids (Seehausen et al. 1999). Unfortunately, sex segregates with three markers in the LF x MZ cross, and none of the ten profusely blotched F<sub>2</sub> seemed to segregate with any one marker. In order to find OB modifiers, the degree of blotching needs to be scored and mapped as a quantitative trait.

Candidate markers for OB and sex. Sex and color segregate with (or near) 2 very attractive candidate loci: *wtl* and *c-ski*, respectively. *Wtl* is an autosomal sex-determining gene in mammals. In particular, *wtl* encodes a zinc-finger transcription factor that is part of the regulatory network for gonadogenesis (Wilhelm and Englert 2002). In humans and mouse, *wtl* maps very closely to *fshb*, which encodes the beta subunit of follicle-stimulating hormone (FSHB), which regulates gonad function in mammals. *Wtl*, or a closely linked gene, may be worth pursuing as a candidate for sex determination in haplochromine cichlids.

The *c-ski* proto-oncogene encodes a transcription factor that binds to DNA in association with other proteins. *C-ski* has been implicated in regulating normal growth and development of several neural crest derivatives, including the craniofacial skeleton, skeletal musculature, and melanocytes. Several lines of evidence suggest *c-ski* acts by regulating the proliferation of progenitor cells. Tissue specific over expression of *c-ski* is correlated with melanoma in humans (Fumagalli et al 1993), and results in muscle hypertrophy in mice (Sutrave et al 1990). In contrast, mice lacking *c-ski* have grossly reduced craniofacial structures (Berk et al 1997).



*C-ski* is X-linked in humans. Two classes of *c-ski* have been identified in tilapia: one is expressed predominantly in the ovaries, the other is expressed mainly in the testes (Huang et al 1999). Thus, *c-ski*, or another linked gene, may be involved in sex-determination in certain organisms. Given its role in melanocyte proliferation and its association with sex, *c-ski* should be pursued vigorously as a candidate for the OB/BB color polymorphism in MZ, and perhaps in all haplochromine cichlids.

### Acknowledgements

Thanks to Janet Conroy, Woo-Jai Lee, J. Todd Strelman, and Karen Carleton who isolated the tilapia-specific microsatellites (UNH169 – UNH1009). J. Todd Strelman designed primers to amplify microsatellites in *wtl*, *prl*, *clc5*, *ins* and *cski*, and performed the restriction digest to map *bmp4*. Woo-Jai Lee kindly provided primers for Genomar (GM) markers. All of these resources contributed greatly to the success of this endeavor.

**Table 4.1**  
**Comparative map.** Corresponding linkage groups between Lake Malawi rock-dwelling cichlids and tilapia. Map order is conserved whenever three or more markers are shared.

mbuna Linkage Groups	Tilapia Linkage Groups	Markers in common
1	3	UNH2199, GM570, UNH973, UNH896, wt1
2	17,18	UNH933, bmp4
3	13	UNH874, UNH1009
4	6	GM198
5	1	UNH948, UNH908
6	10	GM575
7	2	UNH875, UNH2191
8	16	GM150, clc5, GM204
9	9	UNH1003, GM571, UNH906
10	12	UNH216
11	1	ins, UNH915, UNH937, UNH932
12	15	UNH169, cski
13	2	UNH919, UNH983
14	5	UNH989
15	8	prl, UNH911
16	7	UNH958
17	11	UNH974, UNH362, UNH951
18	2	UNH843
19	21	GM493
20	unknown	
21	unknown	
22	22	UNH138
23	23	GM128, GM385
24	4	UNH934, GM479

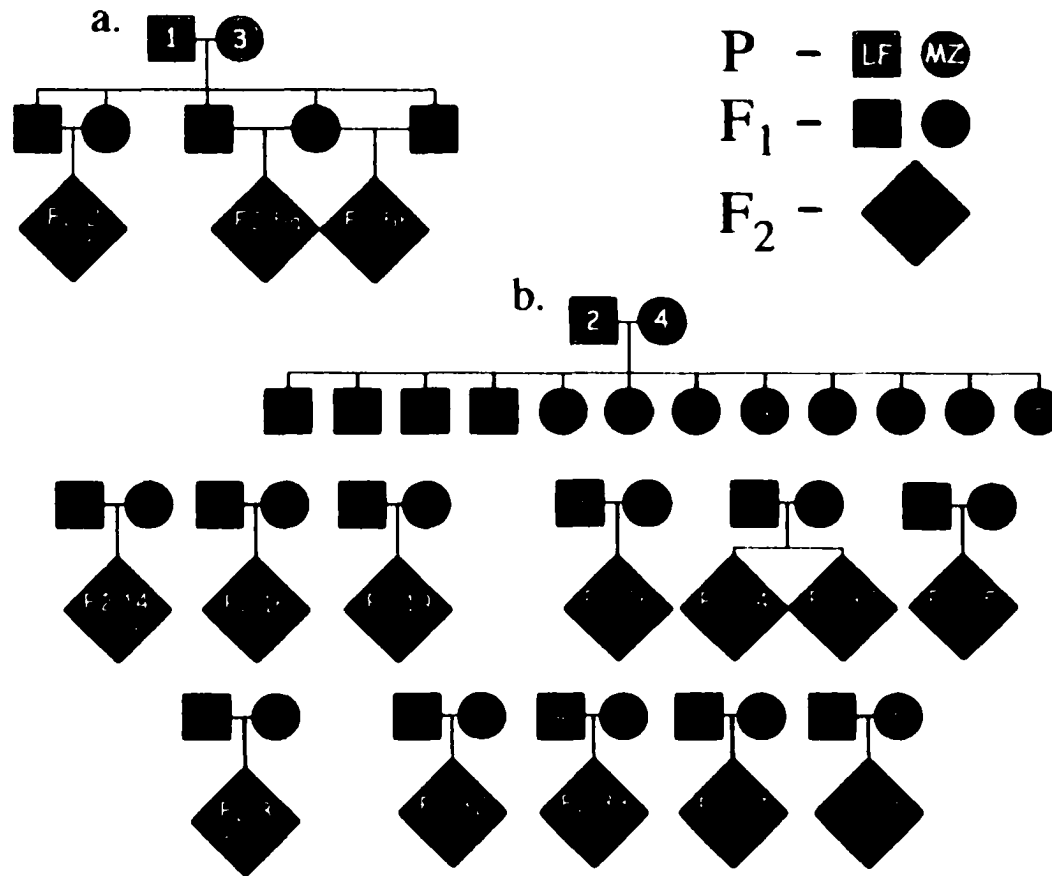
**Table 4.2**

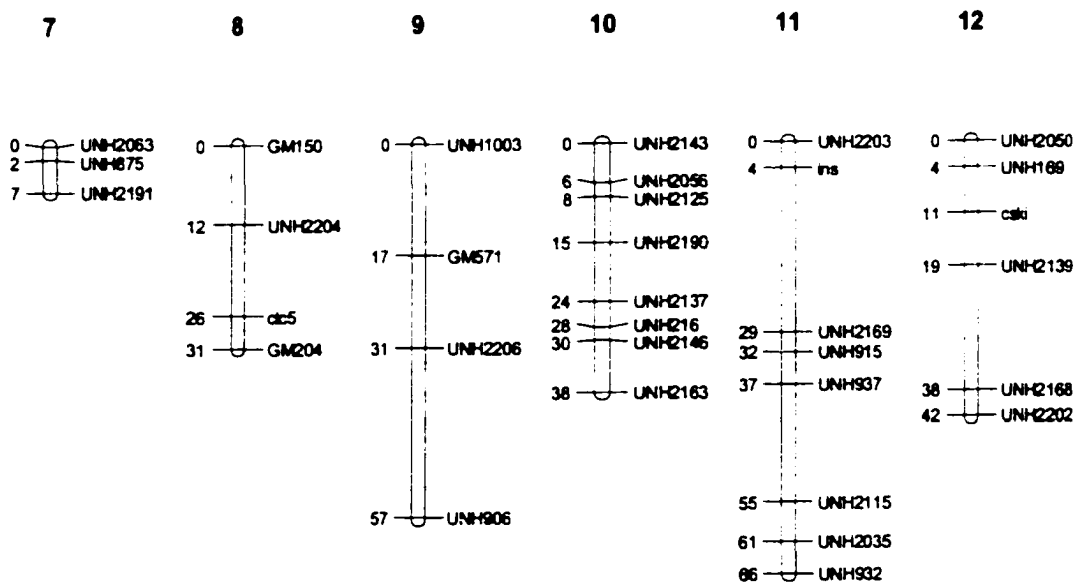
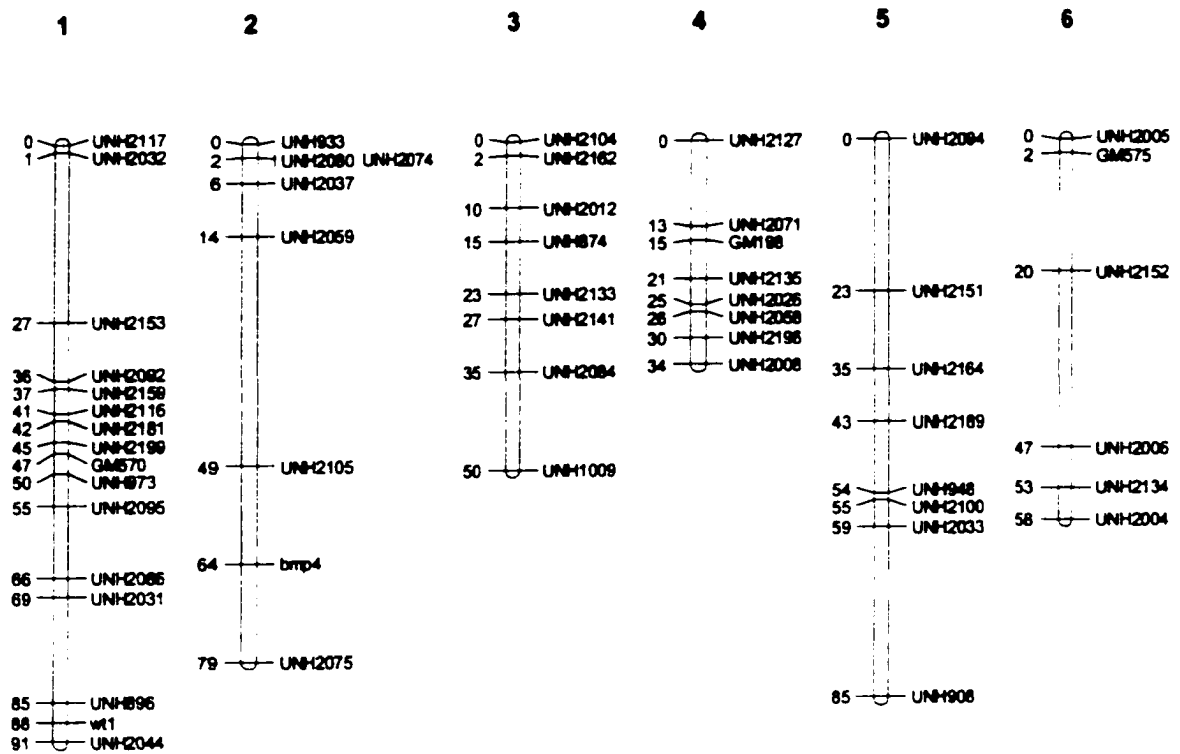
**Segregation of color and sex.** The linkage between OB color and sex breaks down in the F<sub>1</sub> generation. F<sub>2</sub> progeny tend to express the phenotype of their F<sub>1</sub> parents.

P	LF BB male	x	MZ OB female		
F <sub>1</sub>	OB male	OB female	BB male	BB female	n <sub>T</sub>
n =	9	11	11	12	43
% =	0.21	0.26	0.26	0.28	
F <sub>1</sub>	OB male	x	OB female		
F <sub>2</sub>	OB male	OB female	BB male	BB female	n <sub>T</sub>
n =	16	16	2	2	36
% =	0.44	0.44	0.06	0.06	
F <sub>1</sub>	BB male	x	BB female		
F <sub>2</sub>	OB male	OB female	BB male	BB female	n <sub>T</sub>
n =	0	0	26	19	45
% =	0.00	0.00	0.58	0.42	
F <sub>1</sub>	OB male	x	BB female		
F <sub>2</sub>	OB male	OB female	BB male	BB female	n <sub>T</sub>
n =	4	1	1	3	9
% =	0.44	0.11	0.11	0.33	
F <sub>1</sub>	BB male	x	OB female		
F <sub>2</sub>	OB male	OB female	BB male	BB female	n <sub>T</sub>
n =	8	24	19	11	62
% =	0.13	0.39	0.31	0.18	

**Figure 4.1**

**Pedigree of the experimental population.** a. one LF male and one MZ female were mated to produce  $F_1$  family one, which was self-crossed to generate two  $F_2$  families. b. A second LF male and MZ female were mated to produce  $F_1$  family two, which in turn generated 12 additional  $F_2$  families.





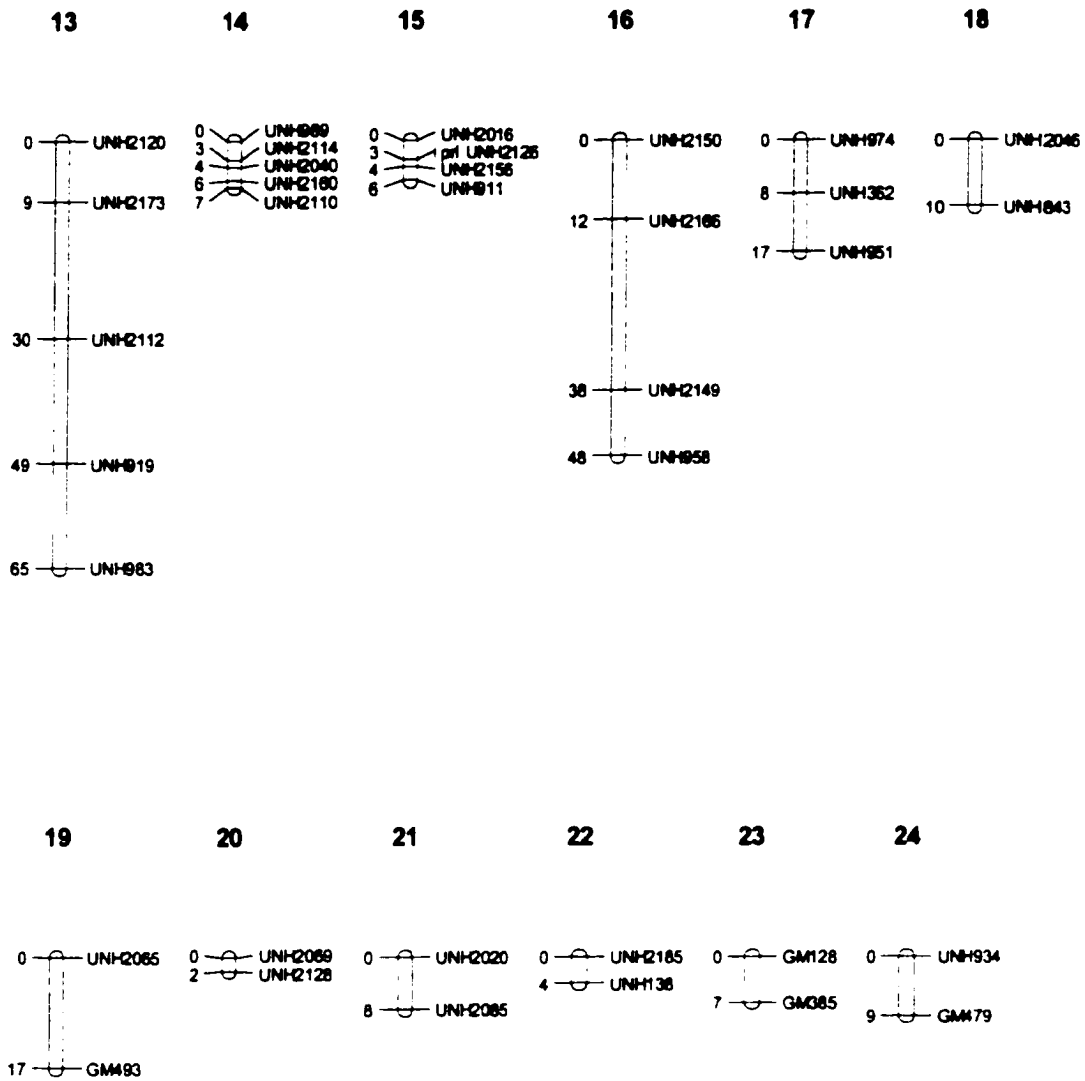
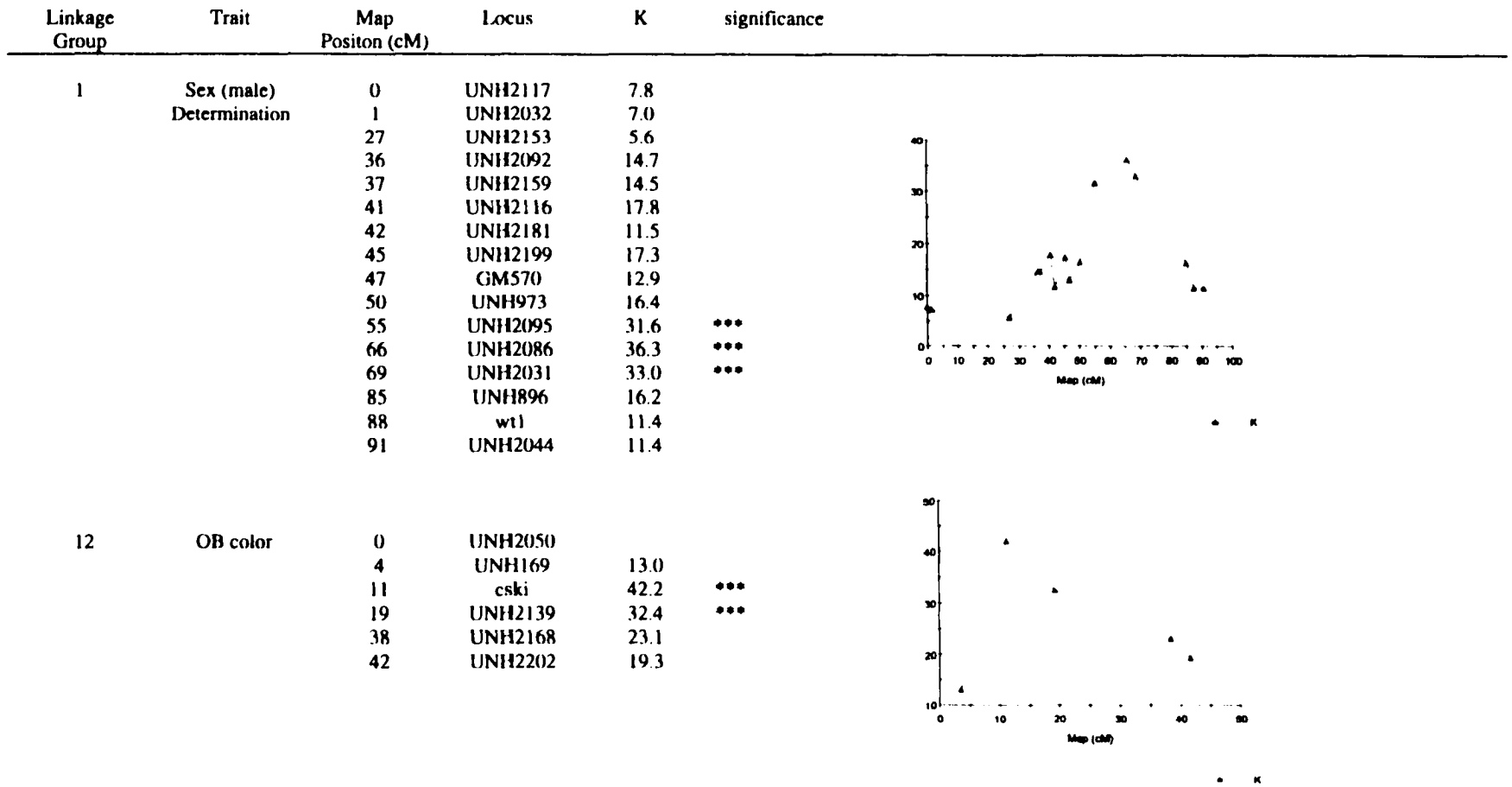


**Figure 4.2**

**A genetic linkage map for Lake Malawi rock-dwelling cichlids.** Microsatellites are coded by laboratory followed by the identifying number. UNH markers were isolated at the University of New Hampshire. GM markers were developed at Genomar Inc., Oslo, Norway.

**Figure 4.3**

**Segregation of sex and color.** The Kruskal-Wallis nonparametric mapping method was used to test the null hypothesis of no segregating QTL at each marker locus. The test statistic,  $K$ , is distributed approximately as a chi-square distribution. Associations that are significant at the  $p < 0.0001$  level are reported as \*\*\*.



## CHAPTER 5

### GENETIC DETERMINANTS AND GENOMIC “HOT-SPOTS” IN THE ADAPTIVE RADIATION OF EAST AFRICAN CICHLIDS

#### Abstract

Cichlid fishes exhibit unparalleled diversity among vertebrate systems. Natural selection on feeding morphology and sexual selection on male nuptial color have played crucial roles in this diversification. Unfortunately, the genetic bases of these fitness related traits remain unknown. In this report we take the first steps in uncovering the genetic determinants responsible for the adaptive radiation in these remarkable fishes. A genetic linkage map was constructed from the F<sub>2</sub> of an intergeneric cross between two rock-dwelling species from Lake Malawi that employ different modes of feeding. *Labeotropheus fuelleborni* feeds by cropping attached algae from the rocky substrate, whereas *Metriaclima zebra* forages on plankton in the water column with a sucking mode of feeding. Quantitative trait loci (QTL) were detected for 15 morphological traits that distinguish the feeding apparatus of *L. fuelleborni* and *M. zebra*. A number of chromosomal regions were identified that contained QTL that affected several traits. We contend that these genomic “hot-spots” represent either pleiotropic units or units of genetic linkage, and may have important implications for the rapid and replicative nature



of cichlid evolution. One such “hot-spot” contains QTL that map on or near *bmp4*, a gene known to play an important role in craniofacial development. In all, our results offer critical insight into the genetic basis of adaptive radiation, and present a number of genomic intervals that should be investigated in finer detail.

## Introduction

East African cichlids are one of the most dramatic examples of adaptive morphological radiation in vertebrates. Vast trophic specializations have evolved repeatedly within Lakes Victoria, Tanganyika and Malawi. Scientists have long endeavored to uncover the factors that have contributed to this evolutionary explosion. Several lines of evidence suggest that functional divergence in feeding morphology has contributed to the radiation and maintenance of cichlid species diversity (Albertson et al. 1999; Bouton et al. 1997, 1998; Danley and Kocher 2001; Liem 1980; Reinthal 1990; Yamaoka et al. 1986). We submit that if functional diversification is predicted by changes in feeding morphology (Liem, 1991), then the genetic basis of adaptive radiation can be examined by mapping QTL that control salient shape differences in the cichlid head.

An F<sub>2</sub> mapping population was generated by crossing two rock-dwelling species from Lake Malawi that employ very different modes of feeding. *Labeotropheus fuelleborni* ("LF" from here on) has a robust sub-terminal mouth that it uses to crop attached algae from the rocky substrate with a specialized biting mode of feeding. *Metriaclima zebra* ("MZ") has a relatively narrow terminally oriented mouth and is one of the only rock-dwelling species that collect plankton in the water column with a suction mode of feeding. LF and MZ coexist at nearly every rocky locality (Ribbink et al. 1983), and partition their environment according to diet, depth, and several other microhabitat characteristics (Albertson in prep; Genner et al. 1999; Reinthal 1990; Ribbink et al. 1983). We chose LF and MZ for our experimental cross because they are closely related species at opposite ends of the biting/sucking continuum.

Using a genetic linkage map developed for the LF x MZ cross, we explored the genetic control of 15 morphological characters that distinguished LF and MZ along a functional axis. Shape variation in the F<sub>2</sub> was assessed using both geometric and traditional linear methods. Geometric variables were used to quantify the total deformation of shape of individual bony elements. Linear measures were used to evaluate specific, functionally relevant characters defined *a priori*.

Our results offer critical insight into the genetic architecture of the cichlid head. We identified QTL that explained between 5 and 26% of the phenotypic variance (PVE). Most QTL were distributed across the genome. We also identified a number of genomic 'hot-spots' where QTL for several characters mapped to a similar chromosomal interval. This observation implicates pleiotropy or genetic linkage as a prominent part of the genetic architecture of the cichlid feeding apparatus. Interestingly, one of the most dramatic hot-spots contained the gene *bmp4*, which is known to play an important role in patterning and differentiation of cartilage in vertebrate embryogenesis.

## Materials and methods

### Mapping pedigree

Hybridization among cichlids has been observed to occur naturally when males of one species are placed in a tank with females of another species (Loiselle 1971; Cragon de Caprona and Fritzsich 1984; McElroy and Kornfield 1993; personal observation). Male LF were placed in a 500 gallon pool with female MZ. All mbuna females incubate their clutch in their mouths. Female MZ were identified as holding a clutch by an enlarged buccal pouch, at which point they were removed from the breeding pool and placed in ten gallon tanks until they released free-swimming fry (~ 3 weeks).

Two  $F_1$  hybrid families were grown to sexual maturity.  $F_2$  families were generated via brother-sister matings of the  $F_1$ . All  $F_2$  were reared in 40 gallon tanks for 3 months, and 500 gallon pools for an additional 6-9 months. To minimize the functional demand on the feeding apparatus,  $F_2$  animals were fed high quality spirulina flake food (Aquatic Ecosystems, FL). In total, 173  $F_2$  were used in this experiment.

### Phenotypic trait measurements

$F_2$  families were collected between 12-18 months, and sacrificed with MS222 in accord with a protocol approved by the University of New Hampshire ACUC. Specimens were prepared for morphometric analysis with dermestid beetles, which cleaned and disarticulated the skeleton. Craniofacial bony elements were collected and digitized using

a SPOT digital camera (Diagnostic Instruments, Inc.) mounted on a Zeiss SV11 dissecting scope. Images were imported into NIH Image (version 2.1) and landmark coordinates were captured in 2-dimensional (x,y) space.

Shape was quantified via geometric morphometrics and traditional linear measures. Our geometric approach is described in detail elsewhere (Albertson and Kocher 2000; and Albertson et al. in review). In brief, landmark coordinates were superimposed using a generalized least-squares fit algorithm in Morphometrika 7.0 (Walker 1999). Using the same program, a series of orthogonal geometric descriptors of shape difference, called partial warps, were generated via thin-plate spline analysis. A principal component analysis was performed on partial warp scores generated from the LF/MZ comparison. Hybrids were then evaluated against this axis by multiplying hybrid partial warp scores by parental eigenvectors in the space of partial warps. In this way, hybrid individuals were evaluated against the axis that differentiated LF and MZ.

Distances between landmarks were used to assess differences in four functionally significant characters: 1) length of the lower jaw in the lateral view, 2) width of the lower jaw in the ventral view, 3) length of the ascending arm of the articular, and 4) length of the palatinad wing of the maxilla. The distance between any two landmarks was calculated as:

$$d = \sqrt{(x_a - x_b)^2 + (y_a - y_b)^2}$$

where d is distance,  $x_a$  and  $y_a$  are the x,y coordinates of landmark a, and  $x_b$  and  $y_b$  are the coordinates of landmark b. Distances were calculated using both raw landmark coordinates, standardized by standard length, and superimposed landmark coordinates. Both approaches gave similar results. Data presented here are from distances calculated after landmark superimposition.

Tooth shape was also evaluated in the  $F_2$ .  $F_2$  dentition in the outer row of the upper and lower jaws is a continuum between the fully tricuspid dentition of LF and the fully bicuspid dentition of MZ. Differences in tooth shape were assessed by evaluating the height of the third cusp in every tooth following the protocol of (Albertson et al. in review).

### Genotyping and Linkage map construction

See the previous chapter (Chapter 4) for the protocols used to genotype microsatellites and construct a genetic linkage map.

### QTL mapping

Morphological traits were analyzed with MapQTL 4.0 (van Ooijen et al. 2002) using interval and multiple-QTL (MQM) methods.

Interval mapping. Interval mapping is a single-QTL model based on the segregation of three possible genotypes. Interval mapping calculates a QTL likelihood map by comparing the likelihoods of a segregating QTL ( $H_A$ ) and no segregating QTL ( $H_0$ ) at each position on the genome. This comparison was achieved using a LOD likelihood ratio statistic.

MQM mapping. The MQM mapping method is a multiple-QTL extension of interval mapping. The framework is similar to multiple regression, where phenotype is

regressed on a single putative QTL in a given marker interval, and at the same time on a number of other markers located elsewhere in the genome (Jansen 1994). Theoretically, using markers as cofactors will eliminate the variation induced by unlinked QTL (Jansen 1994).

In our analysis the genome was first searched for putative QTL using interval mapping. Next, markers close to detected QTL were selected as cofactors. Marker cofactors that accounted for a significant amount of the phenotypic variance were verified using backward elimination multiple regression of phenotype on cofactors. This analysis was performed for every trait using the automatic cofactor selection module in MapQTL 4.0. Markers remaining after backward elimination were used as cofactors in MQM mapping.

Permutation test. Significant LOD thresholds were determined for each trait by a permutation test. Here, phenotypic data were shuffled over individuals while marker data remained fixed. The maximum LOD score over the genome was calculated for each iteration, and the LOD frequency distribution under the null-hypothesis of no QTL was generated. Genome-wide significance levels of  $\alpha = 0.05$  and  $0.01$  were identified for each trait from 1000 permutations of the data.

## Results

## MQM mapping

Results from the QTL analysis are presented in table 5.1, figures 5.1 and 5.2 and appendix 1. Using the MQM model, we detected QTL that explained between 5 and 26% (average = 11%) of the phenotypic variance (PVE) in the F<sub>2</sub>. Significant LOD scores ranged from 2.60 to 10.54 (average = 4.05). We detected QTL on 17/24 linkage groups. In addition, four traits (lower jaw in the ventral view, width of the lower jaw, maxilla, and the length of the palatinad wing of the maxilla) segregated with an unlinked marker, UNH2207. Shape of the premaxilla segregated with another unlinked marker, UNH2011. We refer to these ungrouped markers as linkage groups 25 and 26, respectively.

Fourteen QTL were identified that affected a single trait. In contrast, we detected eight genomic intervals that contained at least two overlapping QTL affecting multiple structures.

Dentition. Phenotypic distributions of tooth shape in the F<sub>2</sub> were roughly trimodal, suggesting that a very small number of genetic determinants control tooth shape in the LF x MZ cross (Albertson et al. in review). We detected QTL on linkage groups 7, 12 and 16 that affected cusp number on the upper and lower jaw.

Dentary. Only one significant QTL on linkage group 2 was detected for the dentary. This observation is consistent with a biometrical study suggesting that only one genetic factor underlies shape difference in the dentary (Albertson et al. in review). Alternatively, since this QTL accounts for very little of the phenotypic variance (10%), there could be many other QTL of small effect that could not be detected with our experimental design.



Articular. We identified QTL on linkage groups 2, 6, and 21 that affected shape of the articular.

Lower jaw in the lateral view. Three significant QTL were found on linkage groups 1, 2, and 6 for shape of the lower jaw in the lateral view.

Length of the lower jaw. MZ had a long narrow lower jaw, which is typical in species that suck plankton from the water column (Liem 1991). LF had a relatively short robust lower jaw like other scraping species. We detected significant QTL on linkage groups 1, 2 and 10 for lower jaw length.

Length of the ascending arm of the articular. LF had a much longer ascending arm of the articular than MZ. This process is where the adductor mandibulae inserts and is a critical lever in the action of jaw adduction (i.e., biting) (Otten 1983). The height of this process has significant function implications. A long ascending arm will increase force transmission of the adductor mandibulae and is a more efficient biting design. In contrast, a short process will increase the speed of jaw rotation and is more typical in species that employ a sucking mode of feeding. We identified QTL that affected the length of the ascending arm of the articular on linkage groups 1, 2 and 21.

Lower jaw in ventral view. We identified QTL on linkage groups 1, 11, 16 and 25 that affected shape of the lower jaw in the ventral view.

Width of the lower jaw. LF had a very wide, almost rectangular, lower jaw, which allows this species to take large uniform bits of algae. In contrast, MZ had a narrow lower

jaw, which is a more efficient design for suction feeding (Liem 1991). We identified QTL that affected jaw width on linkage groups 1, 11, 14, 16, 20 and 25.

Maxilla. We detected QTL that affected shape of the maxilla on linkage groups 2, 5, 9 and 25.

Length of the palatinad wing of the maxilla. LF had a much longer palatinad wing than MZ. This bony structure supports the intermaxillary ligament that is also much larger in LF. The intermaxillary ligament presumably absorbs much of the force applied to the upper jaw as the maxillary shank is pulled posteriorly by the adductor mandibulae during biting (Albertson et al. 2000; Otten 1983). We identified QTL that affected the length of this structure on linkage groups 9 and 25.

Premaxilla. QTL were identified on linkage groups 2, 10, 16 and 26 that affected shape of the premaxilla. Heterozygotes for the QTL on linkage group 2 appeared to be overdominant (Figure 5.1). The QTL on linkage group 10 was in the wrong phase (i.e., the LF/LF genotype produced a MZ phenotype).

Suspensorium. We detected QTL on linkage groups 4, 5 and 18 that affected the suspensorium. The suspensorium did not share QTL with any other structure, suggesting that shape of the suspensory apparatus can be modified independently of the oral jaw apparatus.

Neurocranium. QTL were detected on linkage groups 1 and 8 that affected shape of the skull. The QTL on linkage group 8 was in the opposite phase.

Vomer. We identified QTL on linkage groups 16 and 24 that affected shape of the vomerine process. The QTL on linkage group 24 was in the opposite phase.

### Distribution of QTL

We used a  $X^2$  goodness of fit test to assess whether QTL were distributed randomly throughout the genome. In total, we detected 43 QTL (not including the five QTL that segregated with the single markers, UNH2011 and UNH2207) over 838 cM. If QTL were spread randomly over the genome, we expected to find 1 QTL every ~20 cM (838/43). We compared this expectation with the actual number of QTL detected every 20 cM. Results from the  $X^2$  goodness of fit test suggest that QTL are not randomly dispersed over the genome ( $X^2 = 62$ ,  $df = 41$ ,  $p = 0.019$ ).

We also calculated the expected frequency distribution of QTL for linkage groups, by dividing the length of each linkage group by 20. For example, we expected 4.55 (91/20) QTL to map to linkage group 1, 3.95 (79/20) to map to linkage group 2, and so on. Results from this goodness of fit test reinforce the observation that QTL are not randomly distributed ( $X^2 = 36.03$ ,  $df = 23$ ,  $p = 0.041$ ).

## Discussion

### Selective forces acting on the cichlid feeding apparatus

Most QTL detected exhibited additive effects with little or no dominance (Figure 5.1). These observations implicate directional selection as the predominant force acting

on the oral jaw apparatus. Strong directional selection on jaw morphology is consistent with the hypothesis that trophic specialization among cichlids has occurred in evolutionary bursts (Albertson et al. 1999; Danley and Kocher 2002). There are a few traits, however, that do not show this pattern of additivity.

QTL that underlie differences in the skull showed significant nonadditive effects. The neurocranium and the vomer each had a QTL in the opposite phase (i.e., LF/LF genotype produces MZ morphology), which suggest these structures are under stabilizing rather than directional selection. This hypothesis seems plausible given the relative conservation of skull shape among cichlid taxa compared to other craniofacial elements (Reinthal 1990; Albertson and Kocher 2000).

Alternatively, nonadditive effects could result from epistasis between QTL alleles and the genetic background (Tanksley 1993). In this scenario, several undetected loci would influence the phenotypic expression (i.e., the shape of the skull) of the QTL genotype. Unfortunately, the role of epistasis in producing quantitative variation in natural populations is largely unknown (True et al. 1997), owing mainly to the difficulty in detecting loci with epistatic effects (Gadau et al. 2002; Li et al. 2002). The skull is a large, dynamic structure derived from multiple embryological origins (Hall 1999), and involved in several functional pathways (Liem 1979). Given the variety of forces imposed upon this structure over its ontogeny, genetic background could profoundly influence the shape of the skull.

#### Detecting QTL for geometric and linear shape variables

Genomic morphometrics methods are basis-invariant, such that the position of each landmark is evaluated relative to every other landmark rather than a single point,

line, or plane defined *a priori* (Yaroch, 1996). This attribute is a major advantage when the total deformation of shape is sought. However, when a specific character with known functional or evolutionary potential is evaluated, traditional linear measures are still most useful. We have combined these two morphometric approaches to map QTL that affect the shape of the cichlid head.

In general we were most interested in mapping differences in the total deformation of shape that occurred between LF and MZ. However, several investigations have revealed a number of specific characters that affect the functional design of the cichlid feeding apparatus (i.e., Otten 1983). We investigated the genetic basis of these traits using simple linear measures.

We found that geometric and linear measures often had QTL in common, which underscores the biological relevance of geometric descriptors of shape difference. We also detected QTL unique to each type of shape variable. This observation reinforces the precept that a QTL analysis is only as revealing as the phenotype being measured.

#### Genomic hot-spots.

QTL that underlie differences in the feeding apparatus were not distributed randomly across the genome. Several genomic blocks contained a disproportional number of QTL. In total we identified 8 chromosomal regions that contained two or more overlapping QTL. Of these, linkage groups 16 and 25 each contained an interval with four QTL, linkage group 1 contained a region with five QTL, and linkage group 2 contained an interval with six segregating QTL. These results implicate pleiotropy, or the

cumulative action of several closely linked genes, as a prominent force in the adaptive radiation of cichlid fishes.

We suggest these chromosomal regions represent genomic “hot-spots” where selection on the shape of one element/trait will quickly propagate change to several other morphological characters. If these pleiotropic units are common to various cichlid taxa, they could help account for the rapid, even stereotypical, evolution of trophic forms in several East African assemblages.

#### Role of *bmp4* in the adaptive radiation of cichlids.

Linkage group 2 contains an interval with six segregating QTL. Interestingly, these QTL map on or close to *bmp4*. Bone morphogenic protein 4 (BMP4) is a member of the transforming growth factor beta (TGF $\beta$ ) superfamily which is involved in a variety of developmental processes. Of particular interest is the role of BMP4 in differentiation and patterning of embryonic cartilage (Monsoro-Burq et al. 1996). For example, BMP4 shows spatially and temporally restricted expression patterns in the mouse mandibular process (Semba et al. 2000). Further, BMP4 soaked beads implanted in embryonic mouse and chicken mandibular explants induce ectopic cartilage formation (Nonaka et al. 1999; Semba et al. 2000).

Of the six traits that segregate with *bmp4*, the length of the ascending arm of the articular is perhaps the most interesting. As described above, the length of this process has direct functional consequences, affecting both the speed and force of jaw adduction (Otten 1983). To confirm the association between *bmp4* and the height of this process, F<sub>2</sub> individuals were grouped by their genotype at the *bmp4* locus, and mean differences in the length of the ascending arm of the articular were assessed by a full factorial ANOVA.

As expected, we found highly significant ( $p = 0.018$ ) differences in the length of this process among individuals with different *bmp4* genotypes.

In all, these data are highly suggestive that *bmp4*, or a closely linked gene or regulator, affects the length of this functionally relevant trait, and has a pleiotropic effect on several other traits. At the very least, *bmp4* should be a prominent figure in future investigations of the molecular basis of adaptive radiation in cichlids.

### Conclusions

This study offers an exciting first look into the genetic basis of adaptive radiation in cichlid fishes. We suggest that the rapid and replicative nature of cichlid evolution may, in part, be attributed to pleiotropic effects of genes that control shape of the feeding apparatus. These results are consistent with findings in other rapidly evolving systems (True et al. 1997; Bradshaw et al. 1998; Peichel et al. 2001), where QTL that affect different traits map to the same interval. Further, we present strong evidence that a well characterized gene, *bmp4*, plays an important role in the functional differentiation between LF and MZ. This observation moves BMP4 from the domain of developmental genetics in model systems and places it firmly within the scope of evolutionary biology.

Our results have provided a foundation for further investigations into the genetic architecture of cichlid evolution. Future experiments should proceed in two general directions. First, additional marker loci and  $F_2$  progeny are needed to more accurately map and better estimate the effects of QTL in the LF x MZ cross (Lander and Botstein 1989; Beavis 1998). The addition of more  $F_2$  will also facilitate the detection of QTL with much smaller magnitudes of effect (Bradshaw et al. 1998). Second, the genetic architecture of the cichlid feeding apparatus should be evaluated in other species.

Particular attention should be given to the genomic hot-spots and candidate loci identified in this experiment. It will be very interesting to see if the same intervals are implicated in the divergence among other cichlid taxa.

### Acknowledgements

This work was performed in collaboration with J. Todd Streebman and Thomas D. Kocher. Thanks to A. Ambali, the University of Malawi, and the Malawi Government for assistance with collection of specimens. Access to dermestid beetles was provided by M. Scott. All illustrations were done by R. Craig Albertson. This work was supported by a National Science Foundation Grant (IBN 9905127) awarded to T. D. Kocher.



**Table 5.1**

**Location and effect of QTL.** For each QTL detected the name, linkage group, map position (cM), LOD score, percent variance explained (%), and effect are indicated. The phenotypic mean of *L. fuelleborni* and *M. zebra* is given as a reference. QTL were detected via MQM mapping. LOD thresholds were calculated via permutation test for each trait. Genome-wide significance levels were evaluated at the 95%\* and 99%\*\* levels.

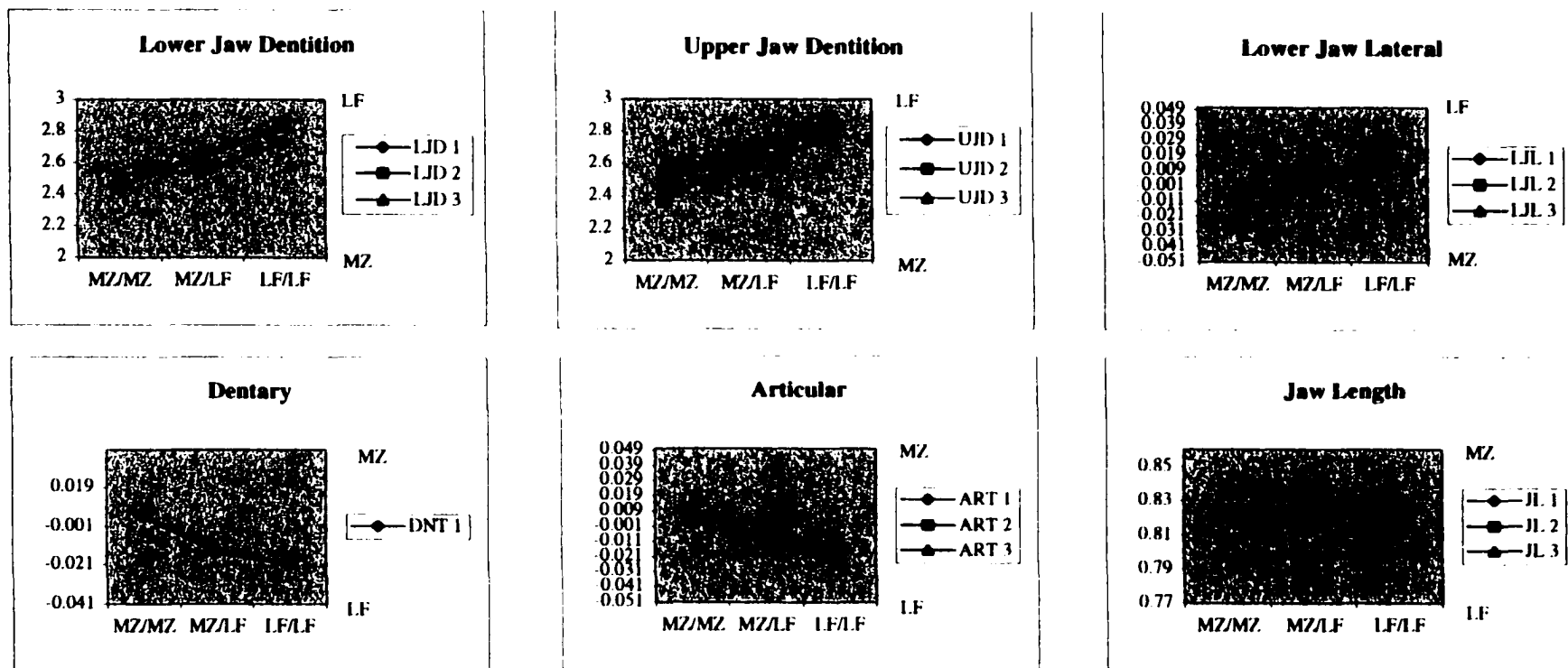
Phenotypic class	Trait	Phenotypic mean of parental lines		QTL Name	Linkage Group	Map Position (cM)	LOD	PVE (%)	Phenotypic mean of genotypic classes					
		<i>M. zebra</i>	<i>L. fuelleborni</i>						MZ/MZ	MZ/LF	LF/LF			
DENTITION	LOWER JAW DENTITION	2	3	LJD 1	7	2.3	3.31**	7.2	2.52626	2.53667	2.72537			
				LJD 2	12	0	4.97**	12.8	2.44607	2.64727	2.84146			
				LJD 3	16	0	6.29**	18.4	2.45154	2.6289	2.83632			
	UPPER JAW DENTITION	2	3	UJD 1	7	2.3	3.43**	5.4	2.54492	2.58911	2.75492			
				UJD 2	12	0	4.52**	18.9	2.37457	2.64905	2.88409			
				UJD 3	16	0	5.28**	10.7	2.49628	2.66656	2.83208			
LOWER JAW IN THE LATERAL VIEW	LOWER JAW (LATERAL)	-0.01092	0.117	LJL 1	1	68.8	10.54**	17.8	-0.0224602	-2.40E-05	0.0200489			
				LJL 2	2	54.5	6.37**	11.4	-0.00942844	-0.00355648	0.0168462			
				LJL 3	6	51.8	5.08**	8.7	-0.00768034	0.00216174	0.0146111			
	DENTARY	0.0386	-0.0414	DNT 1	2	6	2.82*	6.8	0.00475923	-0.0142725	-0.0205283			
				ARTICULAR	0.1038	-0.1111	ART 1	2	64.1	2.65*	7.9	0.0101784	-0.0108625	-0.024777
							ART 2	6	2	2.84*	6.3	0.00300781	0.000337266	-0.0190248
	ART 3	21	5	5.69**	14	0.0100765	-0.0122344	-0.0247945						
	LOWER JAW LENGTH	0.8736	0.7633	JL 1	1	73.8	3.25*	9.2	0.835058	0.82889	0.814656			
				JL 2	2	59.5	4.02**	12	0.835191	0.835044	0.814137			
JL 3				10	38.2	3.43**	7.4	0.82082	0.815355	0.831301				

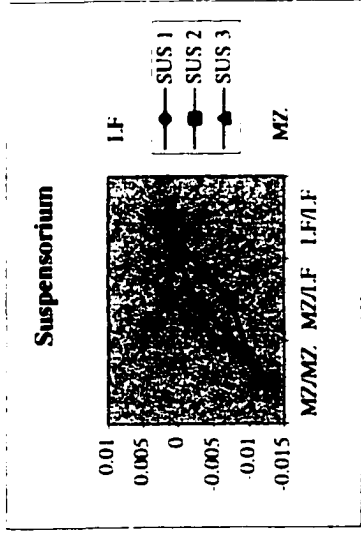
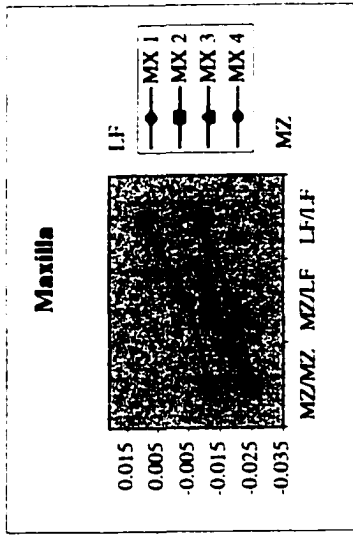
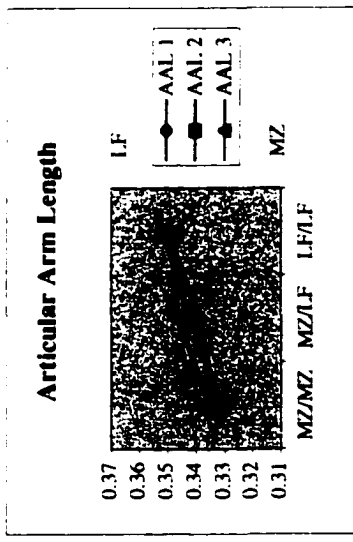
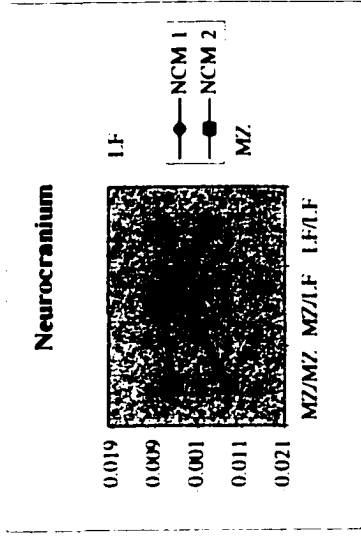
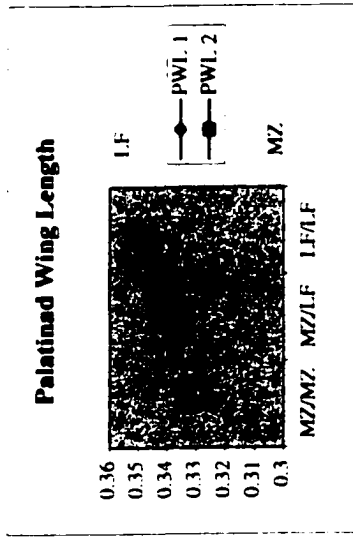
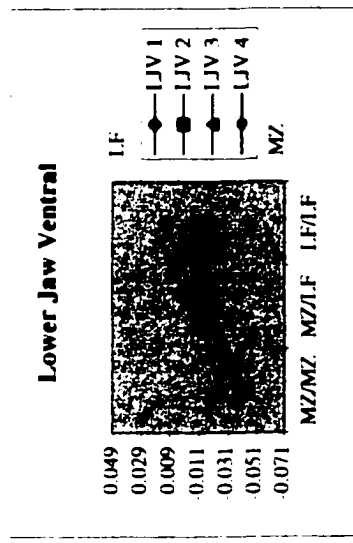
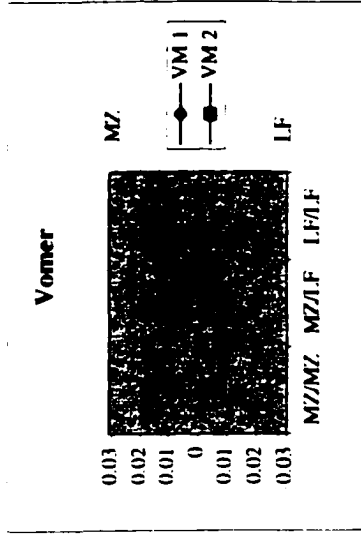
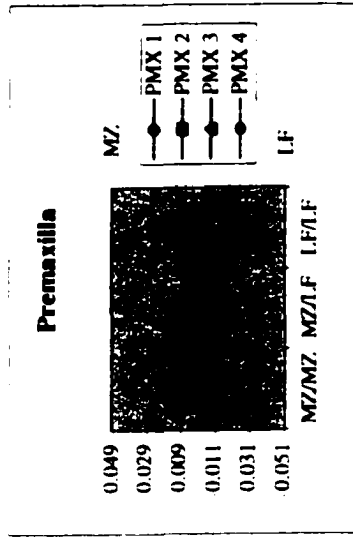
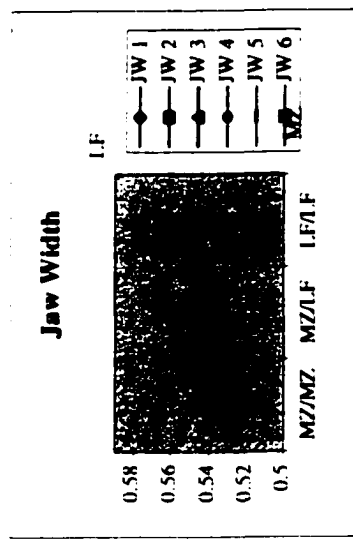
ARTICULAR ARM LENGTH	0.284	0.393	AAL.1	1	78.8	4.66**	11.8	0.333455	0.338901	0.349589
			AAL.2	2	64.1	6.16**	15.8	0.331163	0.342034	0.351485
			AAL.3	21	0	3.45**	6.5	0.335258	0.346298	0.347391
LOWER JAW IN THE VENTRAL VIEW			LJV.1	1	55.3	3.1*	6.6	-0.0405397	-0.0204032	-0.0152148
	-0.1531	0.1531	LJV.2	11	28.9	3.66**	7.1	-0.0419663	-0.0189129	-0.0107195
			LJV.3	16	17.1	3.37**	9.4	-0.044053	-0.0172386	-0.0153691
			LJV.4	25	9	4.5**	11.4	-0.0258888	-0.0108315	0.0120751
LOWER JAW WIDTH	0.4361	0.7575	JW.1	1	55.3	3.86**	6.7	0.523927	0.54273	0.550232
			JW.2	11	18.9	5.5**	13.2	0.514642	0.54243	0.554635
			JW.3	14	3.6	3.5**	6.3	0.523937	0.533411	0.550223
			JW.4	16	0	3.18*	8.7	0.52068	0.54742	0.545481
			JW.5	20	0	3.09*	5.4	0.527206	0.547627	0.546954
			JW.6	25	9	4.67**	11.9	0.540485	0.559074	0.575793
UPPER JAW			MX.1	2	78.9	3.54**	7.3	-0.0242611	-0.0112567	-0.0109008
MAXILLA	-0.0743	0.0792	MX.2	5	22.8	3.34*	7	-0.0249336	-0.0125434	-0.0102298
			MX.3	9	35.9	2.75*	7.2	-0.0257248	-0.0188318	-0.00940122
			MX.4	25	9	5.55**	14.6	-0.0116094	-0.00480108	0.0099156
MAXILLARY PALATINAD WING LENGTH	0.2711	0.4407	PWL.1	9	35.9	3.84**	14.5	0.32389	0.332668	0.350734
			PWL.2	25	9	3.41**	9.1	0.332679	0.336859	0.351484

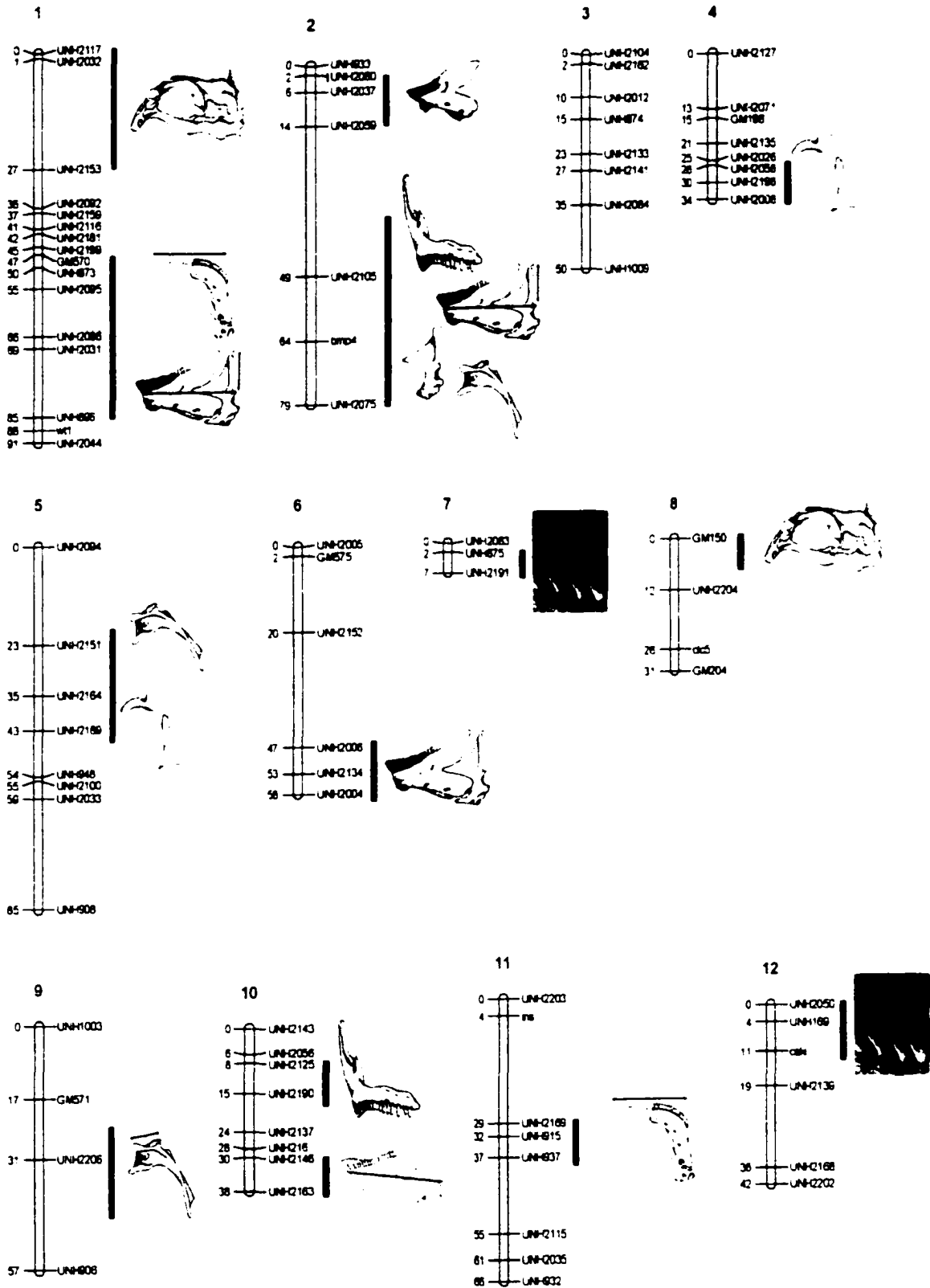
PREMAXILLA	0.1	-0.1077	PMX 1	2	39.2	2.92*	14.6	-0.0154403	0.00482777	-0.020426
			PMX 2	10	12.9	3.3**	9.5	-0.00240249	-0.0127704	0.00788976
			PMX 3	16	48.2	3.78**	10.8	-0.00064369	-0.00499344	-0.0258686
			PMX 4	26	1	2.7*	9.1	0.0395746	-0.00305389	-0.0355872
SUSPENSORY APPARATUS			SUS 1	4	34.2	2.83*	6.6	-0.0111072	-0.00731458	0.00281098
	-0.0531	0.0531	SUS 2	5	27.8	3.07*	7.6	-0.0132773	0.00126556	0.000293677
			SUS 3	18	0	2.53*	7.9	-0.0132875	-0.00250525	0.00219376
SKULL			NCM 1	1	11.3	3.3**	11.8	-0.00827923	0.000840141	0.00639797
	-0.0449	0.0478	NCM 2	8	0	2.6*	9	0.00435281	0.00755542	-0.00467436
VOMER			VM 1	16	0	3.7**	18.6	0.0160261	0.00480814	-0.00851651
	0.0514	-0.0514	VM 2	24	8.5	3.1**	20.7	-0.00694909	-0.00963887	0.0144591

**Figure 5.1**

**Phenotypic effects of genotype at each QTL.** The phenotypic mean is plotted for each genotype (MZ/MZ, MZ/LF, LF/LF) at every QTL. The y-axis is recorded in phenotypic units. "LF" and "MZ" indicate the orientation of phenotypic values relative to *L. fuelleborni* and *M. zebra*.







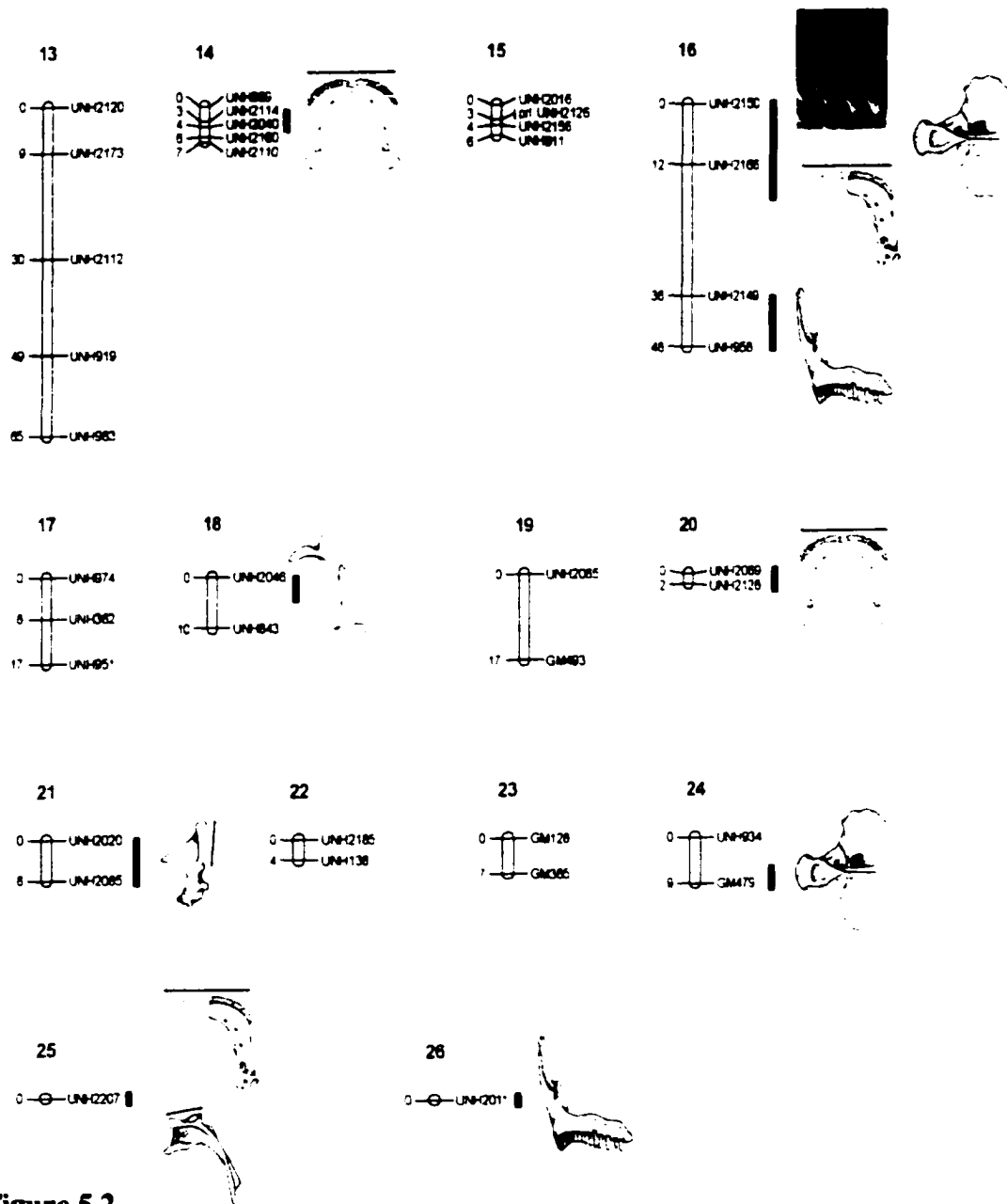


**Figure 5.2**

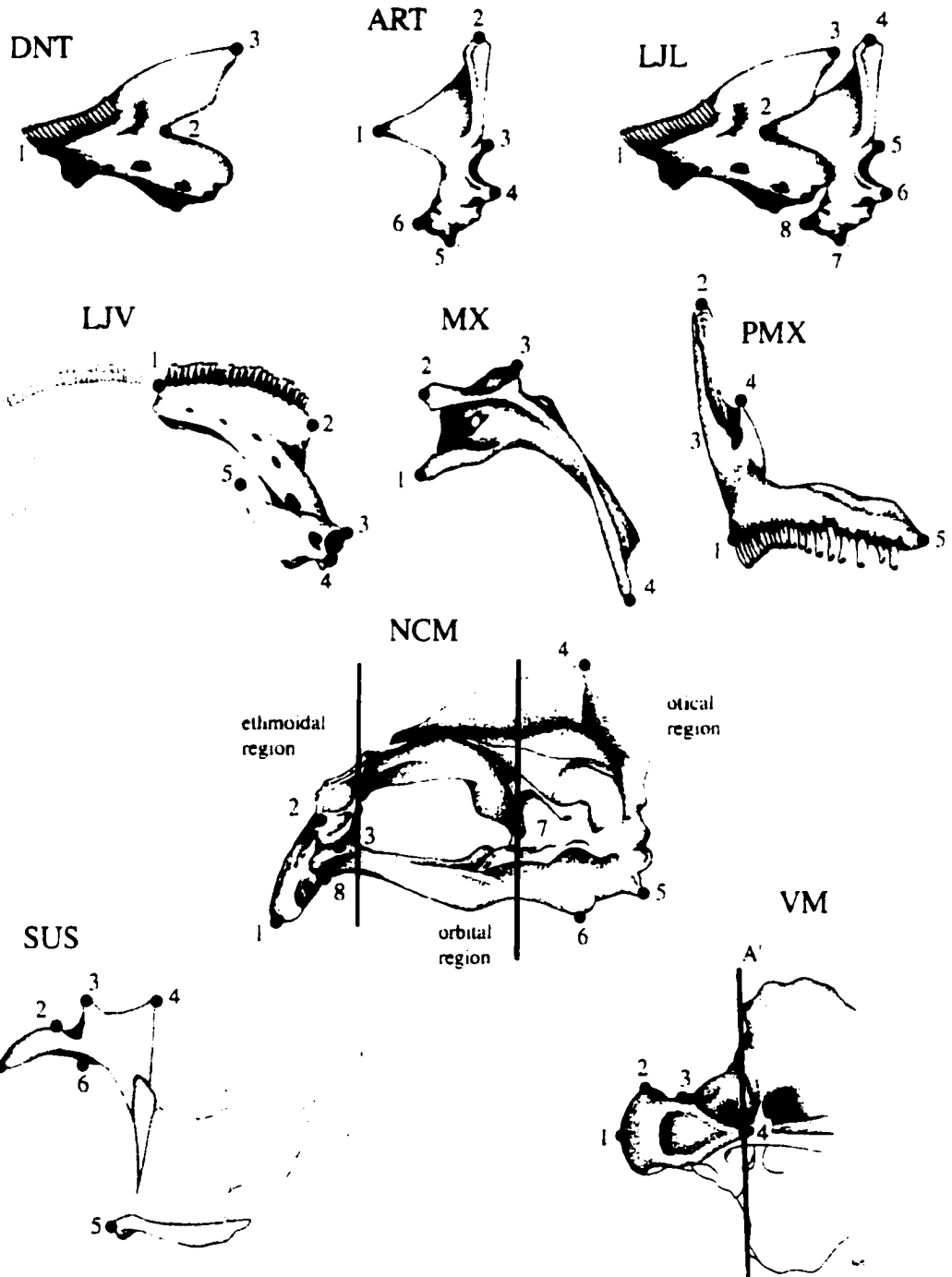
**QTL position on the mbuna genetic linkage map.** Marker names are to the right of linkage groups, map positions (cM) are to the left. Black bars indicate 95% confidence intervals where QTL, or several overlapping QTL were detected. The map locations of QTL affecting feeding morphology are represented by illustrations. Individual bony elements indicate QTL affecting geometric variables. Red bars indicate QTL affecting linear measures. Where geometric and linear variables map to the same interval red bars overlay stippled illustrations. When only traditional shape variables map to an interval, bars are shown with line drawings.

## APPENDICES



## Appendix A

Landmarks used for thin-plate spline analysis in Chapter 3.



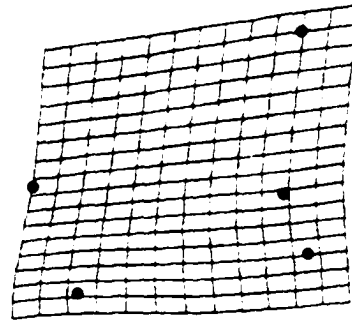
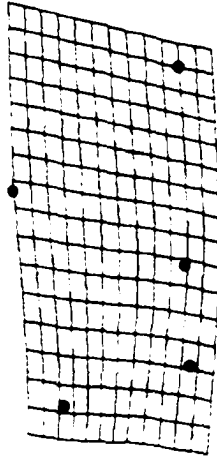
## **Appendix B**

**Deformation of shape along the first principal component axis. The genetic basis of shape difference was determined both biometrically (Chapter 3) and via QTL analysis (Chapter 5) for principal component scores along this axis.**

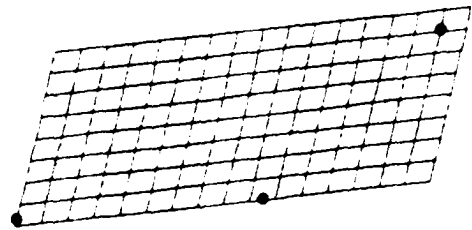
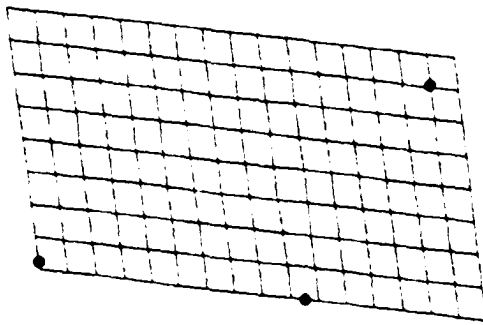
ART

LF

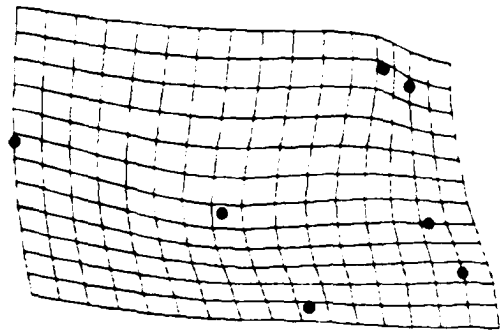
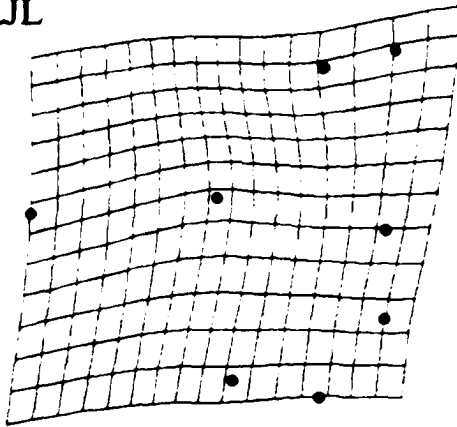
MZ



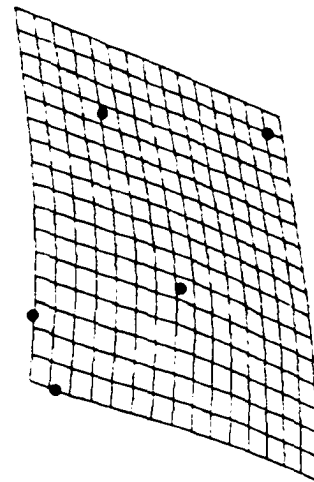
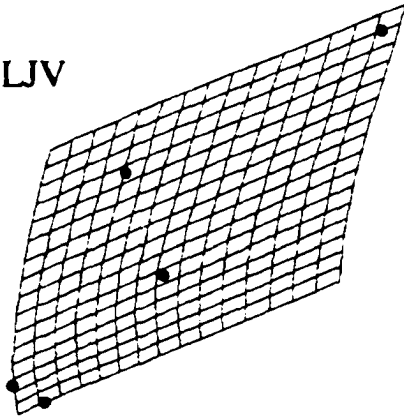
DNT



LJL



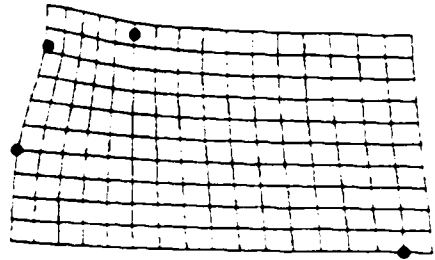
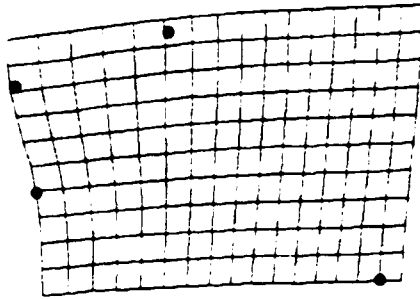
LJV



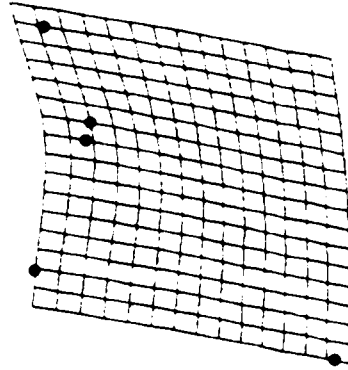
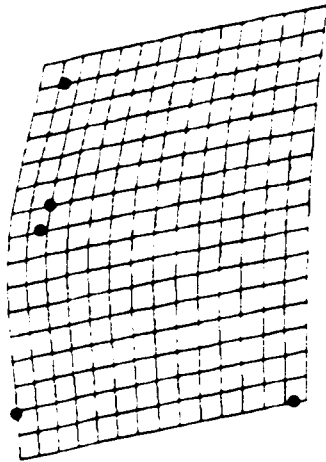
LF

MZ

MX



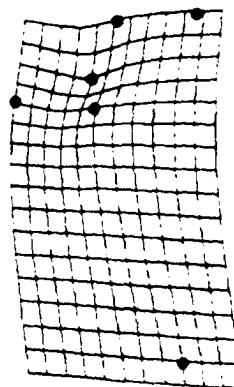
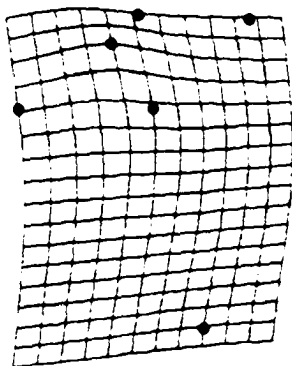
PMX



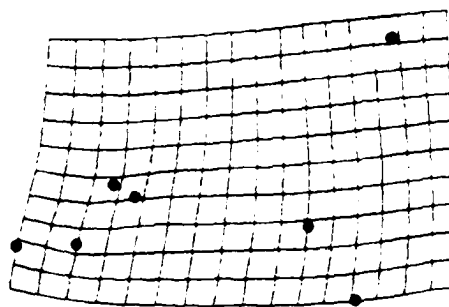
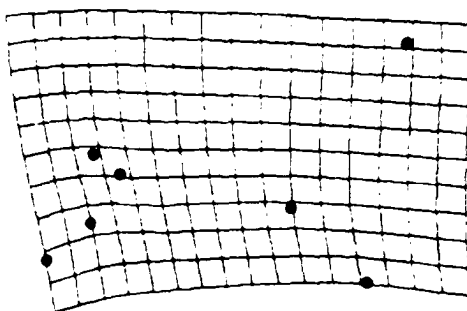
LF

MZ

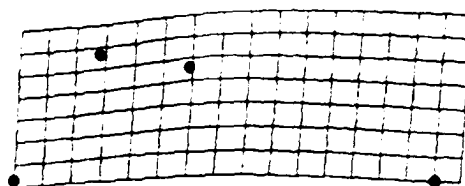
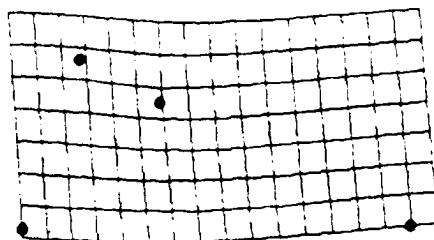
SUS



NCM

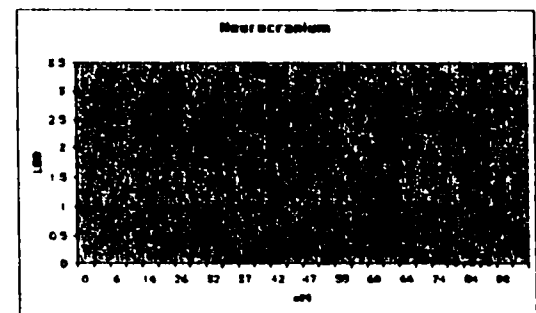
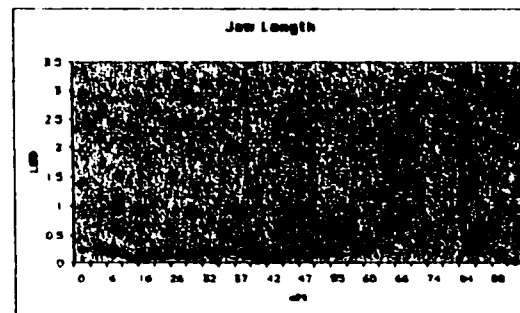
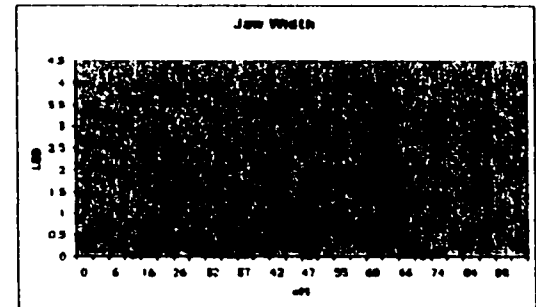
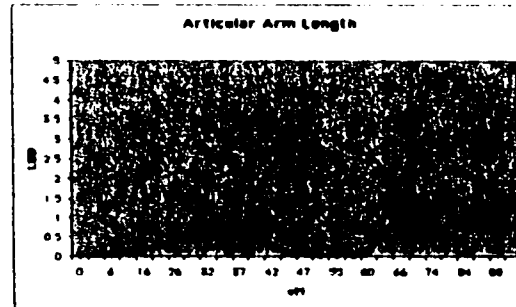
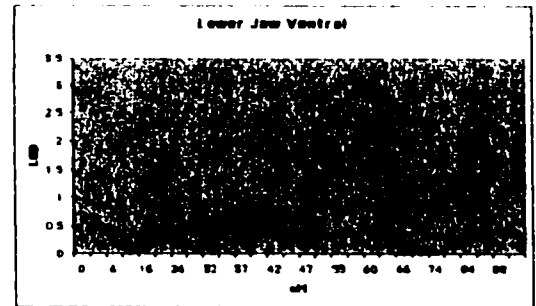
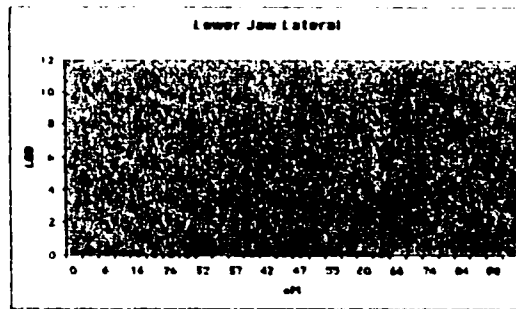
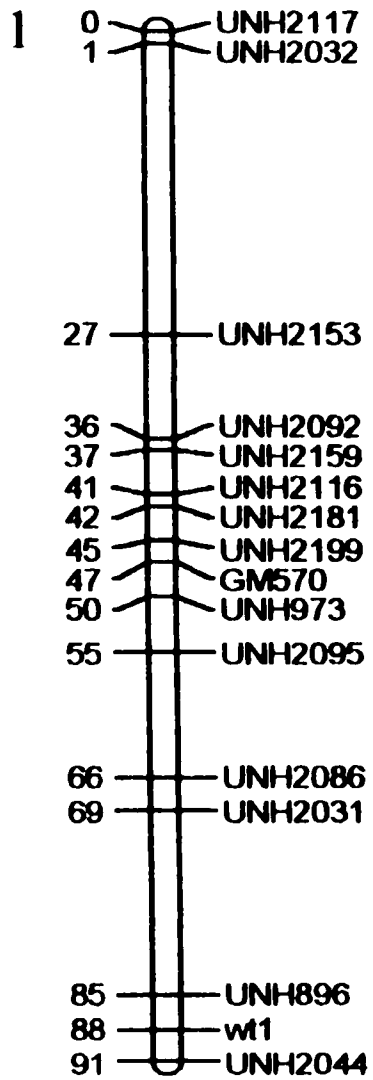


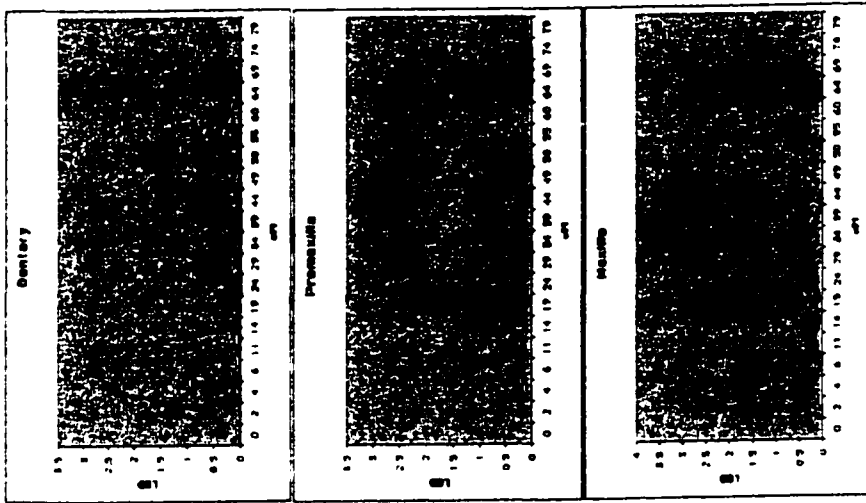
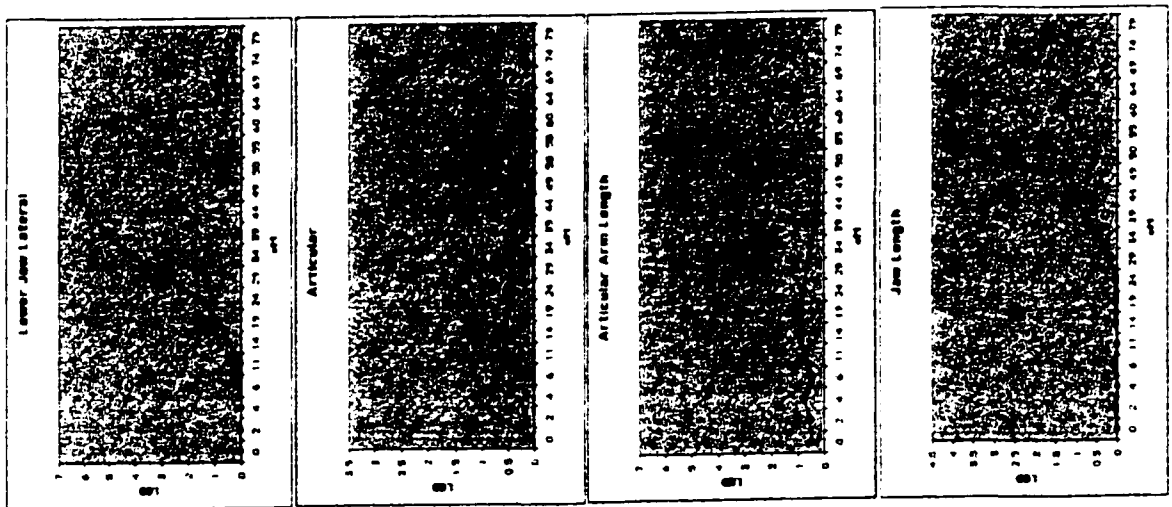
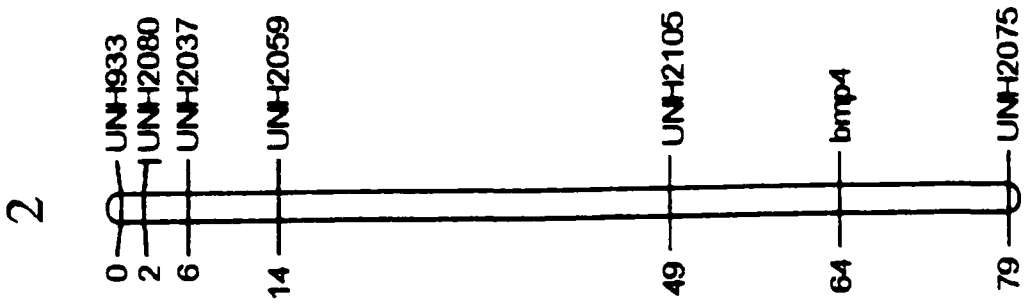
VM



## Appendix C

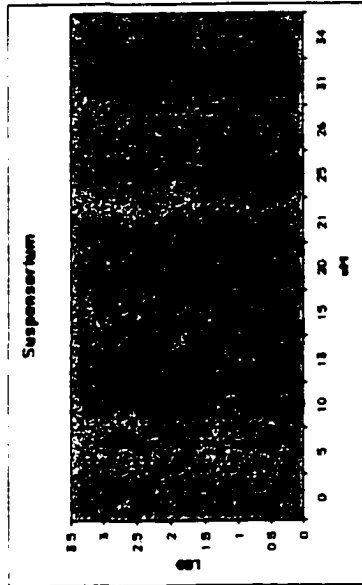
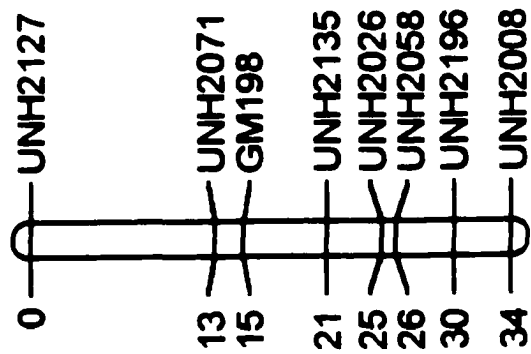
Results from MQM mapping organized by linkage group. Linkage groups are presented on the left. Graphical depictions of QTL are shown to the right. LOD scores (LOD) were plotted against chromosomal positions (cM) for every trait. LOD thresholds at the 95% level were determined by 1000 permutations of the data. Significant LOD scores for each trait were as follows: lower jaw dentition = 2.4, upper jaw dentition = 2.3, lower jaw in the lateral view = 3.0, dentary = 2.4, articular = 2.4, jaw length = 2.7, articular arm length = 2.7, lower jaw in the ventral view = 2.8, jaw width = 2.8, maxilla = 2.7, palatinal wing length = 2.3, premaxilla = 2.5, suspensorium = 2.5, neurocranium = 2.6, vomer = 2.3.

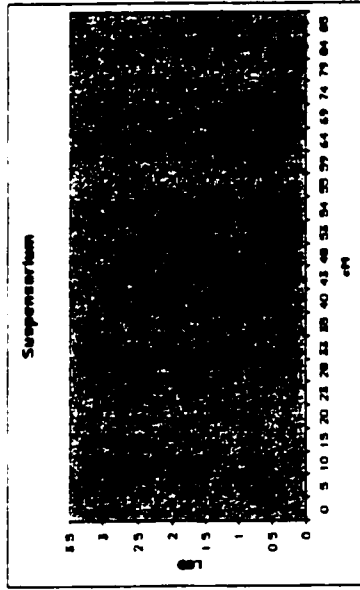
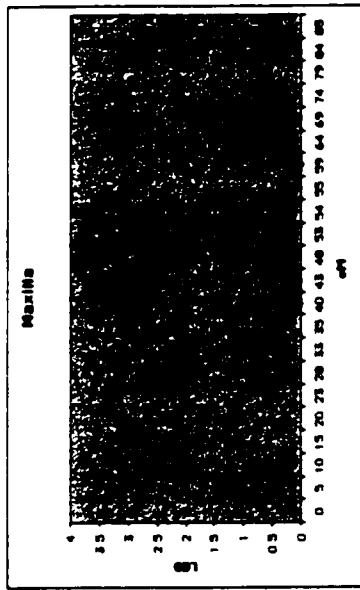
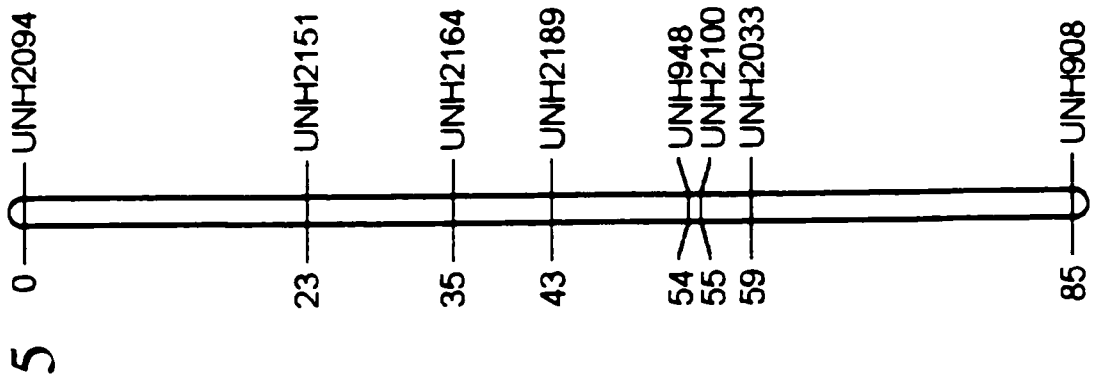




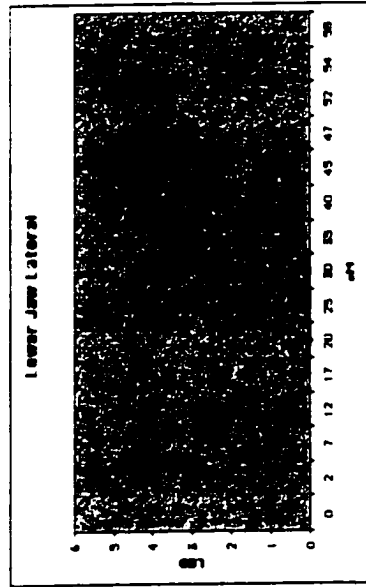
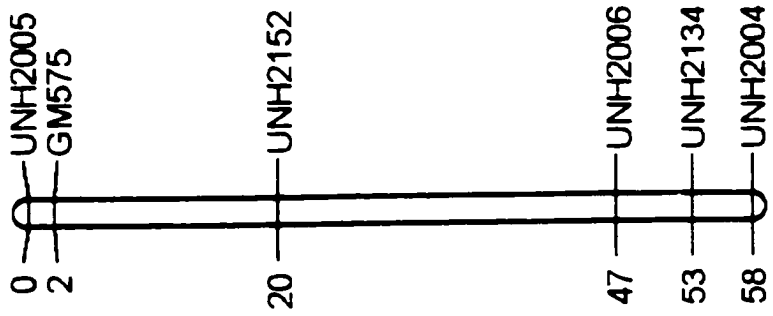


4



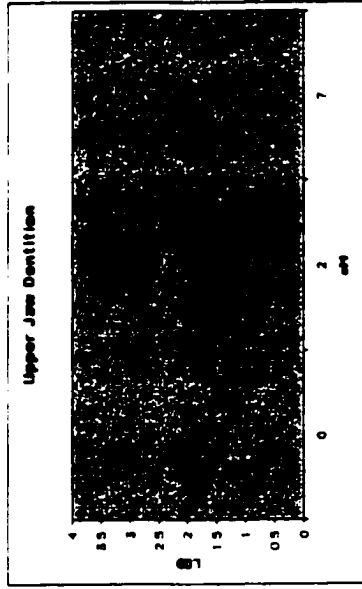
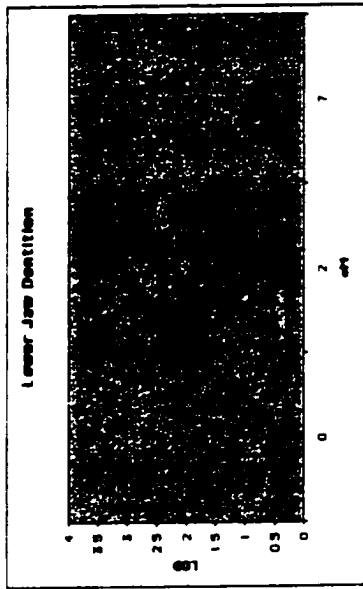


6

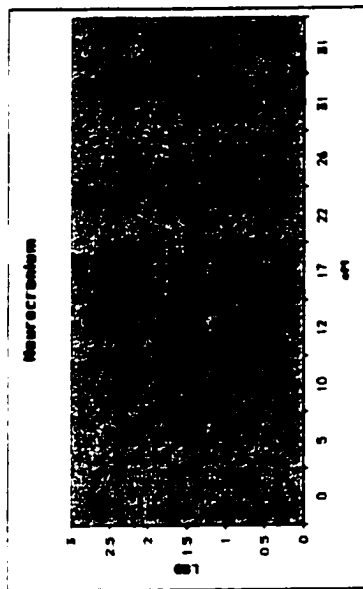
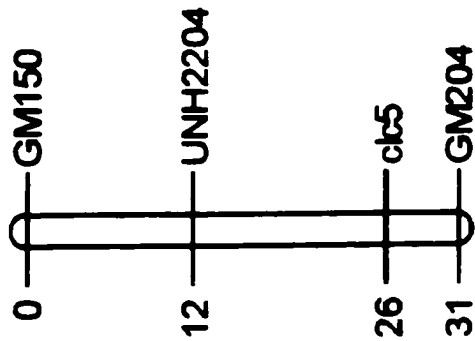


7

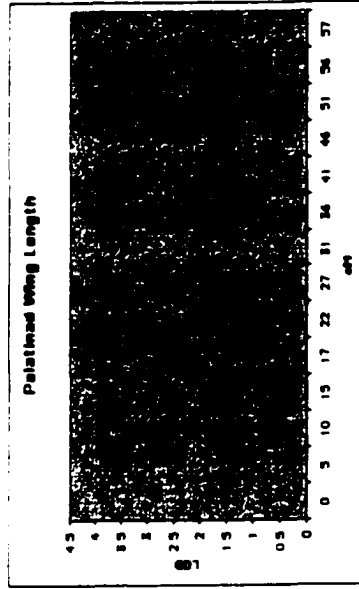
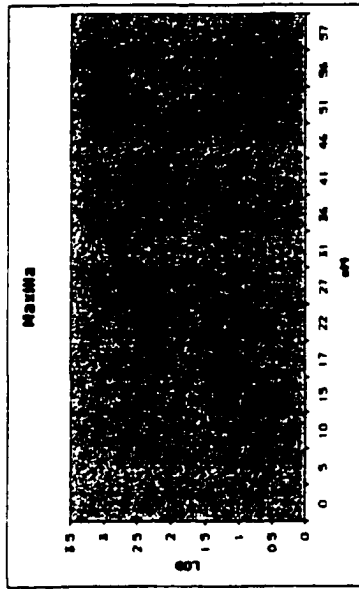
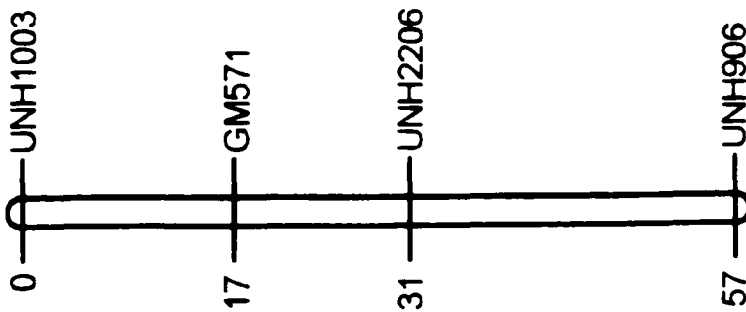
0 UNH2063  
2 UNH875  
7 UNH2191



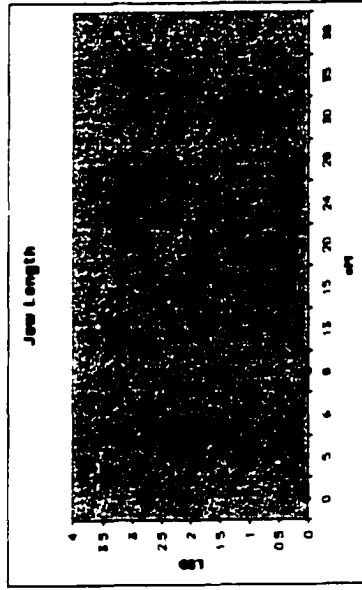
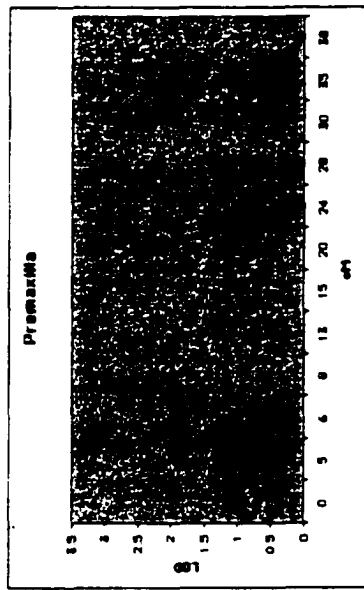
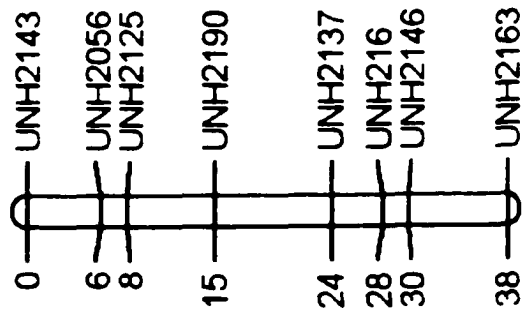
8



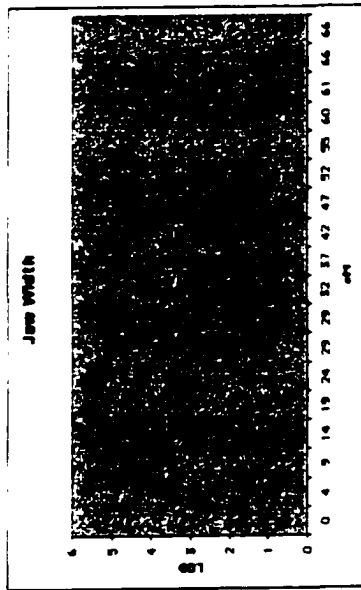
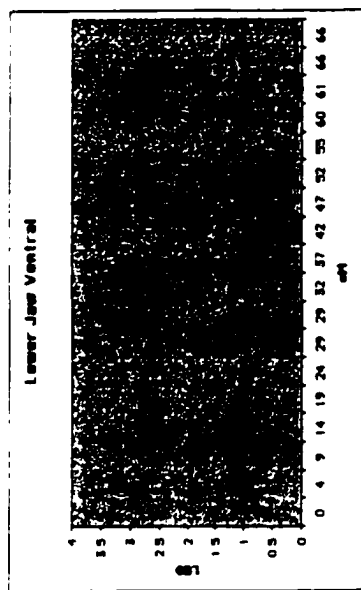
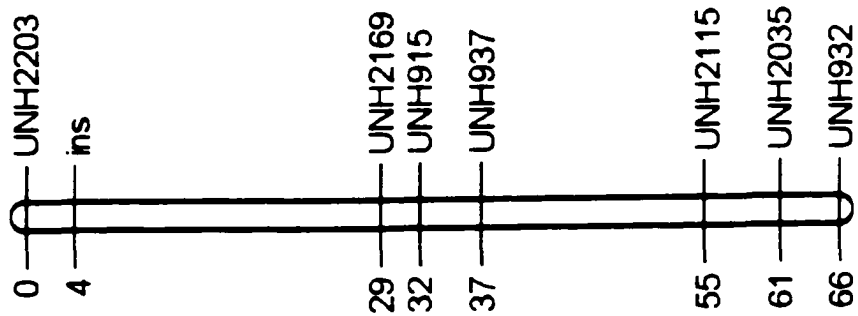
9



10

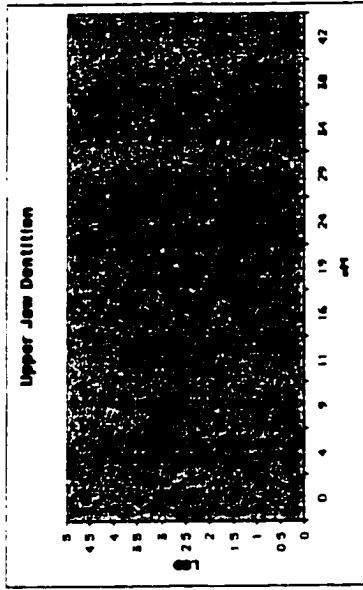
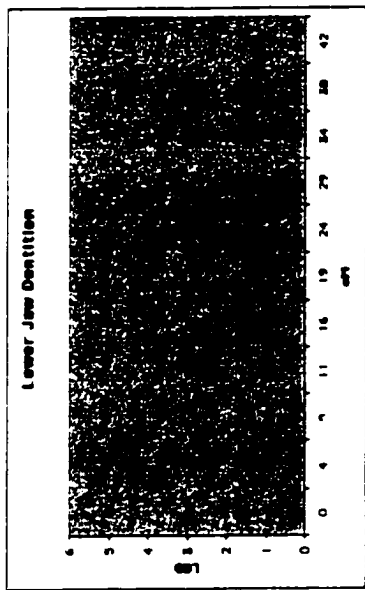
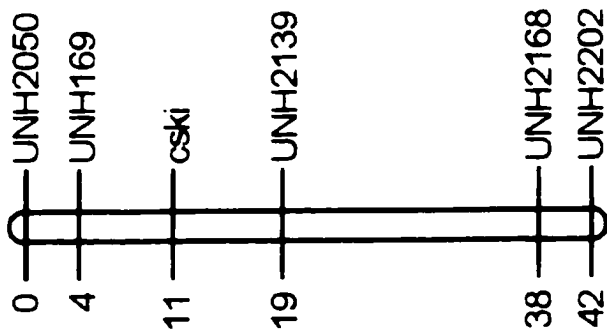


11



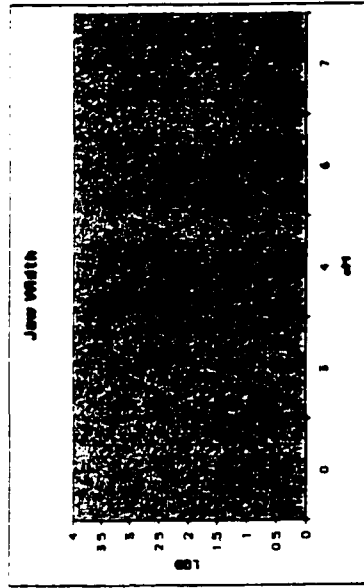


12

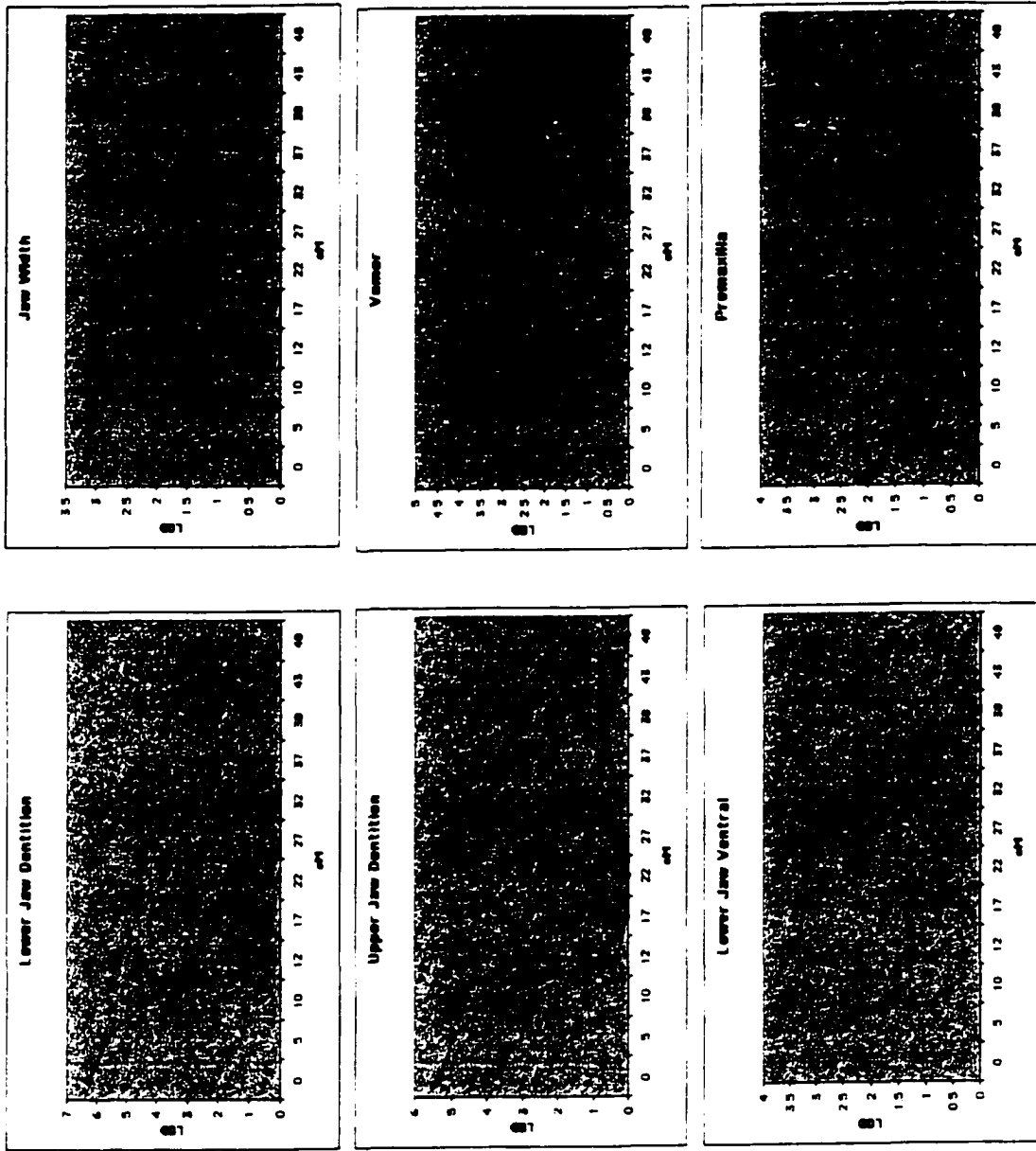
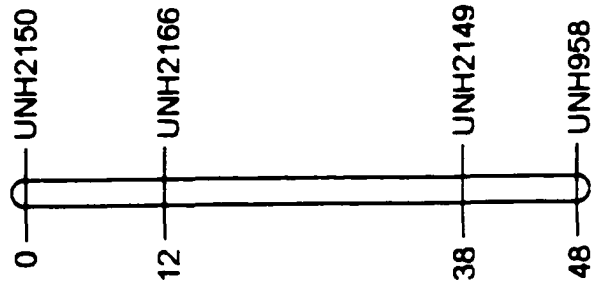


14

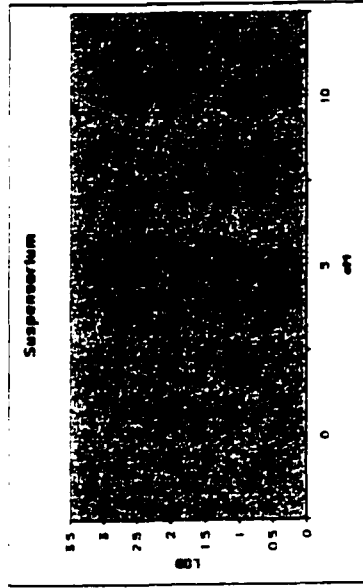
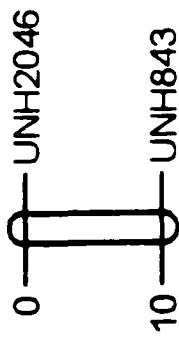
0 UNH989  
3 UNH2114  
4 UNH2040  
6 UNH2160  
7 UNH2110



16

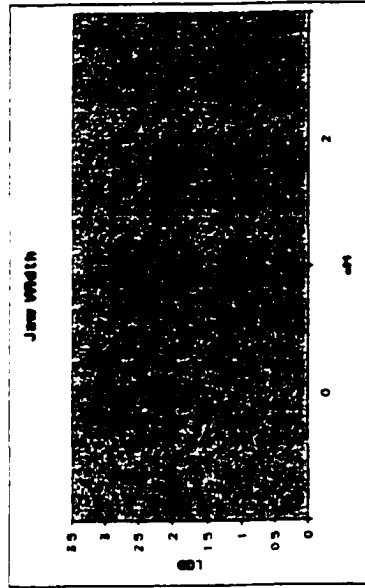


18

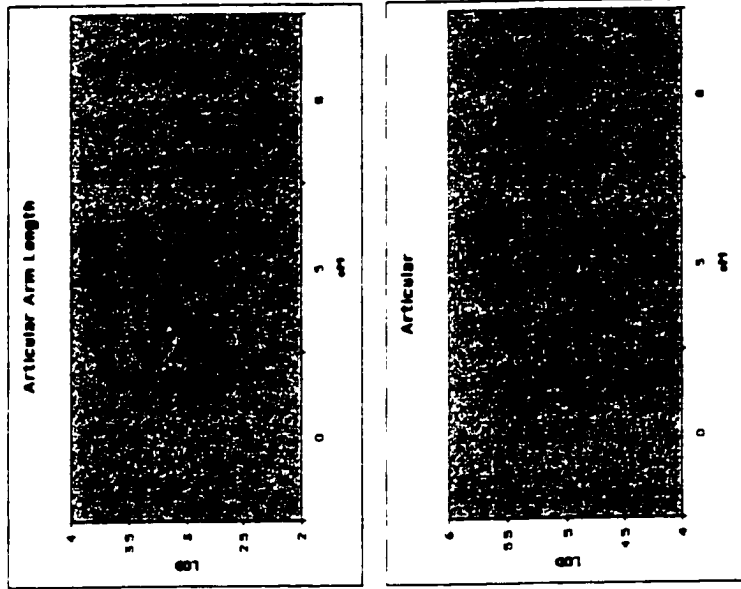
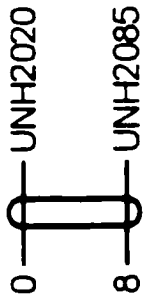


20

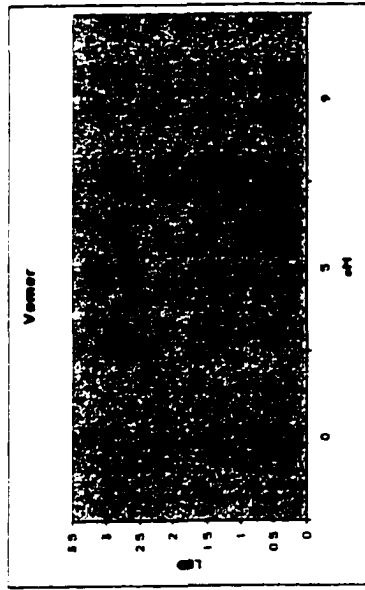
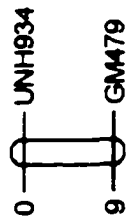
0 UNH2069  
2 UNH2128



21



24



## Literature Cited

- Adams, D.C., and F.J. Rohlf, 2000. Ecological character displacement in *Plethodon*: biomechanical differences found from a geometric morphometric study. Proc. Natl. Acad. Sci. USA. 97(8):4106-4111.
- Albertson, R. C., J. A. Markert, P. D. Danley, and T. D. Kocher, 1999. Phylogeny of a rapidly evolving clade: The cichlid fishes of Lake Malawi, East Africa. Proc. Natl. Acad. Sci. 96:5107-5110.
- Albertson R.C., and T.D. Kocher, 2001. Assessing morphological differences in a adaptive trait: a landmark-based morphometric approach. J. Exp. Zool. 289:385-403.
- Amid, C., A. Bahr, A. Mujica, N. Sampson, S.E. Bikar, A. Winterpacht, B. Zabel, T. Hankeln, E.R. Schmidt, 2001. Comparative genomic sequencing reveals a strikingly similar architecture of a conserved syntenic region on human chromosome 11p15.3 (including gene ST5) and mouse chromosome 7. Cytogene. Cell Genet. 93(3-4):284-90.
- Alexard, J., M. Rothenberg, G. L. Henery, and D. Y. R. Stainier. 1999. *casanova* plays an early and essential role in endoderm formation in zebrafish. Dev. Biol. 215:343-357.
- Atchley, W. R., 1993. Genetic and Developmental Aspects of Variability in the Mammalian Mandible. In: J. Hanken and B. K. Hall, editors. The Skull, Volume One: Development. University of Chicago Press, Chicago. p 207-247.
- Atchley, W. R., S. Newman, and D. E. Cowley. 1988. Genetic divergence in mandible form in relation to molecular divergence in inbred mouse strains. Genetics 120:239-253.
- Atchley, W. R. and B. K. Hall, 1991. A model for development and evolution of complex morphological structures. Biol. Rev. 66:101-157.
- Arai, R., and A. Koike, 1980. A karyotype study on two species of freshwater fishes transplanted to Japan. Bull. Nat. Sci. Mus. (Tokyo) 6:275-278.



- Bagheri-Fam, S., C. Ferraz, J. Demaille, G. Scherer, and D. Pfeifer, 2001. Comparative genomics of the SOX9 region in human and *Fugu rubripes*: conservation of short regulatory sequence elements within large intergenic regions. *Genomics*. 78(1-2):73-82.
- Barel, C. D. N. 1983. Toward a constructional morphology of cichlid fishes (Teleostei, Perciformes). *Neth. J. Zool.* 33: 357-424.
- Barel, C. D. N. , F. Witte, and M. J. P. vanOijen, 1976. The shape of the skeletal elements in the head of a generalized Haplochromis species: *H. elegans* Trewavas 1933 (Pisces, Cichlidae). *Neth. J. Zool.* 26:163-265.
- Beavis W.D., 1998. QTL analysis: power precision, and accuracy. In: *Molecular Dissection of Complex Traits* (A. H. Paterson, ed.). Boca Raton: CRC Press; 145-162.
- Berk, M., S.Y. Desai, H.C Heyman, and C. Colmenares, 1997. Mice lacking the *ski* proto-oncogene have defects in neurulation, craniofacial, patterning, and skeletal muscle development. *Genes Dev.* 11(16):2029-39.
- Bookstein, F. L. 1989. Principal warps: thin-plate splines and the decomposition of deformations. *IEEE Trans. Pattern Analysis Machine Intelligence.* 11:567-585.
- Bookstein, F. L. 1991. *Morphometric tools for landmark data: geometry and biology.* Cambridge University Press, New York.
- Bouton, N., O. Seehausen, and J.J.M. van Alpen 1997. Resource partitioning among rock-dwelling haplochromines (Pisces: Cichlidae) from Lake Victoria. *Ecol. Fresh. Fish*, 6:225-240.
- Bouton, N., N. van Os, and F. Witte 1998. Feeding performance of Lake Victoria rock cichlids: testing predictions from morphology. *J. Fish Biol. (Suppl. A)*, 53:118-127.
- Bradshaw, H. D., K. G. Otto, B. E. Frewen, J. K. McKay and D. W. Schemske. 1998. Quantitative trait loci affecting differences in floral morphology between two species of monkeyflower (*Mimulus*). *Genetics* 149:367-382.

- Cheverud, J.M., 1982. Phenotypic, genetic, and environmental morphological integration in the cranium. *Evolution* 36:499-516.
- Cheverud, J.M., 2001. The genetic architecture of pleiotropic relations and differential epistasis. In: *The Character Concept in Evolutionary Biology* (G. P. Wagner, ed). Academic Press; 411-433.
- Cheverud, J. M., S. E. Hartman, J. R. Richtsmeier and W. R. Atchley. 1991. A quantitative genetic analysis of localized morphology in mandibles of inbred mice using finite element scaling analysis. *J. Craniofac. Genet. Dev. Biol.* 11:121-137.
- Churchill, G. A. and R. W. Doerge. 1992. Empirical threshold values for quantitative trait mapping. *Genetics* 138:963-971.
- Clouthier, D. E., S.C. Williams, H. Yanagisawa, M. Wieduwilt, J.A. Richardson, and M. Yanagisawa. 2000. Signaling pathways crucial for caniofacial development revealed by endothelin-A receptor-deficient mice. *Dev. Biol.* 217(1):10-24.
- Crapon de Caprona, M. -D. , and B. Fritsch, (1984) Interspecific fertile hybrids of Haplochromine Cichlidae (Teleostei) and their possible importance for speciation. *Neth. J. Zool.* 34 (4): 503-538.
- Crossley, P.H., and G.R. Martin, 1995. The mouse *Fgf8* gene encodes a family of polypeptides and is expressed in regions that direct outgrowth and patterning in the developing embryo. *Dev.* 121(2)439-51.
- Danley, P.D., and T.D. Kocher, 2001. Speciation in rapidly diverging systems: Lessons from Lake Malawi. *Molecular Ecology* 10:1075-1086.
- De Beer, G. R. 1985. *The Development of the Vertebrate Skull*. U. Chicago Press, Chicago.
- Dominey, W.J. 1984. Effects of sexual selection and life history on speciation: Species flocks in African cichlids and Hawaiian *Drosophila*. in *Evolution of Fish Species Flocks*, eds. Echelle, A.A. & Kornfield, I. (University of Maine at Orono Press).
- Echelle, A. A. and I. Kornfield, 1984. *Evolution of fish species flocks*. University of Maine at Orono Press, Orono, Maine.

- Fryer, G., 1959. The trophic interrelationship and ecology of some littoral communities of Lake Nyasa with special reference to the fishes and a discussion of the evolution of a group of rock-frequenting Cichlidae. *Proc. Zool. Soc. London*, 132:153-281.
- Fryer, G. and T. D. Iles, 1972. *The Cichlid Fishes of the Great Lakes of Africa: Their Biology and Evolution*. Oliver and Boyd, Edinburgh.
- Fumagalli, S., L. Doneda, N. Nomura, and L. Larizza, 1993. Expression of the *c-ski* proto-oncogene in human melanoma cell lines. *Melanoma Res.* 3(1):23-7.
- Futuyma, J.F., 1986. *Evolutionary Biology*. Sunderland, MA: Sinauer Associates, Inc.
- Gadau, J., R.E. Page, and J.H. Werren, 2002. The Genetic Basis of the Interspecific Differences in Wing Size in *Nasonia* (Hymenoptera; Pteromalidae). Major quantitative trait loci and epistasis. *Genetics*. 161(2):673-84.
- Genner, M.J., G.F. Turner, and S.J. Hawkins, 1999. Foraging of rocky habitat cichlid fishes in Lake Malawi: coexistence through niche partitioning? *Oecologia* 121:283-292.
- Greenwood, P. H. 1974. The cichlid fishes of Lake Victoria, East Africa: the biology and evolution of a species flock. *Bull. Br. Mus. Nat. Hist. (Zool. ) (Suppl. )* 6: 1-134.
- Gower, J. C. 1975. Generalized Procrustes analysis. *Psychometrika* 40:33-51.
- Grant, P.R., and B.R. Grant, 1997. Genetics and the origin of bird species. *Proc. Natl. Acad. Sci. USA*. 94:7768-7775.
- Gold, J.R., 1979. Cytogenetics. In *Fish Physiology*, Vol 8. W.S. Hoar, D.J. Randall, and J.R. Brett (eds.). Academic Press, New York pp. 353-405.
- Hall, B. K. 1999. *The Neural Crest in Development and Evolution*. Springer-Verlag New York, Inc. , New York, NY.
- Hanken, J. 1993. Model systems versus outgroups: alternative approaches to the study of head development and evolution. *Amer. Zool.* 33:448-456.

- Hatfield, T. 1997. Genetic divergence in adaptive characters between sympatric species of stickleback. *Am. Nat.* 149:1009-1029.
- Holzberg, S., 1978. A field and laboratory study of the behavior and ecology of *Pseudotropheus zebra* (Boulenger), an endemic cichlid of Lake Malawi (Pisces: Cichlidae). *Z. Zool. Syst. Evol-Forsch.* 16:171-186.
- Huang, C.J., J.Y. Lin, H.J. Tsai, 1999. Two distinct *c-ski* cDNAs of fish, tilapia (*Oreochromis aurea*). *Mol Reprod Dev.* 54(3):223-31.
- Jansen, R.C., 1994. Controlling the type I and type II errors in mapping quantitative trait loci. *Genetics.* 138(3):871-81.
- Johnson, T. C., C. A. Scholz, M. R. Talbot, K. Kelts, R. D. Ricketts, G. Ngobi, K. Beuning, I. Ssemmanda, and J. W. McGill. 1996. Late Pleistocene desiccation of Lake Victoria and rapid evolution of cichlid fishes. *Science* 273:1091-1093.
- Kappen, C., J.M. Salbaum, 2001. Comparative genomics of a conserved chromosomal region associated with a complex human phenotype. *Genomics.* 73(2):171-8.
- Kimmel, C.B., C.T. Miller, and C.B. Moens, 2001. Specification and morphogenesis of the zebrafish larval head skeleton. *Dev. Bio.* 233:239-257.
- Kocher, T. D., J. A. Conroy, K. R. McKaye, and J. R. Stauffer. 1993. Similar morphologies of cichlids in lakes Tanganyika and Malawi are due to convergence. *Mol. Phyl. Evol.* 2:158-165.
- Kocher, T. D. , J. A. Conroy, K. R. McKaye, J. R. Stauffer and S. F. Lockwood, 1995. Evolution of ND2 gene in East African cichlids. *Mol. Phyl. Evol.* 4:420-432.
- Kocher, T. D., W. -J. Lee, H. Sobolewska, D. Penman, and B. McAndrew. 1998. A genetic linkage map of a cichlid fish, the tilapia, (*Oreochromis niloticus*). *Genetics* 148:1225-1232.
- Köntges, G., and A. Lumsden, 1996. Rhombencephalic neural crest segmentation is preserved throughout craniofacial ontogeny. *Dev.* 122:3229-3242.
- Kornfield, I. 1984. Descriptive genetics of cichlid fishes. pp. 591-616. in *Evolutionary Genetics of Fishes*. Turner, B.J. (ed.). Plenum Publishing.

- Kornfield, I.L., U. Ritte, C. Richler and J. Wahrman, 1979. Biochemical and cytological aspects of species differentiation in Old World cichlid fishes. *Evolution* 33:1-14.
- Lande, R., O. Seehausen, and J.J.M. van Alphen, 2001. Mechanisms of rapid sympatric speciation by sex reversal and sexual selection in cichlid fish. *Genetica* 112-113:435-443.
- Lander, E. S., and D. Botstein. 1989. Mapping mendelian factors underlying quantitative traits using RFLP linkage maps. *Genetics* 121:185-199.
- Lauder, G. V. 1979. Feeding mechanics in primitive teleosts and in the halecomorph fish *Amia calva*. *J. Zool. (London)* 187:543-578.
- Leamy, L.J., E.J. Routman, and J.M. Cheverud, 1999. Mouse Skull Morphological Integration. *Am. Nat.* 153:201-214
- Li, X., G. Masinde, W. Gu, J. Wergedal, S. Mohan, D.J. Baylink, 2002. Genetic dissection of femur breaking strength in a large population (MRL/MpJ x SJL/J) of F<sub>2</sub> Mice: single QTL effects, epistasis, and pleiotropy. *Genomics*. 79(5):734-40.
- Liem, K. F. 1974. Evolutionary strategies and morphological innovations : cichlid pharyngeal jaws. *Syst. Zool.* 22:425-441.
- Liem, K.F., 1979. Modulatory multiplicity in the feeding mechanism of cichlid fishes, as exemplified by the invertebrate pickers of Lake Tanganyika. *J. Zool., London* 189:93-125.
- Liem, K. F. 1980. Adaptive significance of intra- and interspecific differences in the feeding repertoires of cichlid fishes. *Amer. Zool.* 20:25-31.
- Liem, K. F. 1991. Functional morphology. pp. 129-150 in *Cichlid Fishes: Behavior, Ecology and Evolution* (M. H. A. Keenleyside, ed. ), Chapman and Hall, London.
- Lillo, F., S. Basile, and R.N. Mantegna, 2002. Comparative genomics study of inverted repeats in bacteria. *Bioinformatics*. 18(7):971-9.
- Loiselle, P. V. 1971. Hybridization in cichlids. *Buntb. Bull.* 27: 9-18.

- Lynch, M., and B. Walsh, 1998. *Genetics and Analysis of Quantitative Traits*. Sunderland, MA: Sinauer Associates.
- Mackay, T. F. 1996 The nature of quantitative genetic variation revisited: lessons from *Drosophila* bristles. *Bioessays* 18:113-121.
- Martin, A.P., and E. Bermingham, 1998. Systematics and evolution of lower Central American cichlids inferred from analysis of cytochrome b gene sequences. *Mol. Phylogenet. Evol.* 9(2):192-203.
- McElroy, D. M. and I. Kornfield, 1993. Novel jaw morphology in hybrids between *Pseudotropheus zebra* and *Labeotropheus fuelleborni* (Teleostei: Cichlidae) from Lake Malawi, Africa. *Copeia* 1993, 933-945.
- McKaye, K. R. 1991. Sexual selection and the evolution of the cichlid fishes of Lake Malawi, Africa. Pp 241-257 in *Cichlid Fishes: Behavior, Ecology, and Evolution* (M.H.A. Keenleyside, ed.), Chapman and Hall, London.
- McKaye, K. R. and A. Marsh, 1983. Food switching by two specialized algae-scraping cichlid fishes in Lake Malawi, Africa. *Oecologia* 56:245-248.
- McKaye, K. R., S. M. Louda, and J. R. Stauffer. 1990. Bower size and male reproductive success in cichlid fish lek. *American Naturalist* 35:592-613.
- McKaye, K.R., E. van den Berghe, T.D. Kocher, and J.R. Stauffer, 1998. Assortative mating by taxa of the Midas cichlid, '*Cichlasoma*' *citrinellum*: sibling species or taxa speciating??? In: *International Symposium on Tropical Fish Biology*, Southampton, UK, July 13-16, 1998.
- McKaye, K.R., J.R. Stauffer, E.P. van den Berghe, R. Vivas, L.J. Lopez Perez, J.C. McCrary, R. Waid, A. Konings, W.-J. Lee, and T.D. Kocher, 2002. Behavioral, Morphological and Genetic Evidence of Divergence of the Midas Cichlid Species Complex in Two Nicaraguan Crater Lakes. *Cuadernos de Invest. de la U.C.A.* 12:19-47.
- McPhail, J. D. 1992. Ecology and evolution of sympatric sticklebacks (*Gasterosteus*): evidence for genetically divergent populations in Paxton Lake, Texada Island, British Columbia. *Can. J. Zool.* 70:361-369.

- McPhail, J. D. 1994. Speciation and the evolution of reproductive isolation in the sticklebacks (*Gasterosteus*) of south-west British Columbia. Pp. 399-437 in M.A. Bell and S.A. Foster, eds. *Evolutionary Biology of the Three-Spine Stickleback*. Oxford Univ. Press, Oxford.
- Meyer, A. 1993. Phylogenetic relationships and evolutionary processes in East African cichlid fishes. *Trends. Ecol. Evol.* 8: 279-284.
- Meyer, A. , Kocher, T. D. , Basasibwaki, P. and A. C. Wilson, 1990. Monophyletic origin of Lake Victoria cichlid fishes suggested by mitochondrial DNA sequences. *Nature* 347, 550-553.
- Mezey, J.G., J.M. Cheverud, and G.P. Wagner, 2000. Is the genotype-phenotype map modular? A statistical approach using mouse quantitative trait loci data. *Genetics* 156:305-311.
- Monsoro-Burq, A.H., D. Duprez, Y. Watanabe, M. Bontoux, C. Vincent, P. Brickell, and N. Le Douarin, 1996. The role of bone morphogenetic proteins in vertebral development. *Development.* 122(11):3607-16.
- Moran, P. , I. Kornfield and P. Reinthal, 1994. Molecular systematics and radiation of the haplochromine cichlids of Lake Malawi. *Copeia* 1994:274-288.
- Nagelkerke, L.A.J., F.A. Sibbing, J.G.M. J.G.M. van den Boogaart, E.H.R.R. Lammens, and J.W.M. Osse, 1994. The barbs (*Barbus* spp.) of Lake Tana: a forgotten species flock? *Env. Bio. Fish.* 39:1-22.
- Noden, D. M. 1986. Origins and patterning of craniofacial mesenchymal tissues. *J. Craniofacial Gen. Dev. Biol.* 2:15-31.
- Nonaka, K., L. Shum, I. Takahashi, K. Takahashi, T. Ikura, R. Dashner, G.H. Nuckolls, and H.C. Slavkin, 1999. Convergence of the BMP and EGF signaling pathways on Smad1 in the regulation of chondrogenesis. *Int J Dev Biol.* 43(8):795-807.
- Orr, H.A., and J.A. Coyne, 1992. The genetics of adaptation: a reassessment. *Am. Nat.* 140:725-742.
- Otto, S.P., and C.D. Jones, 2000. Detecting the Undetected: Estimating the Total Number of Loci Underlying a Quantitative Trait. *Genetics* 156: 2093-2107.

- Otten, E. 1983. The jaw mechanism during growth of a generalized *Haplochromis* species: *H. elegans* Trewavas, 1933 (Pisces, Cichlidae). *Neth. J. Zool.* 33:55-98.
- Owen, R. B. , R. Crossley, T. C. Johnson, D. Tweddle, I. Kornfield, S. Davison, D. H. Eccles, and D. E. Engstrom, 1990. Major low levels of Lake Malawi and implication for speciation rates in cichlid fishes. *Proc. R. Soc. Lond. B.* 240, 519-533.
- Peichel, C.L., K.S. Nereng, K.A. Ohgi, B.L.E. Cole, P.F. Colosimo, C.A. Buerkley, D. Schluter, and D.M. Kingsley, 2001. The genetic architecture of divergence between threespine stickleback species. *Nature* 414:901-905.
- Peters, H., and R. Balling, 1999. Teeth: where and how to make them. *Trend. Genet.* 15(2):59-65.
- Piotrowski, T., T. F. Schilling, M. Brand, Y. Jiang, C. Heisenberg, D. Beuchle, H. Grandel, F. J. M. van Eeden, M. Furutani-Seiki, M. Granato, P. Haffter, M. Hammerschmidt, D. A. Kane, R. N. Mullins, J. Odenthal, R. M. Warga, and C. Nusslein-Volhard. 1996. Jaw and branchial arch mutants in zebrafish II: anterior arches and cartilage differentiation. *Development* 123:345-356.
- Piotrowski, T., and C. Nusslein-Volhard. 2000. The endoderm plays an important role in patterning the segmented pharyngeal region in zebrafish. *Dev. Biol.* 225:339-356.
- Post, A., 1965. Vergleichende untersuchungeh der Chromosomenzahlen bei Susswasser-Teleostern. *Z. Zool. Syst. Evolutionsforsch.* 3:47-93.
- Reinthal, P. N. 1990. The feeding habits of a group of tropical herbivorous rock-dwelling cichlid fishes from Lake Malawi, Africa. *Environmental Biology of Fishes* 27:215-233.
- Ribbink, A. J. , A. C. Marsh, C. C. Ribbink, and B. J. Sharp, 1983. A preliminary survey of the cichlid fishes of rocky habitats in Lake Malawi. *S. Afr. J. Zool.* 18:149-310.
- Ridgway, M. S., and J. D. McPhail. 1984. Ecology and evolution of sympatric stickleback (*Gasterosteus*): mate choice and reproductive isolation in the Enos Lake species pair. *Can. J. Zool.* 62:1813-1818.



- Rohlf, F. J. 1999. TPSRegression. Geometric morphometric software for the PC. <http://life.bio.sunysb.edu/morph/software.html>.
- Rohlf, F. J. and L. F. Marcus, 1993. A revolution in morphometrics. *Trends. Ecol. Evol.* 8:129-132
- Rohlf, F. J. and D. Slice, 1990. Extensions of the Procrustes method for the optimal superimposition of landmarks. *Syst. Zool.* 39:40-50.
- Ruber, L., E. Verheyen, and A. Meyer, 1999. Replicate evolution of trophic specialization in an endemic cichlid fish lineage from Lake Tanganyika. *Proc. Natl. Acad. Sci. USA* 31:10230-10235.
- Santagati, F., J.K. Gerber, J.H. Blusch, C. Kokubu, H. Peters, J. Adamski, T. Werner, R. Balling, K. Imai, 2001. Comparative analysis of the genomic organization of *Pax9* and its conserved physical association with *Nkx2-9* in the human, mouse, and pufferfish genomes. *Mamm Genome.* 12(3):232-7.
- Sato, A., H. Tichy, C. O'hUigin, P.R. Grant, B.R. Grant, and J. Klein, 2001. On the origin of Darwin's finches. *Mol. Biol. Evol.* 18(3):299-311.
- Schilling, T. F. 1997. Genetic analysis of craniofacial development in the vertebrate embryo. *BioEssays* 19:459-468.
- Schilling, T.F., T. Piotrowski, H. Grandel, M. Brand, C. Heisenberg, Y. Jiang, D. Beuchle, M. Hammerschmidt, D.A. Kane, R.N. Mullins, F.J.M. van Eeden, R.N. Kelsh, M. Furutani-Seiki, M. Granato, P. Haffter, J. Odenthal, R.M. Warga, T. Trowe, and C. Nusslein-Volhard, 1996. Jaw and branchial arch mutants in zebrafish I: branchial arches. *Development* 123:329-344.
- Schliewen, U. K., D. Tautz and S. Paabo. 1994. Sympatric speciation suggested by monophyly of crater lake cichlids. *Nature* 368:629-632.
- Scholtz, C.A., and Rosendahl, B.R., 1988. Low lake stands in Lake Malwai and Tanganyika, East Africa, delineated with multifold seismic data. *Science* 240: 1645-1648.
- Schulter, D., and J.D. McPhail. 1993. Character displacement and replicate adaptive radiation. *Trend. Ecol. Evol.* 8:197-200.

- Seehausen, O., van Alphen, J. J. M. and F. Witte, 1997. Cichlid fish diversity threatened by eutrophication that curbs sexual selection. *Science* 277, 1808-1811.
- Seehausen, O., J.J.M. van Alphen, and R. Lande, 1999. Color polymorphism and sex ratio distortion in a cichlid fish as an incipient stage in sympatric speciation by sexual selection. *Ecology letters* 2:367-378.
- Semba, I., K. Nonaka, I. Takahashi, K. Takahashi, R. Dashner, L. Shum, G.H. Nuckolls, and H.C. Slavkin, 2001. Positionally-dependent chondrogenesis induced by BMP4 is co-regulated by *Sox9* and *Msx2*. *Dev Dyn.* 217(4):401-14.
- Skulason, S., D.L.G. Noakes, and S.S. Snorrason. 1989. Ontogeny of trophic morphology in four sympatric morphs of arctic charr *Salvelinus alpinus* in Thingvallavatn, Iceland. *Biol. J. Linn. Soc.* 38:281-301.
- Skulason, S., S.S. Snorrason, D.L.G. Noakes, and M. M. Ferguson. 1996. Genetic basis of life history variations among sympatric morphs of arctic charr *Salvelinus alpinus*. *Can J. Fish. Aquat. Sci.* 53:1807-1813.
- Sokal, R.R., and F.J. Rohlf, 1981. *Biometry*, 2<sup>nd</sup> Edition. W.H. Freeman and Co., San Francisco, CA.
- Stauffer, J. R. Jr. , Bowers, N. J. , Kellogg, K. A. and K. R. McKaye, 1997. A revision of the blue-black *Pseudotropheus zebra* (Teleostei: Cichlidae) complex from Lake Malawi, Africa, with description of a new genus and ten new species. *Proc. Acad. Nat. Sci. Phil.* 148, 189-230.
- Stauffer, J.R., and K.R. McKaye, 2002. Descriptions of three new species of cichlid fishes (Teleostie: Cichlidae) from Lake Xiloa, Nicaragua. *Cuadernos de Invest. de la U.C.A.* 12:19-47.
- Sutrave, P., A.M. Kelly, and S.H. Hughes, 1990. Ski can cause selective growth of skeletal muscle in transgenic mice. *Genes Dev.* 4(9):1462-72.
- Tanksley, S.D., 1993. Mapping polygenes. *Annu. Rev. Genet.* 27:205-233.
- Thompson, D'A. W. 1917. *On Growth and Form*. Cambridge Univesity Press.

- Thompson, K.W., 1981. Karyotypes of six species of African Cichlidae (Pisces: Perceiforms). *Experientia* 37:351-352.
- Tichy, H., and L. Seegers, 1999. The *Oreochromis alcalicus* flock (Teleostei: Cichlidae) from lakes Natron and Magadi, Tanzania and Kenya: a model for the evolution of "new" species flocks in historical times? *Ichthyol. Explor. Freshwaters*, 10:147-174.
- Trendall, J., 1988. The distribution and dispersal of introduced fish at Thumbi West Island in Lake Malawi, Africa. *J. Fish Biol.* 33:357-369.
- Trewavas, E., 1935. A synopsis of the cichlid fishes of Lake Nyasa. *Ann. Mag. Nat. Hist.* 10:65-118.
- True, J. R., J. Liu, L. F. Stam, Z. -B. Zeng, and C. C. Laurie. 1997. Quantitative genetic analysis of divergence in male secondary sexual traits between *Drosophila simulans* and *Drosophila mauritiana*. *Evolution* 51: 816-832.
- Tucker, A.S., K.L. Matthews, and P.T. Sharpe, 1998. Transformation of tooth type induced by inhibition of BMP signaling. *Science* 282:1136-1138.
- Van Ooijen, J.W., H. Sandbrink, C. Purimahua, R. Vrieling, R. Verkerk, P. Zabel, and P. Lindhout, 1993. Mapping quantitative genes involved in a trait assessed on an ordinal scale: A case study with bacterial canker in *Lycopersicon peruvianum*. In *Molecular Biology of Tomato*, ed. J.I. Yoder (Technomic Publishing Co. Inc., Lancaster PA).
- Van Ooijen, J.W., and R.E. Voorrips, 2001. JoinMap 3.0, Software for the calculation of genetic linkage maps. Plant Research International, Wageningen, the Netherlands.
- Van Ooijen, J.W., M.P. Boer, R.C. Jansen, and C. Maliepaard, 2002. QTLMap 4.0, Software for the calculation of QTL positions on genetic maps. Plant Research International, Wageningen, the Netherlands.
- Volpe, J.P., and M.M. Ferguson. 1996. Molecular genetic examination of the polymorphic arctic charr *Salvelinus alpinus* of Thingvallavatn, Iceland. *Mol. Ecol.* 5:763-772.

- Walker, J. 1999. Morphometrika. Geometric morphometric software for the Power Macintosh. <http://jaw.fmnh.org/Software/Morphometrika.html>.
- Westerbergh, A., and J. Doebley, 2002. Morphological traits defining species differences in wild relatives of maize are controlled by multiple quantitative trait loci. *Evolution* 56(2):273-283.
- White, S., and J. Doebley. 1998. Of genes and genomes and the origin of maize. *Trends Genet.* 14:327-332.
- Wijngaarden, P.J., and P.M. Brakefield, 2000. The genetic basis of eyespot size in the butterfly *Bicyclus anynana*: an analysis of line crosses. *Heredity* 85:471-479.
- Witte, F. 1984. Consistency and functional significance of morphological differences between wildcaught and domestic *Haplochromis squamipinnis*. *Neth. J. Zool.* 34:596-612.
- Wong, S., G. Butler, and K.H. Wolfe, 2002. Gene order evolution and paleopolyploidy in hemiascomycete yeasts. *Proc Natl Acad Sci U S A.* 99(14):9272-7.
- Yamaoka, K., M. Hori, and S. Kuratani, 1986. Ecomorphology of feeding in 'goby-like' cichlid fishes in Lake Tanganyika. *Physiol. Ecol. Japan*, 23:17-29.
- Yaroch, L. A. 1996. Shape analysis using the thin-plate spline: *Neanderthal* cranial shape as an example. *Yearbook of Phys. Anth.* 39:43-89.
- Zelditch, M.L., 1987. Evaluating models of developmental integration in the laboratory rat using confirmatory factor analysis. *Syst. Zool.* 36:368-380.
- Zeng, Z.-B., 1992. Correcting the bias of Wright's estimates of the number of genes affecting a quantitative character: a further improved method. *Genetics*, 131:987-1001.
- Zeng, Z.-B., D. Houle, and C.C. Cockerham, 1990. How informative is Wright's estimator of the number of genes affecting a quantitative character? *Genetics*, 126:235-247.